ADVANCES IN INORGANIC CHEMISTRY, VOL. 40

OCTACYANO AND OXO- AND NITRIDOTETRACYANO COMPLEXES OF SECOND AND THIRD SERIES EARLY TRANSITION METALS

JOHANN G. LEIPOLDT, STEPHEN S. BASSON, and ANDREAS ROODT

Department of Chemistry, University of the Orange Free State, Bloemfontein 9300, South Africa

I. Introduction

The aim of this chapter is to summarize the chemistry of octacyano complexes and oxo- and nitridocyano complexes of molybdenum, tungsten, niobium, tantalum, technetium, and rhenium, with special emphasis on structural and kinetic properties.

These complexes are excellent models for theoretical studies. The octacyano complexes of molybdenum and tungsten are stable and inert toward substitution reactions and therefore very suitable for theoretical studies of redox reactions and application of the Marcus theory. The photoreactivity of these systems is also proving to be important. The oxo- and nitridocyano complexes of Mo(IV), W(IV), Tc(V), Re(V), and Os(VI) are very good candidates for kinetic studies of substitution reactions with both mono- and bidentate ligands and are of interest especially in view of the large variations in the observed reactivity.

Copyright © 1993 by Academic Press, Inc.
All rights of reproduction in any form reserved.

Apart from the above-mentioned theoretical applications, there is also the possibility of practical applications. The octacyano complexes of Mo(V) and W(V), for example, find excellent use in the oxidation of organic substances which require a mild oxidizing agent. It was also recently observed that derivatives of the dioxotetracyano complexes of Mo(IV) and W(IV) can take up dioxygen, which leads to the activation of the O_2 molecule. The complexes are thus candidates as catalysts in oxidation reactions with dioxygen as well as oxygen-transfer reactions.

These and other applications in for example the field of analytical chemistry have led to an increasing number of articles during the past two decades. Although this chapter does not cover all aspects, it gives a fairly comprehensive account of research output on the octacyano complexes. It is moreover the first review covering the chemistry of oxo- and nitridotetracyano complexes, which has developed extensively during the past decade.

II. Octacyano Complexes

A. Stereochemistry

The stereochemistry of octacyano complexes is at present concerned with the d^1 and d^2 ions of niobium, molybdenum, and tungsten. They are the only elements for which octacoordinated cyano complexes have been unequivocably identified by single-crystal X-ray crystallographic studies. Older structural data on cyano complexes can be found in a review by Griffith (*1*) and Sharpe's book (*2*). Whereas it was claimed that salts of $[Re(CN)_8]^{3-}$ and $[Re(CN)_8]^{2-}$ ions could be synthesized (*3–5*), the reported preparative methods were reinvestigated (*6*) and found to give mixtures of $K_4[Re(CN)_7]\cdot 2H_2O$ and $K_3[ReO_2(CN)_4]$. We have also investigated the reaction between $K_2[ReI_6]$ and KCN in hot methanol and our findings are the same (see also Section IIID3). The only known cyano complex of tantalum at present is the cluster compound, $H_4[Ta_6Cl_{12}(CN)_6]\cdot 12H_2O$, with Ta—C = 2.21(4) Å and C—N = 1.16(5) Å bond distances (*7*).

Octacyano-metal ions, being discrete ML_8 moieties, can have different spatial arrangements. Those that have been considered include, with point symmetry in parentheses, the square antiprism (D_{4d}–$\bar{8}2m$), dodecahedron (D_{2d}–$\bar{4}2m$), cube (O_h–$m3m$), hexagonal bipyramid (D_{6h}–$6/mmm$), puckered hexagonal bipyramid (D_{3d}–$\bar{3}m$), 4,4-bicapped trigonal prism (C_{2v}–mm), and 3,3-bicapped trigonal prism (D_{3h}–$\bar{3}m2$). It is very seldom that the full point symmetry of these

polyhedra do occur in actual crystal structure determinations. Those forms which have been encountered in structure analyses of octacyano complexes are shown in Fig. 1.

Calculations, based on VSEPR theory so as to minimize repulsion between ligands in some of these afore-mentioned forms, have shown that repulsion energy coefficients for the square antiprism, dodecahedron, and cube are about the same but that the antiprism should be the most stable configuration for a ML_8 polyhedron (*8*). This principle has also been applied to $K_4[Mo(CN)_8]\cdot 2H_2O$, for which, in contrast

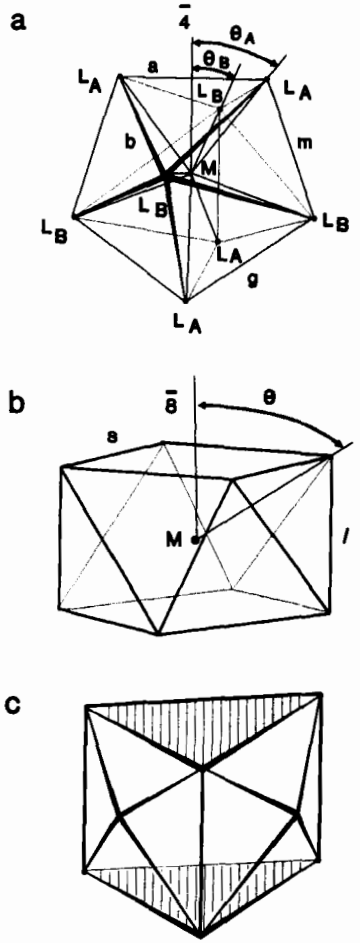

FIG. 1. Perspective views of a (a) dodecahedron, (b) square antiprism, and (c) 4,4-bicapped trigonal prism.

to the actual dodecahedral form of $[Mo(CN)_8]^{4-}$ ions in the structure determination (*9*), it was calculated that the square antiprism has better steric merit especially to accommodate short-range interactions with water molecules and/or cations in its immediate environment. The repulsion energy calculations for the above-mentioned preferred stereochemical forms have also shown that there is no large energy barriers between any two of these forms and that facile interconversions may occur. These in turn can be related to the direct physical environment of $[M(CN)_8]^{4-}$ ions in the solid state as well as in solution. It is thus no guarantee that if a specific solid-state geometry was identified that the same will apply to a solution of the complex. The anion geometry of octacyano complexes as determined by physical methods such as ESR, NMR, Mössbauer spectroscopy, etc., is thus often in conflict with those of crystal structure determinations and with good reason. It is imperative for comparison and interpretation of the different physical methods that crystal structure determinations of octacyano complexes be continued—after all a cubic geometry has not yet been identified for these complexes, although such a case has been reported for $Cs_4[U(NCS)_8]$ (square antiprism) (*10*) and $(Et_4N)_4[U(NCS)_8]$ (cube) (*11*).

Shape parameters (*12, 13*), determined from metal–ligand bond distances, specified angles, and edge lengths, can be used to typify a polyhedron as a hard sphere model (HSM) or, if ligand-to-ligand repulsion energies have been minimized, as a so-called most favorable polyhedron (MFP). The simplest HSM case is that for the square antiprism: all metal–ligand bond distances equal to r, $\Theta = 59.3°$ (Fig. 1), and all edge lengths equal to 1.2156 r. Minimization of repulsion energy gives elongation along the $\bar{8}$-axis so that for the MFP model $\Theta = 57.1°$. The majority of cyano complexes having approximate D_{4d} anion symmetry exhibit the latter value: $Na_3[W(CN)_8]\cdot 4H_2O$ (59.1°) (*14*) (see Fig. 2);

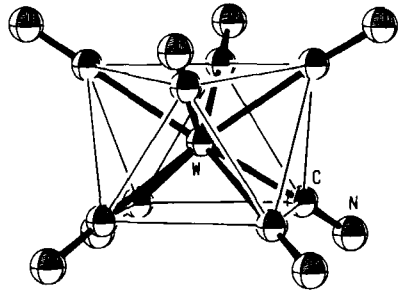

FIG. 2. Perspective view of a square antiprismatic $[W(CN)_8]^{3-}$ ion in $Na_3[W(CN)_8] \cdot 4H_2O$ (*14*).

TABLE I

SHAPE PARAMETERS FOR DODECAHEDRAL ANION GEOMETRIES

Shape parameter	$[(n\text{-But})_4N]_3$ = $[Mo(CN)_8]^a$	$K_4Mo(CN)_8$ = $2H_2O$	$(HPic)_4$ = $[Mo(CN)_8]^b$	MFP	HSM
θ_A (°)	37.2	36.0	35.6	35.2	36.9
θ_B (°)	72.5	72.9	73.6	73.5	69.5
$M—L_A/M—L_B$	1.00	1.00	1.01	1.03	1.00
a	1.21	1.18	1.16	1.17	1.20
m	1.15	1.16	1.16	1.17	1.20
g	1.23	1.24	1.24	1.24	1.20
b	1.48	1.48	1.47	1.49	1.50

[a] Corden *et al.* (*19*).

[b] Basson *et al.* (*20*); $HPic^-$ = 2-carboxypyridinium ion.

$H_4[W(CN)_8]\cdot 6H_2O$ (57.6°) (*15*); $H_4[W(CN)_8]\cdot 4HCl\cdot 12H_2O$ (56.1°) (*16*); $Cd_2[Mo(CN)_8]\cdot 2N_2H_4\cdot 4H_2O$ (57.9°) (*17*), and $Tl_4[Mo(CN)_8]$ (57.2°) (*18*). The ideal dodecahedron (Fig. 1), as a result of two interpenetrating bisphenoids, can have two symmetry-equivalent sets of metal–ligand bonds, namely $M—L_A$ and $M—L_B$ types. The angles Θ_A and Θ_B that $M—L_A$ and $M—L_B$ form with the quasi-$\bar{4}$-axis, bond ratio $M—L_A/M—L_B$, and edge lengths referred to as a unit length in M—L distances can also be used to identify a HSM or MFP polyhedron type (Table I) (*19, 20*). Inspection of the data in Table I shows that the MFP model are here favored as well and, although the point symmetry of a dodecahedron allows two different sets of bond distances to be observed, these are the same for $[(n\text{-But})_4N]_3[Mo(CN)_8]$ and $K_4[Mo(CN)_8]\cdot 2H_2O$.

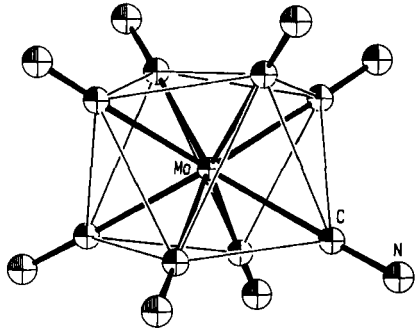

FIG. 3. Perspective view of a dodecahedral $[Mo(CN)_8]^{4-}$ ion in $(HNEt_3)_2(H_3O)_2[Mo(CN)_8]$ (*21*).

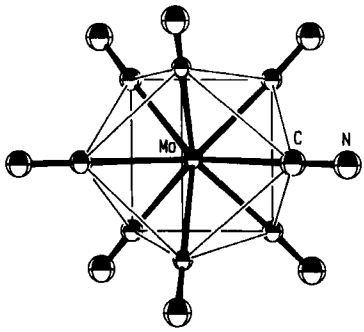

FIG. 4. Perspective view of a 4,4-bicapped trigonal prismatic $[Mo(CN)_8]^{3-}$ ion in $Cs_3[Mo(CN)_8] \cdot 2H_2O$ (*22*).

It does happen from time to time that visual inspection of an ML_8 polyhedron in a crystal structure determination shows obvious deviations from the ideal dodecahedron or square antiprism. This was experienced in structure determinations of, for example, $(HNEt_3)_2(H_3O)_2[Mo(CN)_8]$ (*21*) (Fig. 3) and $Cs_3[Mo(CN)_8]\cdot 2H_2O$ (*22*) (Fig. 4), and for these the anions could be described as distorted versions of the dodecahedral $Mo(CN)_8$ moiety. Fortunately, the shape determining method of Muetterties and Guggenberger (*23*), which makes use of dihedral interfacial angles of the polyhedron, offers a near unambiguous method for analyzing these coordination polyhedra. The ideal and observed values for a number of cyano complexes are given in Table II, which upon inspection shows that the polyhedron in $Na_3[W(CN)_8]\cdot 4H_2O$ (Fig. 2) is approximately halfway between a square antiprism and a bicapped

TABLE II

SHAPE ANALYSIS ACCORDING TO THE INTERFACIAL ANGLE METHOD[a]

ML_8 polyhedron analyzed	δ (°)	ϕ (°)	Reference
Ideal dodecahedron	29.5, 29.5, 29.5, 29.5	0.0	
Ideal 4,4-bicapped trigonal prism	0.0, 21.8, 48.2, 48.2	14.1	
Ideal square antiprism	0.0, 0.0, 52.4, 52.4	24.5	
$H_4[W(CN)_8] \cdot 6H_2O$	0.0, 2.9, 48.7, 48.7	22.7	*15*
$H_4[W(CN)_8] \cdot 4HCl \cdot 12H_2O$	5.2, 5.2, 46.3, 52.5	22.0	*16*
$Na_3[W(CN)_8] \cdot 4H_2O$	2.7, 9.6, 45.7, 48.2	18.9	*14*
$[(n\text{-But})_4N]_3[Mo(CN)_8]$	29.4, 29.4, 33.1, 33.1	1.0	*19*
$(HNEt_3)_2(H_3O)_2[Mo(CN)_8]$	17.3, 22.6, 38.9, 38.9	9.2	*21*
$Cs_3[Mo(CN)_8] \cdot 2H_2O$	0.0, 22.7, 47.4, 48.5	17.5	*22*
$(HPic)_4[Mo(CN)_8]$	30.3, 30.3, 34.2, 34.2	2.8	*20*

[a] Muetterties and Guggenberger (*23*).

trigonal prism, that in *bis*(triethylammonium)dihydronium octacyanomolybdate(IV) is halfway between a dodecahedron and a bicapped trigonal prism, and that in $Cs_3[Mo(CN)_8]\cdot 2H_2O$ should be considered a 4,4-bicapped trigonal prism. The last form is the first example of its kind for octacyano complexes. A closer analysis of the $[Mo(CN)_8]^{3-}$ polyhedron in this compound showed that the bonding angles (α) between the capping ligands and the central atom as well as the angles, Θ, between the six prism ligands and the quasi-threefold axis averaged 124.7° and 46.4°, respectively. For an ideal bicapped trigonal prism (*24*), $\alpha = 120$ and $\Theta = 45°$ for a d^0 and $\alpha = 140$ and $\Theta = 49°$ for a d^2 metal ion so that the experimental values obtained here for a d^1 central ion agree well with the increase for these angles from a d^0 to a d^2 case. The two cyano ligands situated between the capping ligands tend to shear away from one another, which, if not checked by strong Coulombic interactions of 3.35–3.38 Å with neighboring Cs^+ ions, would have led to a square antiprismatic geometry. There is also no lengthening, as permitted by theory (*24*), of metal–capping–ligand bond distances relative to those of the triangular faces of the polyhedron. This is similar to the situation observed for the D_{2d} geometries of $[(n\text{-But})N]_3[Mo(CN)_8]$ and $K_4[Mo(CN)_8]\cdot 2H_2O$. This phenomenon pertains to almost all M—L bond distances of octacyano complexes studied so far and the absence of π-bonding effects is perhaps due to the ability of the cyano ligand to strike a balance between its σ-donor and its π-acceptor abilities. The only meaningful M—C bond differences observed so far is for the D_{2d} geometry in $K_5[Nb(CN)_8]$ (*25*), in which the respective Nb—C distances of 2.282(4) Å and 2.242(4) Å for the corresponding A and B sites (Fig. 1) of the dodecahedron were determined. The structural data for $K_4[Nb(CN)_8]\cdot 2H_2O$ (*26*), which is also isomorphous to $K_4[Mo(CN)_8]\cdot 2H_2O$, showed to the contrary equal Nb—C (2.255 Å) distances. It is interesting to observe that the last value is halfway between the bond distances of its Nb(III) analogue. No analysis of the cation–anion contacts in $K_5[Nb(CN)_8]$ was given but we presume that they will be less effective compared with those of $K_4[Nb(CN)_8]\cdot 2H_2O$ and $K_4[Mo(CN)_8]\cdot 2H_2O$, especially considering the high anionic charge of the Nb(III) complex. It could be that in this case excessive anionic charge, due to ineffective Coulombic interaction with surrounding cations, was canalized via a permitted π-bond differentiation between A and B sites of the dodecahedron following Orgel's proposal (*27*).

Considering cation–anion interactions, the present structural data can, broadly speaking, be divided into two classes of compounds: those that contain a potential of excessive hydrogen bond-making species such as H^+, HCl, and water of crystallization and those having less or no water of crystallization combined with alkali metal or other size-

and charge-related ions. To the first class belong complexes such as $H_4[W(CN)_8]\cdot 6H_2O$, $H_4[W(CN)_8]\cdot 4HCl\cdot 12H_2O$, $Cd_2[Mo(CN)_8]\cdot 2N_2H_4\cdot 4H_2O$, $(HNEt_3)_2(H_3O)_2[Mo(CN)_8]$, $(HPic)_4[Mo(CN)_8]$, and $Na_3[W(CN)_8]\cdot 4H_2O$, and to the second class belong the remaining ones, including also $Ag_4(NH_3)_5[Mo(CN)_8]\cdot 1.5H_2O$ (*28*). This compound was prepared by reacting $AgNO_3$ and $K_4[Mo(CN)_8]\cdot 2H_2O$ in concentrated aqueous ammonia.

Hydrogen bonds play an important part in stabilizing the three-dimensional framework for the first group of complexes. The packing of $M(CN)_8$ polyhedra is layer-like and neighboring square antiprisms have interstitially spaced polyhedra of relative small coordination numbers, such as tetrahedra of H_2O molecules for $H_4[W(CN)_8]\cdot 6H_2O$, which interconnect these adjoining moieties through hydrogen bonding or sharing N atoms on the corners, or N—N edges of the antiprism, with those of the cations' polyhedra. Greater instability arises when the water of crystallization is used to fill structural cavities and becomes zeolitic in nature as was found in, for example, $Cd_2[Mo(CN)_8]\cdot 2N_2H_4\cdot 4H_2O$ and $H_4[W(CN)_8]\cdot 4HCl\cdot 12H_2O$. In the case of $(HPic)_4[Mo(CN)_8]$, four N atoms of the dodecahedron are strongly hydrogen bonded at 2.54 Å with four carboxylic groups. The remaining four N atoms have short cation–anion, i.e., $M—C\equiv N\cdots N^+$, contacts of 2.78 Å. Thus only four of the eight cyano ligands engage in cation–anion interaction with the $M—L_A$ sites on the dodecahedron, whereas the $M—L_B$ sites are the hydrogen-bonded ones. It was found that $Mo—C_A$ bond distances (2.166(5) Å), although not significant, tend to be longer than the $Mo—C_B$ distances of 2.153(6) Å as a result of these different types of Coulombic interactions.

To summarize, for the first group of complexes it seems, as a result of smaller cations or water molecules, that a more flattened version of the $M(CN)_8$ polyhedron, such as the square antiprism, is the preferred choice since it could adapt more efficiently to the smaller dimensions of the cation's polyhedron. If there is no cation polyhedron, then the dodecahedron, which allows dissimilar $M—L_A$ and $M—L_B$ bonds, is better adapted for charge neutralization, as was found in the cases of $(HPic)_4[Mo(CN)_8]$ and $(HNEt_3)_2(H_3O)_2[Mo(CN)_8]$.

In the second group of complexes, the cation radii are larger and as a result have larger coordination numbers so that more N atoms of cyano ligands can participate as an integral part of these polyhedra. As a result of this, fewer H_2O molecules are needed for completion of the cation's polyhedron or hydrogen bond stabilization of the three-dimensional framework. In $K_4[Mo(CN)_8]\cdot 2H_2O$ and its niobium analogue, the potassium ions are solely responsible for charge neutraliza-

tion on cyano groups, whereas H_2O molecules fill only the vacancies on these polyhedra by ion–dipole interactions. The effective coordination number on each potassium ion is 5. In $Tl_4[Mo(CN)_8]$ this increased to 7 and 8 due to a larger cation radius and in $Cs_3[Mo(CN)_8]$ to cubic and 4,4,4-tricapped trigonal–prismatic environments. In $Ag_4(NH_3)_5[Mo(CN)_8]\cdot 1.5H_2O$, which has a distorted square antiprismatic anion geometry, the $Mo(CN)_8$ groups are connected to a puckered layer via four of their N ends, which are tetrahedrally coordinated to silver.

It has also been reported that $(Me_4N)_3Li[Mo(CN)_8]\cdot 3.5H_2O$ and $Cs_7Na[Mo(CN)_8]_2\cdot 2H_2O$ have dodecahedral and approximate square antiprismatic anion geometries, respectively, but no structural details are available (*29*). Structural results have also been published for $(NH_4)_4[Mo(CN)_8]\cdot 0.5H_2O$ and $Rb_4[Mo(CN)_8]\cdot 3H_2O$ (*30*). In the ammonium compound, the $[Mo(CN)_8]^{4-}$ ions exist in two different geometries, dodecahedral and square antiprismatic. The rubidium complex has D_{2d} anion geometry.

B. Kinetics and Mechanism of Redox Reactions of Octacyanomolybdate and -Tungstate Ions

Redox reactions of octacyano complexes are attractive to kineticists for several reasons, of which their inertness to substitution, stability over a wide pH range, almost negligible protonation in acidic media, and favorable redox potentials are some of the more important. The above-mentioned properties are not rigid and exceptions do occur. Ion association and/or substitution of some cyano ligands has been reported for $[Mo(CN)_8]^{4-}$ with $[Cr(H_2O)_6]^{3+}$ (*31, 32*), $[Fe(H_2O)_6]^{3+}$ (*33*), and Ti(IV) (*34*) and for $[W(CN)_8]^{4-}$ with $[Cr(H_2O)_6]^{3+}$ (*35, 36*). There seems to be a difference of opinion regarding the mechanism and product formulation for these anation reactions, especially regarding the intactness or lack thereof of the cyano complexes' coordination sphere. This is an area where more research with, for example, trivalent aqua cations is to be done to clarify the ambiguity. No electron transfer occurs in these reactions and any mechanistic details are beyond the scope of this review.

An impressive number of articles on the redox kinetics of octacyano complexes have been produced during the past two decades. The material in this chapter covers the period between 1969 and 1991. Interested readers may find a good deal on the relatively few older mechanistic studies in reviews on mechanisms of redox reactions (*37*) and cyanide complexes of the early transition metals (*1*). A book by Sharpe (*2*) on

the chemistry of cyano complexes also covers some redox studies up to 1974. In order to make an assessment of the available published articles, it seemed best to classify material according to the mutual properties studied. The theoretical background relating to linear free-energy relationships and more specifically the well-known Marcus expressions as mechanistic criteria to assess the nature of outer-sphere reactions is nowadays well taken care of in standard textbooks on the topic of kinetics and mechanisms, and readers are referred to a source of this kind (*38*).

1. Free-Energy Relationships

a. Metal-Based Systems—MnO_4^-, MnO_4^{2-}, and Ag(III). Neither MnO_4^- or MnO_4^{2-} readily exchanges its ligands with solvent or other ligands, and their reactions with the kinetically inert $[M(CN)_8]^{3-/4-}$ ions are therefore suitable to outer-sphere mechanistic analysis using Marcus theory. The reduction of $[MnO_4]^-$ by $[Mo(CN)_8]^{4-}$ (*39*) and $[W(CN)_8]^{4-}$ (*40, 41*) proceeds with the expected overall stoichiometry of MnO_4^-:$[M(CN)_8]^{4-}$ = 1:5 in acid solution.

The protonation behavior of MnO_4^- results in the reaction taking place along two reaction pathways, the reaction sequence being

$$H^+ + [MnO_4]^- \overset{K}{\rightleftharpoons} HMnO_4 \quad K = 2.99 \times 10^{-3}\,M^{-1}\,(42) \tag{1}$$

$$[MnO_4]^- + [M(CN)_8]^{4-} \xrightarrow{k_1} [MnO_4]^{2-} + [M(CN)_8]^{3-} \tag{2}$$

$$HMnO_4 + [M(CN)_8]^{4-} \xrightarrow{k_2} HMnO_4^- + [M(CN)_8]^{3-}. \tag{3}$$

The observed linear dependence on hydrogen ion concentration is accounted for in the derived rate equation of

$$\text{rate} = (k_1 + k_2K[H^+])[MnO_4^-][M(CN)_8^{4-}]. \tag{4}$$

The pathways involving MnO_4^- ((Eq. (2)) and protonation products of $[M(CN)_8]^{4-}$ are thermodynamically the least favorable and make only a small contribution to the total reaction rate. The Marcus relation

$$k_{12} = (k_{11}k_{22}K_{12}f)^{1/2}, \tag{5}$$

where k_{12} is the rate constant of the redox reaction, $k_{11}(HMnO_4/HMnO_4^-$, $1.1 \times 10^{-3}\ M^{-1}\ sec^{-1})$ and k_{22} ($[Mo(CN)_8]^{3-}/[Mo(CN)_8]^{4-}$, $3 \times 10^4\ M^{-1}\,sec^{-1}$; $[W(CN)_8]^{3-}/[W(CN)_8]^{4-}$, $4 \times 10^4\ M^{-1}\,sec^{-1}$) are the

electron-exchange rate constants for the couples, K_{12} is the equilibrium constant for the redox reaction, and f is a function defined by

$$\log f = (\log K_{12})^2/4\log(k_{11}k_{22}/10^{22}), \tag{6}$$

was applied to calculate rate constants for Eq. (3) with good effect, i.e., $k_{12}(\text{calc}) = 2.39 \times 10^7\ M^{-1}\ \text{sec}^{-1}$ ($[Mo(CN)_8]^{4-}$) and $6.57 \times 10^8\ M^{-1}\ \text{sec}^{-1}$ ($[W(CN)_8]^{4-}$) compared with $k_{12}(\text{obs}) = 1.87 \times 10^7\ M^{-1}\ \text{sec}^{-1}$ ($[Mo(CN)_8]^{4-}$) and $5.78 \times 10^8\ M^{-1}\ \text{sec}^{-1}$ ($[W(CN)_8]^{4-}$). This agreement is seen as good evidence that both cyano complexes react by the outer-sphere mode with permanganate. In addition, although not conclusively indicative of an outer-sphere mechanism, linear free-energy relationships between $\Delta G_{12}{}^0$ and $\Delta G_{12}{}^{\neq}$ values were also established (*40*) using the data of the above cyano complexes and those of $[Fe(CN)_6]^{4-}$ (*43*) or $[Fe(phen)_3]^{2+}$ (*44*).

The oxidation of manganate in alkaline solution is, from a mechanistic viewpoint, less complicated since no protonation, which led to the two-term rate law (*4*), is needed in this case. Kinetic results (*45*) for $[Mo(CN)_8]^{3-}$, $[W(CN)_8]^{3-}$, and $[Fe(CN)_6]^{3-}$ show the rate law to be of the form

$$\text{rate} = k[M(CN)_n{}^{3-}][MnO_4{}^{2-}]. \tag{7}$$

The second-order rate constants for the reaction

$$[M(CN)_n]^{3-} + [MnO_4]^{2-} \longrightarrow [M(CN)_n]^{4-} + [MnO_4]^{-} \tag{8}$$

are in good agreement with $k_{12}(\text{calc})$ according to Eq. (5). That the electron transfer in Eq. (8) proceeds by an outer-sphere mechanism is further illustrated in Fig. 5. The substitution of

$$\log K_{12} = n(\Delta E_{12}{}^0)/0.0591, \tag{9}$$

where n is the number of electrons in the balanced redox reaction and $\Delta E_{12}{}^0$ is the difference E^0(oxidant) $-$ E^0(reductant), in Eq. (5) to yield Eq. (10),

$$\log k_{12} = 0.5(\log k_{11} + \log k_{22} + \log f) + 8.46n(\Delta E^0), \tag{10}$$

predicts linear behavior in a plot of $\log k_{12}(\text{obsd})$ vs E^0(oxidant) using a constant reducing agent. The slope in Fig. 5 is $8.6\ V^{-1}$, which is in good agreement with the theoretical value.

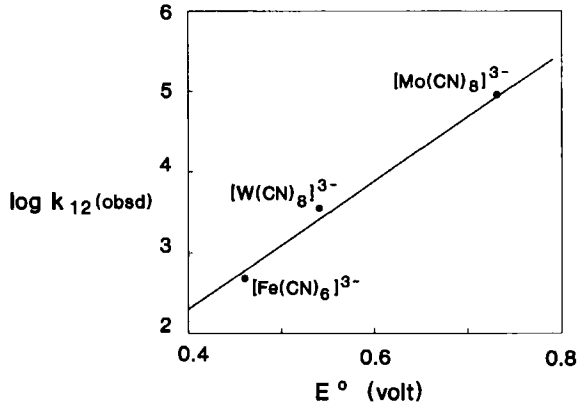

FIG. 5. Plot of log k_{12} (obs) against the reduction potential of the cyano complex (*45*).

Equation (10) is a useful tool to establish outer-sphere mechanisms in cases in which neither the reduction potential nor the self-exchange rate for one of the reactants is known. Such a case has been presented for the reduction of Ag(III) with $[Fe(CN)_6]^{4-}$, MnO_4^{2-}, $[W(CN)_8]^{4-}$, and $[Mo(CN)_8]^{4-}$ in strong alkaline solution (*46*). The reaction

$$[M(CN)_8]^{4-} + [Ag(OH)_4]^- \rightleftharpoons [M(CN)_8]^{3-} + \tfrac{1}{2}[Ag(II)]_2 \qquad (11)$$

goes to completion for tungsten, whereas an equilibrium ($K = 19\ M^{\frac{1}{2}}$ $mol^{-1/2}$, 25°C, $I = [OH^-] = 1.2\ M$) is maintained for a short time in the case of molybdenum. Reduction with the octacyanometalates, according to ESR spectra and stoichiometric measurements, does not proceed further than Ag(II), whereas the remaining stronger reductants give Ag(I)-containing species such as Ag_2O. The regeneration of $[Mo(CN)_8]^{4-}$ after several minutes from the product $[Mo(CN)_8]^{3-}$ in Eq. (11) is accompanied by a precipitated product containing little or no Ag(II). The reason for this is still uncertain but we may suggest that this is due to oxidation of hydroxide ions according to

$$4[Mo(CN)_8]^{3-} + 4OH^- \longrightarrow 4[Mo(CN)_8]^{4-} + O_2 + 2H_2O. \qquad (12)$$

This reaction, being first order in each of the reactant concentrations (*47*), is a hampering factor for studying redox kinetics with $[Mo(CN)_8]^{3-}$ in highly concentrated alkaline solutions.

The mechanism for the Ag(III) reduction, due to the uncertainties in the composition and reductive pathways of the dimer in Eq. (11), is complicated but the rate-determining step (Eq. 13)

$$\text{Ag(III)} + \text{reductant} \longrightarrow \text{Ag(II)} + \text{oxidant} \tag{13}$$

$$\text{Ag(II)} + \text{reductant} \longrightarrow \text{Ag(I)} + \text{oxidant} \tag{14}$$

$$2\text{Ag(II)} \longrightarrow [\text{Ag(II)}]_2 \tag{15}$$

is an established common factor for the above reductants. Application of Eq. (10) gave a linear free-energy relationship with a line slope of 8.9 V^{-1} in the log k_{12} vs $-E^0$(reductant) graph, implying an outer-sphere mechanism. If this is indeed so, it was estimated on the assumption that, if the potential of the $[Ag(OH)_4]^-$–$[Ag(OH)_4]^{2-}$ couple exceeds that of the $[MnO_4]^-$–$[MnO_4]^{2-}$ couple with at least 0.1 V and that $K > 10^3$ for Eq. (15), the redox potential for $Ag(OH)_4^-$ should be 0.7 V and that the self-exchange rate for this couple should be of the order $10–10^2\ M^{-1}\ sec^{-1}$. The above-mentioned equilibrium constant for Eq. (11) also allowed a formal potential estimate of 0.87 V ($[OH^-] = 1.2\ M$, 25°C) for

$$[\text{Ag(OH)}_4]^- + e^- \rightleftharpoons \tfrac{1}{2}[\text{Ag(II)}]_2. \tag{16}$$

b. Hydrazines. Oxidizing agents (1 eq) react with hydrazine to produce either N_2 and NH_3 or N_2 alone, whereas oxidants (2 eq) produce only N_2 as a nitrogen-containing product (*37, 48*). The afore-mentioned and latter pathways can be distinguished on the grounds of stoichiometric determinations being 2:1 and 4:1 for one-electron oxidant/hydrazine reactions. The cyano complexes of Fe(III), Mo(V), and W(V) all react in a 4:1 ratio so that the hydrazinium radical $N_2H_4^+$ (*49*) should be considered a reactive intermediate along the reaction pathway.

Kinetic studies on the oxidation of hydrazine by $[Fe(CN)_6]^{3-}$ in an alkaline water–methanol medium (*50*), in alkaline solution by $[Mo(CN)_8]^{3-}$ and $[W(CN)_8]^{3-}$ (*51*), and in conjunction with its methyl-substituted derivatives by the cyano complexes of Fe(III), Mo(V), and W(V) (*52*) showed that the conjugate base of Eq. (17)

$$\text{R'HNNH}_2\text{R}^+ \overset{K_a}{\rightleftharpoons} \text{R'HNNHR} + \text{H}^+ \tag{17}$$

$$\text{R'HNNHR} + \text{M(CN)}_n^{3-} \overset{k}{\longrightarrow} \text{R'HNNHR}^+ + [\text{M(CN)}_n]^{4-} \tag{18}$$

$$3[\text{M(CN)}_n]^{3-} + \text{R'HNNHR}^+ \overset{\text{fast}}{\longrightarrow} \text{N}_2 + \text{products}, \tag{19}$$

is the reactive species. This mechanism yields Eq. (20), which, on the approximation,

$$\text{rate} = [kK_a/([H^+] + K_a)][\text{hydrazine}]_T[M(CN)_n^{3-}], \quad (20)$$

that $[H^+] = 10^{-pH}$, was used to obtain acid dissociation constants, K_a, of 5.5×10^{-9} (hydrazine), 7.5×10^{-9} (methylhydrazine), and $1.8 \times 10^{-8} M^{-1}$ (1,2-dimethylhydrazine), all at 15°C and $\mu = 0.1$ M. Increased methyl substitution thus gives stronger acids. The cross-reaction rate constant k_{12} was also obtained in a pH region where $[H^+] \ll K_a$, and these, when plotted according to Eq. (10), gave the expected linear relationships with line slopes of 9.7, 8.6, and 8.0 V^{-1} for hydrazine, methylhydrazine, and 1,2-dimethylhydrazine, respectively. These values are again consistent with the theoretical slope of 8.46 V^{-1} according to the Marcus theory. On the assumption that the nuclear tunneling effect for substituted hydrazines would be fairly similar to that of hydrazine, especially considering the slow self-exchange rate constant of $\leq 3 \times 10^{-1} M^{-1}$ sec^{-1} (*53*) for the latter, it could also be assumed that the self-exchange rate constants for methyl- and 1,2-dimethylhydrazine will be of the same order. On this basis upper limits for the reduction potentials (vs NHE) of the redox couples $CH_3N_2H_3^+/CH_3N_2H_3$ and $CH_3HN_2HCH_3^+/CH_3HN_2HCH_3$ were determined (*52*) as ≤ 0.62 and ≤ 0.56 V, respectively compared with ≤ 0.73 V for the $N_2H_4^+/N_2H_4$ couple (*53*).

The Marcus relationship in Eq. (5) assumes that work terms required to bring the reactants together and separate the products are very similar or neglible so that they cancel out for the self-exchange and cross-exchange processes. This is not true for the above cyano complexes of Fe, Mo, and W since the large negative charges of these ions would result in large electrostatic work terms. Recasting the Marcus equation in terms of free energies of activation and work terms (Eq. (21)),

$$\Delta G_{12}^{\neq} - W_{12} = [(\Delta G_{11}^{\neq} - W_{11}) + (\Delta G_{22}^{\neq} - W_{22}) + (\Delta G_{12}^{0} - W_{12} + W_{21})(1 + \alpha)]/2, \quad (21)$$

where

$$\alpha = (\Delta G_{12}^{0} - W_{12} + W_{21})/4[(\Delta G_{11}^{\neq} - W_{11}) + (\Delta G_{22}^{\neq} - W_{22})], \quad (22)$$

a linear relationship between $\Delta G_{12}^{\neq} - \Delta G_{11}^{\neq}/2$ and

$$\underbrace{(\Delta G_{12}^{0} - W_{11} - W_{22} + W_{12} + W_{21})/2}_{\text{(A)}} + \underbrace{(\Delta G_{12}^{0} - W_{12} + W_{21})^2/8(\Delta G_{11}^{\neq} - W_{11} + \Delta G_{22}^{\neq} - W_{22})}_{\text{(B)}}$$

with unit slope and intercept $\Delta G_{22}^{\neq}/2$ is expected. Such a plot (Fig. 6) yielded $\Delta G_{22}^{\neq} \geq 15$ kcal and thus $k_{22} \leq 1.0\ M^{-1}\ \text{sec}^{-1}$ (*52*). This shows that the self-exchange rate constants for the above-mentioned hydrazines are indeed similar and comparable to the independently estimated value of $\leq 0.3\ M^{-1}\ \text{sec}^{-1}$ (*52*).

c. Organic Compounds. Extension of the Marcus theory to the oxidation of organic substrates by using substitution-inert one-electron metal–ion complexes offers the possibility of establishing the inner- or outer-sphere nature of the reaction as well as the determination of self-exchange rate constants and reduction potentials of a radical/ion pair. The systems studied so far involve different homologous series of organic compounds having acid–base equilibria, which in principle offers the possibility of two oxidizable species in solution. The kinetics and mechanism for the oxidation of benzenediols (*54*) and heteroaromatic diols (*55*) by $[Mo(CN)_8]^{3-}$ and a series of Fe(III) and Ir(IV) complexes have been studied in 1.0 M $HClO_4$. The oxidation takes place through two successive one-electron steps,

$$\text{Ox} + \text{H}_2\text{Y} \underset{k_{-1}}{\overset{k_1}{\rightleftharpoons}} \text{Red} + \text{radical} \tag{23}$$

$$\text{Ox} + \text{radical} \xrightarrow{k_2} \text{Red} + \text{Y}, \tag{24}$$

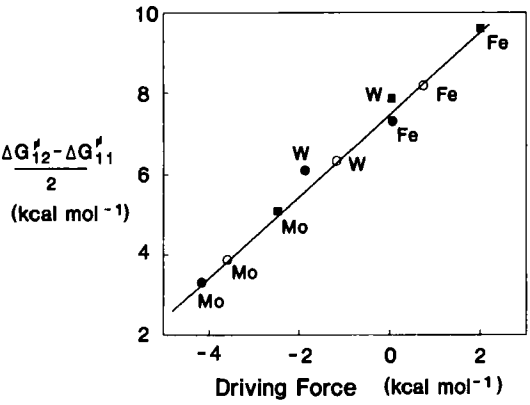

FIG. 6. Marcus relation: Free energies of activation as a function of the driving force (terms (A) + (B) in text) corrected for electrostatic work terms (cyano complexes' reaction with hydrazine (■); methylhydrazine (○); 1,2-dimethylhydrazine (●). Adapted with permission from Dennis *et al.* (*52*). Copyright 1987, American Chemical Society.

where the radical is a semiquinone intermediate. Application of the steady-state condition to the radical intermediate results in the rate equation being

$$-d[\mathrm{Ox}]/dt = 2k_1k_2[\mathrm{Ox}]^2[\mathrm{H_2Y}]/(k_{-1}[\mathrm{Red}] + k_2[\mathrm{Ox}]). \quad (25)$$

Experimental observations suggest $k_2[\mathrm{Ox}] \gg k_{-1}[\mathrm{Red}]$ so that $k_{\mathrm{obs}} = 2k_1$, i.e., simple second-order behavior with Eq. (23), the rate-determining step. Linear relationships, using Eq. (10), suggest that a simple electron abstraction from the diol to give the radical $\mathrm{H_2Y^{+\cdot}}$ operates in this rate-determining step. The Marcus equation (Eq. (21)), recasted in a more compressed form of

$$\Delta G_{12}^{\neq} = W_{12} + \lambda_{12}(1 + \Delta G_{12}^{0\prime}/\lambda_{12})^2/4, \quad (26)$$

predicts a relationship between the free energy of activation, $\Delta G_{12}^{\neq}$, and free energy change, $\Delta G_{12}^{0\prime}$. Here

$$k_{12} = 10^{11}\exp(-\Delta G_{12}^{\neq}/RT \quad (27)$$

$$\lambda_{12} = 2(\Delta G_{11}^{\neq} - W_{11} + \Delta G_{22}^{\neq} - W_{22}) \quad (28)$$

$$\Delta G_{12}^{0\prime} = \Delta G_{12}^{0} + W_{21} - W_{12}, \quad (29)$$

where $\Delta G_{11}^{\neq}$ and $\Delta G_{22}^{\neq}$ are the free energies of activation for the self-exchange reactions with related work terms W_{11} and W_{22}, whereas the work terms W_{12} and W_{21} are involved in bringing reactants and products together. The use of Eq. (26) to evaluate ΔG_{12}^{0} and thus E^0 for the radical/ion pairs in Eq. (23) is based on good judgment and evaluation of the work terms in Eqs. (28) and (29). In the above-mentioned cases for diol oxidations, the W_{12} term in Eq. (29) was taken as zero since uncharged benzenediols react with charged oxidants. This is also predicted by way of the Debye–Hückel expression (*56*)

$$W = z_1z_2e^2/Da(1 + \kappa a), \quad (30)$$

where z_1 and z_2 are the formal charges of the reactants, D is the absolute solvent dielectric, κ is the reciprocal ionic layer thickness, and a is the distance of closest approach. The W_{12} term was also neglected for the diols' oxidations since this involves bringing together more or less similarly charged complex ions with monopositive cation radicals (*54*). These two assumptions lead to $\Delta G_{12}^{0} = \Delta G_{12}^{0\prime}$ for a series of one-

electron oxidants. The work terms in Eq. (28) can be evaluated with the aid of Eq. (30). It was also found that different λ_{12} values hold for different oxidant complexes. For benzene and heteroaromatic diols this reorganizational parameter was estimated as 21 kcal mol^{-1} for $[Mo(CN)_8]^{3-}$ and 30 kcal mol^{-1} for $[Fe(CN)_6]^{3-}$. These values, if, for example, applied through Eqs. (26)–(29) for the reaction between $[Mo(CN)_8]^{3-}$ and $[Fe(CN)_6]^{4-}$ at a low ionic strength, gave excellent agreement between k_{12}(obs) and k_{12}(calc) values (*54*). The estimation of reduction potentials for the $H_2Y^{\cdot+}/H_2Y$ couples in heteroaromatic diols showed that 4,7-diols (A) can be more easily oxidized to the quinone form than the 5,6-diols (B):

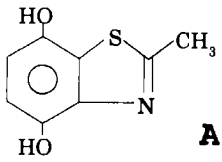

A

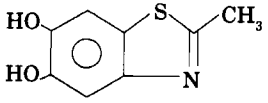

B

This is attributed to the loss of aromaticity of heteroaromatic nuclei in the quinoid form of the 5,6-derivatives relative to 4,7-derivatives (*55*).

The oxidation of ascorbic acid by $[Mo(CN)_8]^{3-}$ and a similar series of Fe(III) and Ir(IV) complexes used for the above-mentioned diols were found to be first order with respect to each of the oxidizing agents and ascorbic acid concentrations (*57*). The second-order rate constants increased with decreasing acidity, whereas addition of the reduced species of oxidizing agents showed no retarding effects. The acid dissociation constants of ascorbic acid were determined at different temperatures and ionic strengths. These, together with the acid-dependence study, suggest a mechanistic sequence of

$$H_2A \overset{K_a}{\rightleftharpoons} HA^- + H^+ \tag{31}$$

$$Ox + H_2A \xrightarrow{k_2} H_2A^{+\cdot} + Red \tag{32}$$

$$Ox + HA^- \xrightarrow{k_3} HA^{\cdot} + Red \tag{33}$$

$$Ox + radicals \xrightarrow{fast} A + Red + nH^+, \tag{34}$$

yielding a derived rate law of

$$-\tfrac{1}{2}d[Ox]/dt = (k_2 + k_3K_a[H^+]^{-1})[Ox][H_2A]. \tag{35}$$

The main contribution to the overall reaction rate comes from the ascorbate anion, HA^-, and although the contribution of the acid-independent path is not relevant for complexes with a low reduction potential, it becomes the more important one for those having higher reduction potentials. An assessment of the reduction potential of the $H_2A^{+\cdot}/H_2A$ couple was made on the assumption that if the electron self-exchange rates for this couple and that of the afore-mentioned benzene and heteroaromatic diols were the same, then the λ values that satisfy Eq. (26) should also hold in this case. On this basis $E^0(H_2A^{+\cdot}/H_2A) = 1.35$ V, which gives a fair agreement between k_2(obs) and k_2(calc) values using the Marcus theory, but it was also reasoned that a lower limit of $2 \times 10^6\ M^{-1}\ sec^{-1}$ for the self-exchange rate for this couple was too low compared with those of other organic substrates, which fall in a narrow range of 10^7–$10^9\ M^{-1}\ sec^{-1}$. Consequently, by lowering λ values with 2 kcal mol^{-1}, it could be shown that an upper limit of 1.40 V for the above couple was also appropriate in giving fair agreement between k_2(obs) and k_2(calc) values. In the case of the ascorbate anion, it was found that the value of $E°(HA^{\cdot}/HA^-)$ should lie in the range 0.85–1.00 V, and rate constants calculated from within this range agreed well with experimental ones, which were corrected beforehand for a diffusional contribution (*58*). The kinetics and mechanism for the oxidation of ascorbic acid by $[Fe(CN)_6]^{3-}$, $[W(CN)_8]^{3-}$, and $[Mo(CN)_8]^{3-}$ in a buffered acidic aqueous methanolic medium suggested a rate law similar to that in the above case (*59, 60*).

The kinetics of oxidation of dithiocarbamate anions to thiuram disulfides in 30% aqueous acetone by $[Mo(CN)_8]^{3-}$, $[W(CN)_8]^{3-}$, and 10 other substitution-inert metal complexes have also been investigated (*61*). Dithiocarbamates decompose in acid solution and oxidations were consequently performed only on the anionic forms in the pH range 9–12, at which no change in rate constants was observed. The only exception was that of thiophenol, which, upon reacting with $[Mo(CN)_8]^{3-}$, showed that the reaction rate contribution due to oxidation of the PhSH form was less than 0.002% that of PhS^-. All of the dithiocarbamates obeyed a simple second-order rate law,

$$-d[M_{ox}]/dt = k[M_{ox}][RS^-], \tag{35}$$

and the rates were greatly affected by the presence of significant amounts of reduced metal complexes.

The following mechanism was proposed:

$$M_{ox} + RS^- \underset{}{\overset{k_1,K_1}{\rightleftharpoons}} M_{red} + RS^{\cdot} \tag{36}$$

$$RS + RS^- \overset{k_2,K_2}{\rightleftharpoons} RSSR^{\cdot -} \tag{37}$$

$$M_{ox} + RSSR^{\cdot -} \overset{k_3,K_3}{\rightleftharpoons} M_{red} + RSSR. \tag{38}$$

If the first step of thio radical formation (Eq. 36) is rate-determining, then

$$\text{rate} = k_1[M_{ox}][RS^-], \tag{39}$$

and the observed second-order kinetics for all the reactions in the absence of metal-complex products, M_{red}, would be consistent with the initial outer-sphere electron transfer taking place during this interaction. However, if the dimerization step to the disulfide radical, Eq. (37), is rate-determining, then

$$\text{rate} = k_2K_1[M_{ox}][RS^-]^2/[M_{red}]. \tag{40}$$

A third possibility, in which a highly favorable outer-sphere oxidation of disulfide radical anions to neutral disulfides, Eq. (38), becomes rate-determining, will yield

$$\text{rate} = k_3K_1K_2[M_{ox}]^2[RS^-]^2/[M_{red}]. \tag{41}$$

Both Eqs. (40) and (41) contain a rate-inhibiting term in the form of M_{red} and it was stated that the rate law describing the $[Mo(CN)_8]^{3-}$/diethyldithiocarbamate reaction in dimethylsulfoxide in the presence of added $[Mo(CN)_8]^{4-}$ matched that of Eq. (41).

Since this study differs from the aforementioned ones in that the solvent medium became partly nonaqueous, redox potentials and electron self-exchange rate constants for metal complexes were unknown. The redox potentials were measured potentiometrically and showed in general a diminishing oxidizing power compared with that of a pure aqueous medium. The self-exchange rate constants for the metal complexes were derived from a least-squares optimization of the observed cross-reaction constants and their dependence on the exchange rate constants according to a rearranged form of Eq. (5),

$$\log[(k_{12})^2/(f_{12}K_{12})] = \log k_{11} + \log k_{22}. \tag{42}$$

Linear equations resulting from 19 cross-reactions were solved to find the best fit of k_{11} and k_{22} parameters. The k_{11} values (with reference to M_{ox}) does not differ much from the known values in aqueous solution.

Marcus theory showed a good correlation between experimental and calculated rate constants using Eq. (5). The k_{22} value was set at 10^7 M^{-1} sec^{-1} for this purpose and is considered as an upper limit for self-exchange of the diethyldithiocarbamate radical/anion pair. From the oxidation rates it was also estimated that $E^0(edtc^{\cdot}/edtc^-) = 0.43(3)V$ vs SCE. A free-energy analysis for the oxidation of diethyldithiocarbamate ($edtc^-$) by $[Fe(CN)_6]^{3-}$ also showed that the initial outer-sphere oxidation of the thiolate anion to its thio radical (Eq. 36) is the main energy barrier to be crossed along the reaction coordinate.

2. *Salt and Anionic Micellar Effects*

One of the main factors influencing the activation barrier in fast electron-transfer reactions is the change in the polarization of the immediate space surrounding the activated complex in solution. The more-well-known salt effects as well as the relatively new field of micellar effects can be used as mechanistic probes in this context. Since micelles have a hydrophobic as well as a hydrophilic part, this creates two different kinds of interfaces where electron transfer can occur if one of either the oxidant or reductant is contained or associated with these molecular aggregates. A futuristic approach could be that studies of this kind may serve as models for enzymatic reactions with complex bioaggregates such as membranes.

Studies so far have concentrated on the use of sodium dodecyl sulfate (SDS) as an anionic micelle because of its influence on fast electron-transfer reactions. A negatively charged metal complex, such as $[Mo(CN)_8]^{4-}$ or $[Fe(CN)_6]^{4-}$, will be electrostatically repelled, whereas positively charged ones, such as $[Os(dipy)_3]^{3+}$, may associate with the hydrophilic parts of the micelle. Neutral complexes such as $[Fe(phen)_2(CN)_2]$ may again be associated through hydrophobic forces of the micelle. Bruhn and Holzwarth (*62*) studied the kinetics of diffusion controlled outersphere electron-transfer reactions for the $[Os(dipy)_3]^{3+}/[Mo(CN)_8]^{4-}$, $[Os(dipy)_3]^{3+}/[Fe(CN)_6]^{4-}$, $[Os(dipy)_3]^{3+}/[IrCl_6]^{2-}$, $[Fe(phen)_2(CN)_2]^{2+}/[Fe(CN)_6]^{4-}$, $[Fe(phen)_2(CN)_2]/[Os(dipy)_3]^{3+}$, and $[Fe(phen)_2(CN)_2]/[IrCl_6]^{2-}$ redox pairs. Increasing concentrations of SDS progressively lowered the reaction rates up to the critical micelle concentration, where a sharp drop from 10^9–10^{10} to 10^6–10^7 M^{-1} sec^{-1} in rate constants occurred. From these and other data it was concluded that only cationic or uncharged metal complexes are attracted by the micelles and that the interaction of, for example, $[Os(dipy)_3]^{3+}$ was an electrostatic one that could be shielded from the micelle using high concentrations of NaCl. $[Fe(phen)_2(CN)_2]$, on the other hand, is taken

up in the hydrophobic core so that electron transfer to $[IrCl_6]^{2-}$ is governed by the equilibrium

$$Fe(II)_B + Ir(IV)_B \underset{k_{D(-mic)}}{\overset{k_{A(-mic)}}{\rightleftharpoons}} Fe(II)_{mic} + Ir(IV)_{mic}, \tag{43}$$

where $K_{Ass} = k_A/k_D = 2.5 \times 10^6 M^{-1}$, B is the bulk of solution, and mic is the micelle.

Electron-transfer studies using $[Ru(bpy)_3]^{3+}$ (*63*) and several substituted 1,10-phenanthroline complexes, $[FeL_3]^{3+}$ (*64*), with $[Mo(CN)_8]^{4-}$ in SDS solutions, resulted in the mechanism (B = bulk)

$$mic + Ox_B^{3+} \overset{K_1}{\rightleftharpoons} Ox_{mic}^{3+} \tag{44}$$

$$Ox_B^{3+} + \{Mo(CN)_8^{4-}\}_B \xrightarrow{k_w} \text{products} \tag{45}$$

$$Ox_{mic}^{3+} + \{Mo(CN)_8^{4-}\}_B \xrightarrow{k_{mic}} \text{products}. \tag{46}$$

If Eq. (44) is constantly equilibrated and k_{obs} is the observed second-order rate constant, then

$$k_{obs} = (k_w + k_{mic}K_1[mic])/(1 + K_1[mic]), \tag{47}$$

Since $K_1[mic] \gg 1$, a linear relationship,

$$k_{obs} = k_w K_1^{-1}[mic]^{-1} + k_{mic}, \tag{48}$$

is obtained. Experimental observations have ruled out any contributions from the k_w term in Eq. (48) so that electron transfer takes place at the micelle–water interface. The conclusion can thus be made that, when FeL_3^{3+} is imbedded in a negatively charged atmosphere, electrostatic repulsion with the negatively charged cyano complex will lead to the limiting diffusional constant of $3.2 \times 10^9 M^{-1}$ sec^{-1} becoming larger than the electron transfer rate constant.

Salt effects have been studied for a large number of electron-transfer reactions. The effect of extremely dilute salt solutions can in most cases be accounted for by the Debye–Hückel formalism, whereas explanations for more concentrated solutions vary. Among these are the associative nature of reactants and counterions as well as specific kinetic effects such as cation bridges between redox pairs to facilitate electron transfer.

Scherer and Willig (*65*) have studied the rate enhancement, due to cations and protons, of electron transfer from the surface of an organic insulator crystal, such as perylene, to oxidized ions, such as $[Fe(CN)_6]^{3-}$ and $[Mo(CN)_8]^{3-}$, in solution. In an electrochemical method such as this, the saturation current directly renders the rate constant for electron transfer at the crystal surface. Furthermore, electron transfer on $[Fe(CN)_6]^{3-}$ or $[Mo(CN)_8]^{3-}$ can be studied in the absence of reduced forms, whereas the salt effect can be measured up to the solubility limit. They found that for the same concentration of added electrolyte, rate constants increased with the increased charge of the cation. Up to $\leq 1\ M$ rate enhancement was of the order $Li^+ < Na^+ < Cs^+$ but at salt concentrations $>3.5\ M$ a reversal that could be explained by different hydrations of the cations took place. They also found a good linear correlation in the shift to higher redox potentials (simultaneously increasing rate constants) with higher salt concentrations.

The continuous-flow method with integrating observation (CFIMO) has been used to study the $[IrCl_6]^2$ $-[W(CN)_8]^{4-}$ reaction (*66*) with alkali metal chlorides as electrolytes. The cations exert an accelerating effect as they descend down the group, so much so that the reaction became diffusion controlled in 1 *M* CsCl. This was interpreted in terms of a promotion of the necessary polarized state in the outer coordination sphere of the reacting anions. In a later study (*67*) of reactions among $[Fe(CN)_6]^{4-}$, $[W(CN)_8]^4$, $[Ag(TPPS)]^{4-}$, and $[IrCl_6]^{2-}$, convincing evidence for electron-transfer catalysis by cations was found. Strong ion associations, such as those between H^+ and $[Fe(CN)_6]^{4-}$ and between di- and trivalent cations at high concentrations and the reactants, do not seem to be the determining factor for catalytic activity. It was felt that, although cations participate in the transition state, they should still be mobile enough to cause the catalytic rate enhancement. An interesting result was that a graphical correlation between observed second-order rate constants and the crystallographic radii of group IA, NH_4^+, $N(Me)_4^+$, $N(Et)_4^+$, and $N(But)_4^+$ cations showed that an optimum radius of 2.3 ± 0.2 Å for the monovalent cations caused the maximum rate enhancement possible, i.e., near the value of $10^{11}\ M^{-1}$ sec^{-1}. Three effects, acting in concert, are believed to be responsible for the catalytic influence of cations: first, they influence the water dipoles in the surrounding solution of the activated complex in such a way that their orientation is faster; second, they allow for a better adjustment of the ligand-to-central-metal bonds before electron transfer, and last, they promote interaction of the redox orbitals that are involved in the reaction so that transfer of charge is facilitated.

The rate of the reaction between $[Fe(CN)_6]^{4-}$ and $[W(CN)_8]^{3-}$ has been studied (*68*) at various ionic strengths for group I cations and the results have been processed with the extended Bronsted–Debye relationship

$$\log k = \log k_0 + 2\alpha Z_A Z_B \sqrt{\mu}/(1 + \beta a_i \sqrt{\mu}), \tag{49}$$

where β is a constant and a_i the distance of closest approach. Setting a_i at 5 or 8 Å did not alter the results to a moderate extent and it was concluded that Li^+ ions were absent in the activated complex but that an increasing number of up to three Cs^+ ions were participating upon descending in group I. It should, however, be kept in mind that positive salt effects such as that above indicate a reduction in the activation barrier but cannot separate the observed trends into rate constants relating to initial and transition state components (*69*). An illustrative example of this is to be found in the oxidation of I^- by $[Mo(CN)_8]^{3-}$ (*70*). The reaction mechanism was proposed as

$$[Mo(CN)_8]^{3-} + I^- \underset{k_{-1}}{\overset{k_1}{\rightleftharpoons}} [Mo(CN)_8]^{4-} + I \tag{50}$$

$$2I \xrightarrow{k_2} I_2 \tag{51}$$

$$I_2 + I^- \xrightarrow{\text{fast}} I_3^-, \tag{52}$$

with the initial k_1 step being rate-determining. Here it was found that a plot of log k_{obs} against $\sqrt{\mu}$, according to the now-extended form of Eq. (49), gave a positive slope of 3.06, in excellent agreement with the product of ionic charges for reactant species in Eq. (50). However, it could be equally well illustrated that a third-order rate expression of

$$-d[Mo(CN)_8{}^{3-}]/dt = k[Mo(CN)_8{}^{3-}][I^-][Na^+], \tag{53}$$

corresponding to the mechanism

$$[Mo(CN)_8]^{3-} + Na^+ \rightleftharpoons Na[Mo(CN)_8]^{2-} \tag{54}$$

$$Na[Mo(CN)_8]^{2-} + I^- \rightleftharpoons Na[Mo(CN)_8]^{3-} + I, \tag{55}$$

can also explain the experimental results. With $[W(CN)_8]^{3-}$, a weaker oxidant than $[Mo(CN)_8]^{3-}$, it was shown (*71*) that additional ion associa-

tion with I^- in preequilibrium must prevail,

$$M^+ + [W(CN)_8]^{3-} \rightleftharpoons M[W(CN)_8]^{2-} \quad (M^+ = Cs^+, Na^+) \tag{56}$$

$$M[W(CN)_8]^{2-} + I^- \rightleftharpoons IM[W(CN)_8]^{3-} \tag{57}$$

$$IM[W(CN)_8]^{3-} + I^- \longrightarrow M[W(CN)_8]^{3-} + I_2^- \tag{58}$$

$$I_2^- + M[W(CN)_8]^{2-} \xrightarrow{\text{fast}} M[W(CN)_8]^{3-} + I_2, \tag{59}$$

with Eq. (58) being rate-determining. Since there is no structural evidence that the inner coordination sphere of octacyano complexes can be enlarged, the proposed ion association in Eq. (57) must be preceded by equilibrium (56). Moreover, the same second-order dependence on $[I^-]$ was also found for the $[Fe(CN)_6]^{3-}/I^-$ reaction (*72*). The difference in order with respect to $[I^-]$ for $[Mo(CN)_8]^{3-}$ and $[W(CN)_8]^{3-}$ seems to reside in Eq. (55), in which the larger driving force for electron transfer in the case of $[Mo(CN)_8]^{3-}$ does not necessitate additional association of an iodide ion.

The kinetics and salt effects for the oxidation of octacyanomolybdate(IV) (*69, 73, 74*) and octacyanotungstate(IV) (*75, 76*) by peroxydisulphate ions have been studied extensively. These reactions are first order with respect to $[S_2O_8^{2-}]$, $[M(CN)_8^{4-}]$, and alkali metal ion concentrations. The alkali metal ion rate enhancement follows the order $Li^+ < Na^+ < K^+ < Rb^+ < Cs^+$ with an increase by a factor of 17 between Li^+ and Cs^+ for the case of $[Mo(CN)_8]^{4-}$ at 40°C. It is still not clear how the first-order dependence in alkali metal ion concentrations should function in a mechanism (*74*). The magnitude for the association constants in equilibria, such as

$$K^+ + S_2O_8^{2-} \rightleftharpoons KS_2O_8^- \quad K = 3.3\,M^{-1}\,(77) \tag{60}$$

$$K^+ + Mo(CN)_8^{4-} \rightleftharpoons K[Mo(CN)_8]^{3-}, \tag{61}$$

predicts that at high concentrations of alkali metal ions a leveling effect should be observed so that the reaction will not be first order in $[M^+]$ at all concentrations. A more recent analysis (*69*) for concentrated salt solutions up to 6 *M* strength confirmed that ion pairs play a key role in determining reactivities in these systems. Rate data, which indicated a positive salt effect, were analyzed for hydration effects of added salts on the ion-pair reactions. It was concluded that solvation effects operate on the initial association of reactants rather than on the actual electron-transfer step. In conjunction with preequilibria

(Eqs. (60) and (61)), the rate-determining step can for the time being be presented as

$$KS_2O_8^- + K[Mo(CN)_8]^{3-} \longrightarrow [Mo(CN)_8]^{4-} + 2K^+ + SO_4^{2-} + SO_4^{\cdot-} \quad (62)$$

followed by a subsequent fast reaction,

$$K[Mo(CN)_8]^{3-} + SO_4^{\cdot-} \longrightarrow [Mo(CN)_8]^{4-} + SO_4^{2-} + K^+. \quad (63)$$

The formulation of $[M(CN)_8(SO_4)]^{5-}$, being the suggested (*76*) product in Eq. (62), can be discarded for reasons mentioned above in the oxidation of iodide ions.

The kinetics of the reduction of octacyanomolybdate(V) and —tungstate(V) by sulfite ions has been studied over a wide pH range (*78*). A first-order dependency on the alkali metal ion concentration (Fig. 7), which is similar to that of peroxydisulphate, has been established. The following mechanism was proposed:

$$HSO_3^- \overset{K_a}{\rightleftharpoons} SO_3^{2-} + H^+ \quad (64)$$

$$Cat^+ + [M(CN)_8]^{3-} \overset{K_2}{\rightleftharpoons} [(NC)_7MCN{:}Cat]^{2-} \quad (65)$$

$$[(NC)_7MCN{:}Cat]^{2-} + SO_3^{2-} \overset{K_3}{\rightleftharpoons} [(NC)_7MCN{:}Cat{:}SO_3]^{4-} \quad (66)$$

$$[(NC)_7MCN{:}Cat{:}SO_3]^{4-} \overset{k_1}{\longrightarrow} [M(CN)_8]^{4-} + SO_3^{\cdot-} + Cat^+ \quad (67)$$

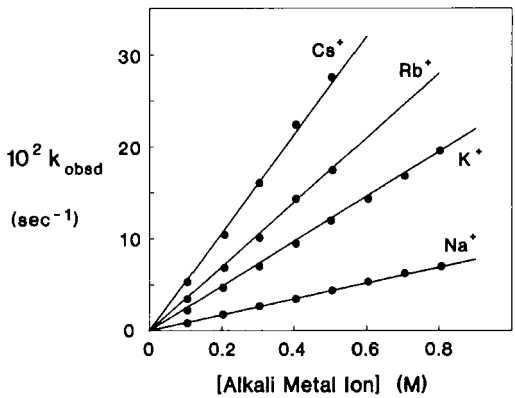

FIG. 7. Alkali metal ion catalysis for the $[W(CN)_8]^{3-}$—SO_3^{2-} reaction in alkaline solution. Reprinted from Dennis *et al.* (*78*). Copyright 1983, Pergamon Press Ltd.

$$[M(CN)_8]^{3-} + HSO_3^- \overset{K_4}{\rightleftharpoons} (NC)_7MCN{:}H{:}SO_3]^{4-} \quad (68)$$

$$[(NC)_7MCN{:}H{:}SO_3]^{4-} \xrightarrow{k_2} [M(CN)_8]^{4-} + SO_3^- + H^+ \quad (69)$$

$$[M(CN)_8]^{3-} + SO_3^- \xrightarrow{\text{fast}} [M(CN)_8]^{4-} + SO_4^{2-}. \quad (70)$$

This mechanism, in which Eqs. (67) and (69) are rate-determining, corresponds to the following rate law:

$$\text{rate} = \{(k_1K_aK_2K_3[Cat^+] + k_2K_4[H^+])/(K_a + [H^+])\}[SO_3^{2-}]_T[M(CN)_8^{3-}]. \quad (71)$$

Equation (65) represents the contact ion-pair formation between complex cyanide and alkali metal ions and Eq. (66) the bridging of the lone pair on $:SO_3^{2-}$ with the cation of the contact ion pair. Isomer I is the dominant form of SO_3^{2-} in aqueous medium (*79*)

$$:SO_3^{2-} + H^+ \rightleftharpoons \underset{\text{I}}{H{:}SO_3^-} \rightleftharpoons \underset{\text{II}}{HO\ddot{S}O_2^-} \quad (72)$$

so that the hydrogen bond formation between HSO_3^- and $[M(CN)_8]^{3-}$ (Eq. (68)) could explain the absence of any alkali metal ion catalysis in acidic solution. The formation of a contact ion-pair complex containing both the oxidant and the reductant as well as the alkali metal ion mediator in Eq. (66), is in principle the same as that proposed for the $[W(CN)_8]^{3-}/I^-$ reaction in Eq. (57). This type of interaction is more specific than that defined by an association equilibrium constant, which is a thermodynamic quantity. It is expected that the product of Eq. (65) could be a close Coulombic interaction between two to three nitrogen atoms of neighboring cyano ligands and the alkali metal ion—a situation that resembles that in the more ordered solid state as was evidenced in crystal structure determinations of octacyano complexes. A linear relationship, using Eq. (10) with rate constants of this study and those of $[Fe(CN)_6]^{3-}$ (*80*), also supports the possibility that an outer-sphere mechanism is operative for these sulfite oxidations.

3. Hydroxylamine, Nitrite, and Arsenite

Hydroxylamine can be oxidized to various products (*48*). Oxidation by $[Fe(CN)_6]^{3-}$ in a weak acidic medium (*81*) proceeds via the NH_2O radical to N_2, and it has been found that traces of Fe(II) or Cu(II) catalyze the reaction (*82*). The kinetics for oxidation by $[Mo(CN)_8]^{3-}$ at pH 1–2 showed a first-order dependence on $[H^+]$ and a negative salt

effect (*83*). Dinitrogen was identified as a reaction product. Oxidation by $[W(CN)_8]^{3-}$ over a wide pH range (Fig. 8) showed that three reactive species, i.e., NH_3OH^+, NH_2OH, and NH_2O^-, are involved (*84*).

From the mechanism

$$NH_3OH^+ + [W(CN)_8]^{3-} \underset{k_{-1}}{\overset{k_1}{\rightleftharpoons}} [W(CN)_8]^{4-} + NH_2O^{\cdot} + 2H^+ \qquad (73)$$

$$\Updownarrow K_{a1}$$

$$NH_2OH + [W(CN)_8]^{3-} \underset{k_{-2}}{\overset{k_2}{\rightleftharpoons}} [W(CN)_8]^{4-} + NH_2O^{\cdot} + H^+ \qquad (74)$$

$$\Updownarrow K_{a2}$$

$$NH_2O^- + [W(CN)_8]^{3-} \xrightarrow{k_3} [W(CN)_8]^{4-} + \tfrac{1}{2}N_2 + H_2O \qquad (75)$$

with the rate law

$$\text{rate} = \{(k_1[H^+]^2 + k_2K_{a1}[H^+] + k_3K_{a1}K_{a2})/([H^+]^2 + K_{a1}[H^+] + K_{a1}K_{a2})\}[NH_3OH^+]_T[W(V)], \qquad (76)$$

where $[W(V)] = [W(CN)_8^{3-}]$, it was established that the relative ordering of $k_1:k_2:k_3 = 1:6\times10^2:4\times10^6$ and that $pK_{a1} = 5.6$ and $pK_{a2} = 13.5$. The $NH_2O^{\cdot}$ radicals in Eqs. (73) and (74) decompose to N_2.

The preparative procedure (*85*) for $Cs_3[M(CN)_8]\cdot2H_2O$ complexes, which make use of HNO_3 as an oxidizing agent, was found to give variable yields depending on the sample of concentrated nitric acid

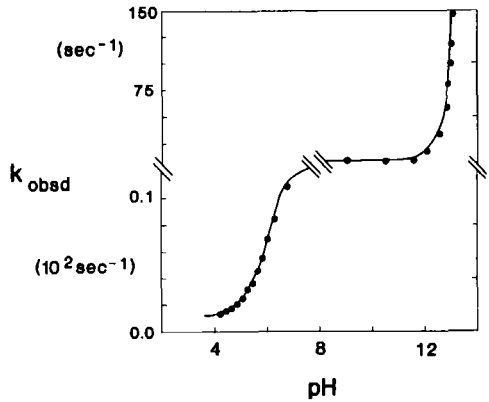

FIG. 8. pH profile for the oxidation of hydroxylamine by $[W(CN)_8]^{3-}$ ions. Reprinted from van Wyk *et al.* (*84*). Copyright 1987, Pergamon Press Ltd.

employed. Suspecting that aging and daylight exposure, which result in nitrous acid, could be the reason for variable yields, the procedure was reinvestigated using sodium nitrite as an oxidizing agent. This modified method gives excellent results (*86*). A kinetic study (*87*) on the oxidation of $[W(CN)_8]^{4-}$ by nitrite ions in perchloric acid medium (pH 0.2–2.0) revealed that reaction rates increased at higher acid concentrations and that only the protonated form of an acid–base equilibrium was reactive. Since the pK_a (3.37) of HNO_2 fall outside the active pH range of the above-mentioned equilibrium, it was proposed that $H[W(CN)_8]^{3-}$ is the active reducing agent. The mechanism

$$[W(CN)_8]^{4-} + H^+ \overset{K_4}{\rightleftharpoons} H[W(CN)_8]^{3-} \tag{77}$$

$$H[W(CN)_8]^{3-} + HNO_2 \xrightarrow{k} [W(CN)_8]^{3-} + NO + H_2O \tag{78}$$

gives a derived rate law

$$\text{rate} = \{kK_4[H^+]/(1 + K_4[H^+]\}][W(CN)_8{}^{4-}][HNO_2], \tag{79}$$

with $k = (3.1 \pm 0.1) \times 10^4\ M^{-1}\ \text{sec}^{-1}$ and $pK_{a4} = 1.39$ at zero ionic strength for $H_4[W(CN)_8]$. This is one of the rare examples in which a protonated form of an octacyano complex is an active participant in a reaction. This mechanistic study also stresses the need for relatively high acid concentrations in the preparative procedure for $Cs_3[M(CN)_8] \cdot 2H_2O$ complexes.

The kinetics and mechanism for the oxidation of As(III) by $[Mo(CN)_8]^{3-}$ (*88*) and $[W(CN)_8]^{3-}$ (*89*) in alkaline medium showed a first-order dependence on $[OH^-]$ and alkali metal ion concentrations, respectively. The hdyroxide dependence is related to the tribasic character of $As(OH)_3$ and, depending on the alkalinity range of the investigation, will determine which active As(III) species in Eqs. (80–81) will function in the mechanism.

$$As(OH)_3 + OH^- \overset{K_1}{\rightleftharpoons} AsO(OH)_2{}^- + H_2O \tag{80}$$

$$AsO(OH)_2{}^- + OH^- \overset{K_2}{\rightleftharpoons} AsO_2(OH)^{2-} + H_2O \tag{81}$$

$[Mo(CN)_8]^{3-}$ gives a measurable reaction rate at pH 9.0 and $[W(CN)_8]^{3-}$ at 0.05 *M* NaOH so that $AsO(OH)_2{}^-$ and $AsO_2(OH)^{2-}$ will be the respective active As(III) species. The rate-determining step for both cyano complexes can be presented by

$$A[M(CN)_8]^{2-} + As(III) \longrightarrow [M(CN)_8]^{4-} + As(IV) + A^+ \quad (82)$$

followed by

$$A[M(CN)_8]^{2-} + As(IV) \xrightarrow{fast} [M(CN)_8]^{4-} + As(V) + A^+, \quad (83)$$

where A^+ is the alkali metal ions and arsenate is the As(V) product. The first-order dependence in $[A^+]$ for $[W(CN)_8]^{3-}$ is accompanied by only 8% variation in reaction rate constants due to ionic strength effects and thus supports the specific salt effects for Na^+, K^+, Rb^+, and Cs^+ ions observed in this case.

4. Oxyanions of Groups VIB and VIIB

The oxidation of thiosulfate ions by mild oxidizing agents such as iodine and Fe(III) yields tetrathionate ions in neutral aqueous medium. Stronger oxidizing agents such as bromine yield sulfate, whereas hydrogen peroxide gives a mixture of the two products. In alkaline solution iodine produces some sulfate ions and the ratio of sulfate to tetrathionate increases with increasing pH of the solution. This suggests that the oxidation product of thiosulfate is determined in part by the reduction potential of the oxidizing agent and also by the pH of the reaction medium.

The kinetics of the reaction between thiosulfate and $[Mo(CN)_8]^{3-}$ (*90*) as well as $[W(CN)_8]^{3-}$ ions (*91*) have been studied at pH 4–5 and produced different rate laws,

$$\text{rate} = k[Mo(CN)_8^{3-}][S_2O_3^{2-}][Cat^+] \quad (84)$$

and

$$\text{rate} = k[H^+][S_2O_3^{2-}]^2. \quad (85)$$

It is interesting that the specific alkali metal ion catalysis in Eq. (84) is also accompanied by first-order dependence on $[M(CN)_8^{3-}]$, which suggests that this catalysis phenomenon should be ascribed to the presence of an octacyano complex rather than ion association between alkali metal and thiosulfate ions. In the case of $[Mo(CN)_8]^{3-}$, the rate-determining step, Eq. (86), is followed by a fast radical dimerization,

$$(Cat)[Mo(CN)_8]^{2-} + S_2O_3^{2-} \longrightarrow (Cat)[Mo(CN)_8]^{3-} + S_2O_3^{-} \quad (86)$$

$$2S_2O_3^{-} \xrightarrow{fast} S_4O_6^{2-}, \quad (87)$$

where the electron-transfer step involves a bridged activated complex, $[Mo(CN)_8^{3-} \cdots Cat^+ \cdots S_2O_3^{2-}]^{\neq}$. It was found that Cs^+ ions were about six times more effective than Na^+ ions in catalyzing the reaction.

Reproducible zero-order reaction rates for the $[W(CN)_8]^{3-}/S_2O_3^{2-}$ reaction could be obtained only upon addition of Na_2EDTA, which is similar to that of the $[Fe(CN)_6]^{3-}/S_2O_3^{2-}$ reaction (*92*), where an additional term in the rate law,

$$\text{rate} = k[H^+][S_2O_3^{2-}]^2 + k'[H^+][S_2O_3^{2-}]^2[Cat^+], \tag{88}$$

was ascribed to alkali metal ion catalysis. This shows that alkali metal ion association or participation in the activated complex, involving thiosulfate ions, do occur but that the contribution of this term to total reaction rates is negligible in the case of stronger oxidizing agents such as $Mo(CN)_8^{3-}$. The zero-order dependence on $[W(CN)_8^{3-}]$ in Eq. (85) originates from the equilibrium

$$S_2O_3^{2-} + H^+ \rightleftharpoons HS_2O_3^-, \tag{89}$$

followed by two comparable rate-determining steps (*93*),

$$HS_2O_3^- + S_2O_3^{2-} \underset{k_{-1}}{\overset{k_1}{\rightleftharpoons}} [HS_2O_3 \cdot S_2O_3]^{3-} \tag{90}$$

$$[HS_2O_3 \cdot S_2O_3]^{3-} \xrightarrow{k_2} HSO_3^- + SO_3^{2-} + 2S. \tag{91}$$

The fact that the experimental rate constant of 0.5 M^{-2} sec^{-1}, representing Eqs. (89) to (91), agrees well with those of $[Fe(CN)_6]^{3-}$ (0.6 M^{-2} sec^{-1}) and $[W(CN)_8]^{3-}$ (0.3 M^{-2} sec^{-1}) is taken as good evidence that the same rate-determining steps are involved. For $[W(CN)_8]^{3-}$, the product of Eq. (90) is followed by a series of fast reactions.

$$[HS_2O_3 \cdot S_2O_3]^{3-} + 2[W(CN)_8]^{3-} \xrightarrow{\text{fast}} S_4O_6^{2-} + 2[W(CN)_8]^{4-}, \tag{92}$$

where tetrathionate production was verified experimentally.

Contrary to the facile oxidation of sulfite ions, that of selenite and tellurite ions by octacyano complexes do not proceed at all except if a catalyst such as OsO_4 is employed. The kinetics for the Os(VIII)-catalyzed oxidation of SeO_3^{2-} (*94*) and TeO_3^{2-} (*95*) ions by octacyanotungstate(V) and -molybdate(V) ions in alkaline medium has thus been studied. The experimental rate laws are the same and show first-order

dependencies on $[M(CN)_8^{3-}]$, [Os(VIII)], and $[OH^-]$. The proposed mechanism comprises the following steps:

$$OsO_4 + OH^- \overset{K}{\rightleftharpoons} HOsO_5^- \tag{93}$$

$$HOsO_5^- + [M(CN)_8]^{3-} \underset{k_{-2}}{\overset{k_2}{\rightleftharpoons}} \text{complex} \tag{94}$$

$$\text{complex} + E(IV) \underset{k_{-3}}{\overset{k_3}{\rightleftharpoons}} E(V) + [M(CN)_8]^{4-} + HOsO_5^- \tag{95}$$

$$E(V) + [M(CN)_8]^{3-} \xrightarrow{k_4} E(VI) + [M(CN)_8]^{4-}. \tag{96}$$

Equation (94) is the rate-determining step and the formation of this complex has been reported before (*96*). E(IV) represents Se(IV) or Te(IV). The interaction between two negatively charged ions in Eq. (94) is in accord with the observed positive salt effect. The equilibrium constant in Eq. (93) was found to vary between 299 and 302 M^{-1}. Se(IV) reacts much faster than Te(IV), the difference in observed second-order rate constants being three orders of magnitude for Mo(V) and a factor of 300 for W(V).

The oxidation of $[W(CN)_8]^{4-}$ by periodate in neutral and weak basic media is of the first order with respect to both reagents, and a specific cation effect of $Li^+ < Na^+ < K^+ < Rb^+ Cs^+ \ll Mg^{2+}$ was observed (*97*). At pH 7–8, an acid-independant term as well as one that is first order in $[H^+]$ is contributing to second-order rate constants. This linear dependence does not hold below pH 7. Considering the following equilibria,

$$H^+ + H_4IO_6^- \overset{K_1}{\rightleftharpoons} H_5IO_6 \tag{97}$$

$$2H_2O + IO_4^- \overset{K_2}{\rightleftharpoons} H_4IO_6^- \tag{98}$$

$$H^+ + H_3IO_6^{2-} \overset{K_3}{\rightleftharpoons} H_4IO_6^-, \tag{99}$$

as well as the pH range of study, the following rate-determining steps were suggested:

$$[W(CN)_8]^{4-} + IO_4^- \xrightarrow{k_4} [W(CN)_8]^{3-} + IO_4^{2-} \tag{100}$$

$$[W(CN)_8]^{4-} + H_4IO_6^- \xrightarrow{k_5} [W(CN)_8]^{3-} + H_4IO_6^{2-} \tag{101}$$

$$[W(CN)_8]^{4-} + H_3IO_6^{2-} \xrightarrow{k_6} [W(CN)_8]^{3-} + H_3IO_6^{3-}. \quad (102)$$

The I(VI) species formed in Eqs. (100)–(102) react in fast steps to produce IO_3^-, which is unreactive toward further reduction.

At higher acid concentration (pH 0.65–1.55), the mechanism, with regard to the number of possible I(VII) reactive species, becomes less complicated as was put forward for the case of $[Mo(CN)_8]^{4-}$ oxidation (*98*). The observed rate law,

$$d[Mo(CN)_8^{3-}]/dt = 2k[Mo(CN)_8^{3-}][IO_4^-][H^+], \quad (103)$$

does not contain an independent $[H^+]$ term as was observed for $[W(CN)_8]^{4-}$ and $[Fe(CN)_6]^{4-}$ (*99*).

The proposed mechanism, which considers only Eq. (97) as pertaining to IO_4^-, comprises the following additional steps:

$$[Mo(CN)_8]^{4-} + H^+ \overset{K_2}{\rightleftharpoons} H[Mo(CN)_8]^{3-} \quad (104)$$

$$H[Mo(CN)_8]^{3-} + H_5IO_6 \xrightarrow{k} [Mo(CN)_8]^{3-} + I(VI) \quad (105)$$

$$[Mo(CN)_8]^{4-} + I(VI) \xrightarrow{\text{fast}} [Mo(CN)_8]^{3-} + IO_3^-. \quad (106)$$

The derived rate law

$$d[Mo(CN)_8^{3-}]/dt = 2kK_1K_2[Mo(CN)_8^{3-}][IO_4^-][H^+]^2/(1 + K_1[H^+]) \quad (107)$$

will be identical to that in Eq. (103) provided $K_1[H^+] \gg 1$ ($K_1 = 1.8 \times 10^3\ M^{-1}$) and the protonation equilibrium (97) exists. The latter is not unrealistic considering the results of nitrite oxidation (*vide supra*). It was also suggested, by way of lack of any direct evidence, that the inner-sphere oxidative behavior of IO_4^- should also be applicable for $[Mo(CN)_8]^{4-}$, in which a bridged cyano ligand could interact through substitution with the inner coordination sphere of a labile I(VII).

The kinetics of the $[Mo(CN)_8]^{4-}/IO_4^-$ reaction was also studied in ethanol/water mixtures up to 62 wt% alcohol and pH 1.65, using HNO_3 as acid source (*100*). The reaction rate increases gradually, passing over a maximum at around 43 wt% alcohol, and thereafter decreases with increasing alcohol content. These changes were also reflected in the activation parameters: $\Delta G^{\neq}$ remains fairly constant but a substan-

tial increase in $-\Delta S^{\neq}$ was accompanied by a decrease in $\Delta H^{\neq}$ up to the 43 wt% level.

The opposite trend was observed at higher alcohol levels. Since solvents also make an important contribution to the activated state, their changes in structural effects must be contained in these entropy and enthalpy changes. Since nonpolar solvents, or in this case an increasingly more nonpolar reaction medium, will be relatively more unoriented, it is to be expected that reactions in such media will have a large negative entropy of activation. The proposed mechanism differs from the above-mentioned aqueous acidic oxidation in that appreciable amounts of H_5IO_6 (Eq. (97)) are not formed in water/alcohol mixtures so that $H_4IO_6^-$ is the only reactive species. In addition, the protonation of the organic solvent molecule, S, should be taken into account, and it was shown that ratios of [alcohol]/[H_2O] and [H_2O]/[alcohol] were the main contributors to reaction rates in the 43–62 and 0–43 wt% levels, respectively.

The proposed mechanism is as follows:

$$H_3O^+ + S \overset{K_1}{\rightleftharpoons} SH^+ + H_2O \tag{108}$$

$$[Mo(CN)_8]^{4-} + H_3O^+ \underset{k_{-1}}{\overset{k_1}{\rightleftharpoons}} H[Mo(CN)_8]^{3-} + H_2O \tag{109}$$

$$[Mo(CN)_8]^{4-} + SH^+ \underset{k_{-2}}{\overset{k_2}{\rightleftharpoons}} H[Mo(CN)_8]^{3-} + S \tag{110}$$

$$H[Mo(CN)_8]^{3-} + H_4IO_6^- \xrightarrow{k_3} [Mo(CN)_8]^{3-} + I(VI) \tag{111}$$

$$[Mo(CN)_8]^{4-} + I(VI) \xrightarrow{\text{fast}} [Mo(CN)_8]^{3-} + IO_3^-. \tag{112}$$

Equation (111) is the rate-determining step, and upon application of the steady-state principle to $H[Mo(CN)_8]^{3-}$, assuming $[acid]_T = [H_3O^+] + [SH^+]$ and assuming $[H_4IO_6^-]$ and $[acid]_T$ is constant, it was shown that the pseudo-first-order rate constant observed during solvent composition variation will be given by

$$k_{obs} = A\{k_4/(1 + K_1[S]/[H_2O]) + k_4'/(1 + [H_2O]/K_1[S])\}, \tag{113}$$

where $A = 2k_3[H_4IO_6^-][acid]_T$. The dominance of the two terms containing [S] in Eq. (113) was verified experimentally such that when

$k_2/k_1 = 6$ the reaction is mainly SH^+ catalyzed and when $k_1/k_2 = 5.67$ it is mainly H_3O^+ catalyzed.

The oxidation of $[W(CN)_8]^{4-}$ by bromate ions in perchloric acid solution (*101*) was found to be partially autocatalytic due to the following reactions:

$$BrO_3^- + 5Br^- + 6H^+ \longrightarrow 3Br_2 + 3H_2O \tag{114}$$

$$[W(CN)_8]^{4-} + \tfrac{1}{2}Br_2 \longrightarrow [W(CN)_8]^{3-} + Br^-. \tag{115}$$

The autocatalysis originates when BrO_3^- is taken in excess of $[W(CN)_8]^{4-}$ as follows:

$$5[W(CN)_8]^{4-} + BrO_3^- + 6H^+ \longrightarrow 5[W(CN)_8]^{3-} + \tfrac{1}{2}Br_2 + 3H_2O. \tag{116}$$

The rate constant for Eq. (115) has been determined as 0.4 M^{-1} sec^{-1} at 25°C.

The experimental rate law was determined as

$$-d[W(CN)_8^{4-}]/dt = 6(k_0 + k_1[H^+]^2)[BrO_3^-][W(CN)_8^{4-}], \tag{117}$$

with $k_0 = 1.5 \times 10^{-3}$ M^{-1} sec^{-1} and $k_1 = 9.6 \times 10^{-2}$ M^{-2} sec^{-1} at 25°C and I = 0.5 M. The kinetics does not differ much from that of the $[Fe(CN)_6]^{4-}/BrO_3^-$ reaction (*102*), and the mechanism can be presented as

$$BrO_3^- + 2H^+ \overset{K_1}{\rightleftharpoons} H_2BrO_3^+ \tag{118}$$

$$BrO_3^- + [W(CN)_8]^{4-} \xrightarrow{k_0} [W(CN)_8]^{3-} + Br(IV) \tag{119}$$

$$H_2BrO_3^+ + [W(CN)_8]^{4-} \xrightarrow{k_1} [W(CN)_8]^{3-} + Br(IV) + H_2O \tag{120}$$

$$4[W(CN)_8]^{4-} + Br(IV) \xrightarrow{\text{fast}} 4[W(CN)_8]^{3-} + \tfrac{1}{2}Br_2 + 2H_2O. \tag{121}$$

5. Reactions with Radicals

Faraggi (*103*) studied the oxidation of oxygen-saturated solutions of $[Mo(CN)_8]^{4-}$ at different pH values using steady-state and pulse radiolysis techniques. The rate constants for the reaction

$$[Mo(CN)_8]^{4-} + OH \longrightarrow [Mo(CN)_8]^{3-} + OH^- \tag{122}$$

have been measured in the range $10^{-5} < [HClO_4] < 1$ M and in the

presence of different concentrations of alkali metal perchlorates. No meaningful change in the value of $5.8 \times 10^9\ M^{-1}\ \text{sec}^{-1}$ could be observed in contrast to $[Fe(CN)_6]^{4-}$, in which protonation as well as ion association resulted in meaningful changes (*104*). The irradiation of high-acid solutions of $[Mo(CN)_8]^{4-}$ showed that, aside from the $OH^{\cdot}$ radical, perhydroxyl ($HO_2^{\cdot}$) radicals, produced via the $H + O_2$ reaction, also participated, the reaction being

$$[Mo(CN)_8]^{4-} + HO_2^{\cdot} \xrightarrow{H^+} [Mo(CN)_8]^{3-} + H_2O_2. \tag{123}$$

The peroxy radicals has a pK_a of 4.88 according to

$$HO_2^{\cdot} \rightleftharpoons O_2^{-} + H^+, \tag{124}$$

and, in order to determine the rate constant for Eq. (123), the irradiations were performed at pH 2.5–4.0 to prevent formation of the peroxy radical, $O_2^{\cdot-}$. In addition, a high concentration (0.3 *M*) of formate was used to scavenge $OH^{\cdot}$ radicals according to

$$OH^{\cdot} + HCOO^{-} \longrightarrow CO_2^{\cdot-} + H_2O, \tag{125}$$

after which $CO_2^{\cdot-}$ radicals react with oxygen,

$$CO_2^{\cdot-} + O_2 \longrightarrow O_2^{\cdot-} + CO_2, \tag{126}$$

both reactions having rate constants in the order of $10^9\ M^{-1}\ \text{sec}^{-1}$. The peroxy radical is unreactive toward $[Mo(CN)_8]^{4-}$. In this way it was possible to determine a rate constant of $6 \times 10^4\ M^{-1}\ \text{sec}^{-1}$ for Eq. (123). It was also found that the $O_2^{\cdot-}$ radical, which is relatively stable is weak alkaline solutions, reduces $[Mo(CN)_8]^{3-}$ according to

$$[Mo(CN)_8]^{3-} + O_2^{\cdot-} \longrightarrow [Mo(CN)_8]^{4-} + O_2, \tag{127}$$

with the rate constant being $3 \times 10^5\ M^{-1}\ \text{sec}^{-1}$.

The activation energies for the oxidation of $[Fe(CN)_6]^{4-}$, $[W(CN)_8]^{4-}$, and $[Mo(CN)_8]^{4-}$ by radicals such as $Cl_2^{\cdot-}$, $Br_2^{\cdot-}$, $I_2^{\cdot-}$, $(SCN)_2^{\cdot-}$, and $N_3^{\cdot}$ were found to decrease with the increasing exothermicity of the reaction (*105*). This is in line with an outer-sphere electron-transfer mechanism. The reactivity order for the three metal complexes is $[Mo(CN)_8]^{4-} < [Fe(CN)_6]^{4-} < [W(CN)_8]^{4-}$, which is not the trend expected for the last two if the order of reduction potentials is considered. The difference in

order of reactivities is probably due to the lower self-exchange rate for $[Fe(CN)_6]^{4-}$ compared with that of $[W(CN)_8]^{4-}$.

Huie *et al.* (*106*) have also determined rate constants by pulse radiolysis techniques for the oxidation of the above-mentioned cyano complexes by the carbonate radical at pH $\geq$ 11.2, thus ensuring that only the anionic form in the acid/base equilibrium

$$CO_3H^- \rightleftharpoons CO_3^{\cdot-} + H^+ \ (pK_a = 9.6) \tag{128}$$

reacted. The carbonate radical is a strong oxidant (E^0 = 1.59V vs NHE), resulting in rate constants of 3.6×10^8 ($[Fe(CN)_6]^{4-}$), 2.4×10^8 ($[W(CN)_8]^{4-}$), and 3.5×10^7 ($[Mo(CN)_8]^{4-}$) M^{-1} sec^{-1}. The rate constants for the reactions with $[Fe(CN)_6]^{4-}$ and $[W(CN)_8]^{4-}$ are likely to be limited by diffusion, even though their rate constants are less than 10^9 M^{-1} sec^{-1}. It was suggested that ion association with alkali metal ions reduced the high negative charges on these complexes because only then can calculated diffusion rate constants exceed the experimental rate constants.

6. *Organic Compounds*

The oxidation of formaldehyde by octacyanotungstate(V) ions in strong alkaline medium has been investigated, the reaction stoicheiometry being

$$HCHO + 2[W(CN)_8]^{3-} + 3OH^- \longrightarrow HCO_2^- + 2[W(CN)_8]^{4-} + 3H_2O. \tag{129}$$

The reaction is of the first order with respect to $[W(CN)_8]^{3-}$, formaldehyde, and OH^- concentrations, and product $[W(CN)_8]^{4-}$ ions have no retarding effect upon the reaction rate (*107*). Since the formaldehyde is in the hydrated form, the OH^- concentration dependence should involve a prior neutralization step in the mechanistic sequence of

$$H_2C(OH)_2 + OH^- \underset{k_{-1}}{\overset{k_1}{\rightleftharpoons}} H_2CO(OH)^- + H_2O \tag{130}$$

$$H_2CO(OH)^- + [W(CN)_8]^{3-} \xrightarrow{k_2} [W(CN)_8]^{4-} + H_2\dot{C}O(OH) \tag{131}$$

$$H_2\dot{C}O(OH) + [W(CN)_8]^{3-} \xrightarrow[\text{fast}]{k_3} [W(CN)_8]^{4-} + HCOOH + H^+ \tag{132}$$

$$HCOOH + 2OH^- + H^+ \longrightarrow HCOO^- + 2H_2O. \tag{133}$$

On the assumption that $[H_2O] \gg (k_2/k_{-1})[W(CN)_8^{3-}]$, the following rate

law was derived,

$$\text{rate} = (2k_2K_1/[H_2O])[H_2C(OH)_2][W(CN)_8^{3-}][OH^-], \quad (134)$$

which is in accord with experimental results. A third-order rate constant of $5.1 \times 10^{-3}\,M^{-2}\,\text{sec}^{-1}$ at 14.5°C was obtained. It was suggested that the radical in Eq. (131) had no independent existence since vinyl acetate polymerization tested negative.

It is generally believed that the oxidation of thiourea and related compounds by aqua-metal ions involves an inner-sphere electron-transfer process, whereas an outer-sphere mechanism is more commonly associated with substitution-inert complexes. The stoichiometry of redox reactions with one-electron oxidizing agents is different for acid and alkaline media. The oxidation of both thiourea and thioacetamide by $[Mo(CN)_8]^{3-}$ in the range $0.02 < [HClO_4] < 0.08\,M$ proceeds in a 1:1 ratio, yielding the disulfide as a product (*108*):

$$2(NH_2)_2CS + 2[Mo(CN)_8]^{3-} \longrightarrow 2[Mo(CN)_8]^{4-} + (H_2N)HN{=}CSSC{=}NH(NH_2). \quad (135)$$

In alkaline solution (*109*), 8 eq. of $[M(CN)_8]^{3-}$ are needed to yield sulfate and urea as products:

$$8[M(CN)_8]^{3-} + (NH_2)_2CS + 10OH^- \longrightarrow 8[M(CN)_8]^{4-} + SO_4^{2-} + (NH_2)_2CO + 5H_2O. \quad (136)$$

Protonated thiourea is a strong acid, the pK_a being -1.19 in aqueous solution (*110*). It is thus more likely that the equilibrium

$$(NH_2)_2CS \overset{K}{\rightleftharpoons} (NH_2)HN{=}CS^- + H^+ \quad (137)$$

should be encountered for moderate acid or base concentrations during kinetic studies. Equation (137) was found to comply with experimental observations for the oxidation of thiourea by $[Mo(CN)_8]^{3-}$ in the above-mentioned perchloric acid range (*108*), the reaction sequence being

$$[Mo(CN)_8]^{3-} + (NH_2)_2CS \xrightarrow{k_1} [Mo(CN)_8]^{4-} + (NH_2)HN{=}CS^{\cdot} + H^+ \quad (138)$$

$$[Mo(CN)_8]^{3-} + (NH_2)HN{=}CS^- \xrightarrow{k_2} [Mo(CN)_8]^{4-} + (NH_2)HN{=}CS^{\cdot}, \quad (139)$$

where the two radicals combine in a fast subsequent reaction to yield the disulfide. Equations (137)–(139) yield a rate equation,

$$-d[Mo(CN)_8^{3-}]/dt = (k_1 + k_2K[H^+]^{-1})[\text{thiourea}][Mo(CN)_8^{3-}], \quad (140)$$

which predicts a linear inverse first-order dependence on $[H^+]$, as was found. For thioacetamide, however, the protonation equilibrium

$$MeNH_2CS + H^+ \overset{K_1}{\rightleftharpoons} Me\overset{+}{N}H_3CS \quad (141)$$

was found to be operative. This is probably due to the inductive effect of the methyl group, which shifts electron density toward the sulfur atom, making it a better nucleophile toward H^+ ions. Consequently, the rate-determining steps here were

$$[Mo(CN)_8]^{3-} + Me\overset{+}{N}H_3CS \xrightarrow{k_3} [Mo(CN)_8]^{4-} + MeHNC\dot{S} \quad (142)$$

and

$$[Mo(CN)_8]^{3-} + MeNH_2CS \xrightarrow{k_4} [Mo(CN)_8]^{4-} + MeHN\dot{C}S + H^+. \quad (143)$$

The derived rate (Eq. (144)) showed that a linear dependence of observed rate constants on $[H^+]$ should prevail,

$$-d[Mo(CN)_8^{3-}]/dt = (k_4 + k_3K_1[H^+])[MeNH_2CS][Mo(CN)_8^{3-}], \quad (144)$$

which was also verified experimentally. For two reactions, Eqs. (138) and (143), which are of similar nature, it was found that $k_1 = 10.2$ M^{-1} sec^{-1} and $k_4 = 43.3$ M^{-1} sec^{-1} at 25°C. This is in line with a relatively more electron-rich sulfur atom in thioacetamide, which will enhance electron transfer to the Mo(V) center more effectively than thiourea.

According to experimental results (*109*), the rate equation at pH 8.6–11.15 was determined as

$$\text{rate} = k[M(CN)_8^{3-}][\text{thiourea}][OH^-][Na^+], \quad (145)$$

with rate constants at 25°C of 2×10^5 and 1.6×10^2 M^{-3} sec^{-1} for $[Mo(CN)_8]^{3-}$ and $[W(CN)_8]^{3-}$, respectively. The rate-determining step was given as

$$(NH_2)HN{=}CS^- + Na[M(CN)_8]^{2-} \underset{k_{-1}}{\overset{k_1}{\rightleftharpoons}} [M(CN)_8]^{4-} + (NH_2)HN{=}\dot{C}S, \quad (146)$$

followed by a number of fast steps. A slight retarding effect was observed for $[W(CN)_8]^{4-}$ ions.

The oxidation of thiols in the form of L-cysteine, penicillamine, and thioglycollic acid by $[Mo(CN)_8]^{3-}$ in aqueous acidic solution also formed disulfides as final products (*111*). The reactions show a second-order substrate dependence, and the rates are found to decrease with increasing hydrogen ion concentration. This is attributed to the deprotonation of the —SH and —COOH groups in these thiols prior to electron transfer. The reactions are interpreted in terms of outer-sphere activation. An explanation for the second-order dependence on thiol concentration involves ion association between the cyano complex and a protonated form of the thiol, followed by reaction of this complex with a second thiol molecule.

A number of symmetrically substituted benzoins,

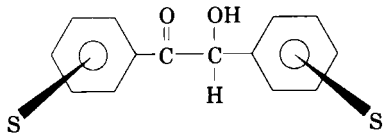

with S = H; *o*-, *p*-, and *m*-OMe; *p*-Cl; and *o*-Cl, has also been oxidized by $[Mo(CN)_8]^{3-}$ (*112*) and $[W(CN)_8]^{3-}$ (*113*) in buffered alkaline aqueous/methanolic (50% v/v) medium. The 1,2-diketone (benzil) product formed via a 2:1 oxidant/benzoin ratio. The experimental rate law was determined as

$$-d[Mo(CN)_8{}^{3-}]/dt = k[\text{benzoin}][Mo(CN)_8{}^{3-}][OH^-]. \quad (147)$$

The proposed mechanism involves a preequilibrium of enolate formation (HBO^-) followed by a rate-determining electron transfer:

$$HBOH + OH^- \overset{K}{\rightleftharpoons} HBO^- + H_2O \quad (148)$$

$$HBO^- + [Mo(CN)_8]^{3-} \xrightarrow{k_2} HBO\cdot + [Mo(CN)_8]^{4-} \quad (149)$$

$$HBO\cdot + [Mo(CN)_8]^{3-} + OH^- \xrightarrow{\text{fast}} BO + [Mo(CN)_8]^{4-} + H_2O. \quad (150)$$

A third-order rate law can be derived:

$$\text{rate} = k_2K[\text{HBOH}][\text{Mo(CN)}_8^{3-}][\text{OH}^-], \quad (151)$$

from which it follows that $k_{obs} = k_2K$.

The relative rates ($k_{substituted}/k_{benzoin}$) correlated very well with the Hammett substituent constants and support a negatively charged intermediate. The effect of substituents correlated with a σ value of 1.36. An interesting variation in k_{rel} with $\Delta S^{\neq}$ was also found: the benzoin with the highest reactivity (S = *o*-Cl) has the most positive $\Delta S^{\neq}$ value ($+62$ J K^{-1} mol^{-1}) whereas the least reactive (S = *o*-OMe) has the largest negative value of $\Delta S^{\neq}$ (-105 J K^{-1} mol^{-1}). This was explained in view of the closest approach through the formation of the activated complex, and thus, the value of $\Delta S^{\neq}$ is a function of the electron-transfer distance. For high negative $\Delta S^{\neq}$ values, the electron transfer takes place at a relative short distance and may be hindered by factors such as solvation, ion pairing, and substituent steric effects.

An interesting application for the oxidation of organic compounds is of electrochemical nature. Octacyano complexes have been used to monitor redox enzymes such as lactate oxidase (from *Pediococcus* sp.) and sarcosine oxidase (from *Arthrobacter* sp.) in a suitable electrochemical system (*114*). Two equivalents of $[M(CN)_8]^{4-}$ can, for example, be oxidized at the electrode surface to $[M(CN)_8]^{3-}$, which in turn can oxidize the flavoproteien to its oxidized form. This in turn reacts with, for example, L-lactic acid to produce pyruvic acid,

$$CH_3CH(OH)COOH \longrightarrow CH_3C(=O)COOH + 2H^+ + 2e^-, \quad (152)$$

after which the cycle can start again. Under conditions of excess amounts of substrate (such as L-lactic acid) and mediator ($[M(CN)_8]^{4-}$), it was found that the rate-determining step is between the mediator and the enzyme. Second-order rate constants of ca. $6 \times 10^4\ M^{-1}$ sec^{-1} (lactate oxidase) and ca. $1 \times 10^4\ M^{-1}$ sec^{-1} (sarcosine oxidase) were determined for $[W(CN)_8]^{4-}$ as mediator.

7. *Innersphere Mechanisms*

The majority of research on the redox kinetics of octacyanotungstate and -molybdate ions points to outer-sphere activation during the electron-transfer step. The behavior of these ions is such that the octacoordinated moiety remained the same and as such the ions are deemed to be substitution inert toward many reactants. However, as was pointed out in the introduction of Section IIB, there are cases in which substitution of cyano ligands occurred but with the exclusion of redox behavior. On the other hand, as we will learn from the photochemistry of these

complexes (Section IIC), it is also possible via irradiation to disrupt the M—CN bond and effect substitution in this way.

Only two papers, those on Cr(VI) (*115*) and V(V) (*116*) oxidation of $[Mo(CN)_8]^{4-}$, consider the question of an inner- or outer-sphere mechanism. The Cr(VI) oxidation follows a rate law of

$$-d[Cr(VI)]/dt = k[HCrO_4^-][Mo(CN)_8^{4-}][H^+]^2, \quad (153)$$

where $k = 8.3 \times 10^{-4}\ M^{-3}\ sec^{-1}$. This reaction seems to be a simple case of a one-electron reduction of Cr(VI) in which the kinetics of the first step determines the rate of the reaction. However, according to the King–Espenson mechanism (*117*), reduction of Cr(VI) to Cr(III) involves three one-electron steps, in which the second step (Eq. (155)) for Cr(V) → Cr(IV) is rate determining:

$$Cr(VI) + R \rightleftharpoons Cr(V) + R^+ \quad (154)$$

$$Cr(V) + R \rightleftharpoons Cr(IV) + R^+ \quad (155)$$

$$Cr(IV) + R \rightleftharpoons Cr(III) + R^+. \quad (156)$$

This raised the question as to why the first step (Eq. (154)) is rate-determining for $[Mo(CN)_8]^{4-}$, whereas for metal ions such as Fe^{2+}, VO^{2+}, and NpO_2^+ the second step, Cr(V) → Cr(IV), is rate-determining. In the case of cyanometalates this may be explained by way of an inner-sphere transfer mechanism in which formation of Cr(IV) (Eq. (158)) is rate-determining, the reaction sequence being

$$2H^+ + HCrO_4^- + [Mo(CN)_8]^{4-} \underset{k_{-1}}{\overset{k_1}{\rightleftharpoons}} [H_3O_4Cr\text{-}NC\text{-}Mo(CN)_7]^{5-} \quad (157)$$

$$[H_3O_4Cr\text{-}NC\text{-}Mo(CN)_7]^{5-} + [Mo(CN)_8]^{4-} \xrightarrow{k_2} [H_3O_4Cr\text{-}NC\text{-}Mo(CN)_7]^{4-}. \quad (158)$$

The derived rate law for this mechanism is

$$\text{rate} = k_1K_2[HCrO_4^-][Mo(CN)_8^{4-}][H^+]^2/(k_{-1} + k_2[Mo(CN)_8^{4-}]). \quad (159)$$

If $k_{-1} \ll k_2[Mo(CN)_8^{4-}]$, then

$$\text{rate} = k_1[HCrO_4^-][Mo(CN)_8^{4-}][H^+]^2, \quad (160)$$

in agreement with Eq. (153). If the above-proposed mechanism is true,

then it appears that reducing agents for Cr(VI) can be categorized as follows: (a) metal cations that form oxygen-bridged complexes to Cr(VI) and give kinetics conforming to Eqs. (154)–156), (b) cyano-metalates that coordinate directly to Cr(VI) and Cr(V) through cyanide bridges and give kinetics conforming to Eq. (160), and (c) outer-sphere reagents such as $[Fe(phen)_3]^{2+}$, which conform to a rate law of

$$\text{rate} = k[HCrO_4^-][Fe(II)]. \tag{161}$$

From a coordination viewpoint, there are two views that support the idea of an inner-sphere coordinated cyano bridge on the Cr(VI) core. First, four-coordinated Cr(VI) or Cr(V) changes to six-coordinate Cr(IV) so that there is room for coordination sphere expansion. Second, it has been shown (*118*) that, in spite of the high negative charge on octa- and hexacyano complexes, they can be used as nucleophiles in substitution of an axial water ligand of mesotetra(4-*N*-methylpyridyl)porphinediaquocobalt(III) ions and that the stability constants of these products are comparable to those of NCS^-.

The production of $[Mo(CN)_8]^{3-}$ from the reaction of $[Mo(CN)_8]^{4-}$ with an excess of VO_2^+ in acidic perchlorate media gives biphasic results that, although not conclusively, was interpreted in terms of two parallel reactions taking place simultaneously (*116*). Two experimental rate laws are thus obtained,

$$d[Mo(CN)_8^{3-}]dt = k[Mo(CN)_8^{4-}][VO_2^+][H^+] \tag{162}$$

and

$$d[Mo(CN)_8^{3-}]/dt = k'[Mo(CN)_8^{4-}][VO_2^+][H^+], \tag{163}$$

with $k = 25(8) \times 10^5\ M^{-2}\ \text{sec}^{-1}$ and $k' = 2.81(8) \times 10^4\ M^{-2}\ \text{sec}^{-1}$. On the basis of a comparison of oxidation rates of several complex ions that are known to obey an inner- or outer-sphere mechanism, it was concluded that the two parallel reactions differ in that one is representative of an outer-sphere mechanism and the other inner-sphere electron transfer. No mechanism has been presented and this reaction probably has to be investigated further.

C. Photochemistry

The photosensitivity of the $[M(CN)_8]^{3-}$ complex ions ((M=Mo(V), W(V)) in aqueous solution was observed as early as 1910 (for Mo) (*119*)

and 1955 (for W) (*120*) and was included in earlier reviews (*1, 2, 13*). Important studies by Balzani and Carassiti (*121*) highlighted the quantum efficiencies for photodecomposition. The work of Samotus and co-workers has to be recognized specifically for the important contributions to the photochemistry of these octacyano systems (*122–124*). Important contributions to this field also came from the Kemp (*125*), Hennig (*126*), and Mohan (*127*) groups.

It was shown during this period that photolysis of the octacyano d^1 species of Mo(V) and W(V) produces the reduced octacyanometalate(IV) complexes as main photoproducts, and much research has concentrated on the first mechanistic step of action. On the other hand, photolysis of the primary photoproduct, $[M(CN)_8]^{4-}$ of Mo(IV) and W(IV), forming $[MO_2(CN)_4]^{4-}$ (and the mono- and the diprotonated $[MO(OH)(CN)_4]^{3-}$ and $[MO(H_2O)(CN)_4]^{2-}$, depending on the solution pH) as the final product during exhaustive photolysis, was also extensively studied. Photolysis of both these metals' d^1 and d^2 systems has also been studied in organic media as an aid in the elucidation of the photolytic mechanisms. The discussion below concentrates on aspects of the research that has been performed with regard to the photochemistry of these M(V) and M(IV) complexes of Mo and W.

1. Octacyano Complexes of Mo(V) and W(V)

The photolysis of the $[M(CN)_8]^{3-}$ complexes in both aqueous and nonaqueous media has been extensively researched in the past decade and is still being actively investigated (*122, 123, 125*). Results supporting these investigations have led to the following representation of the photoreactivity of the $[W(CN)_8]^{3-}$ system.

a. Steps I and II. General agreement has been reached with regard to the normal-intensity photolytic process for the W(V) system in hydroxylic solvents (step II in Scheme 1) such as water and methanol, $[W(CN)_8]^{4-}$ being obtained in high yield (*122–128*). The photochemical behavior of the Mo(V) system is not nearly as well defined as that of W(V), but step II is also accepted (*125, 129*). In the case of the W(V) system, $\dot{O}H$ radicals were observed by spin-trapping experiments with suitable agents such as phenyl *N-tert*-butyl nitrone (*129*) and 4-*N,N*-dimethylamino nitrosobenzene (*130*), in agreement with step II in Scheme 1 (*131*). In the case of Mo(V), $CN^{\cdot}$ radicals have also been detected during spin-trapping experiments (*132, 133*) in methanolic solution, as well as the spin adduct of $\dot{O}CH_3$. Laser flash photolysis results (*134*) were used as further evidence that step II is one of the primary processes associated with the photolysis of the $[M(CN)_8]^{3-}$

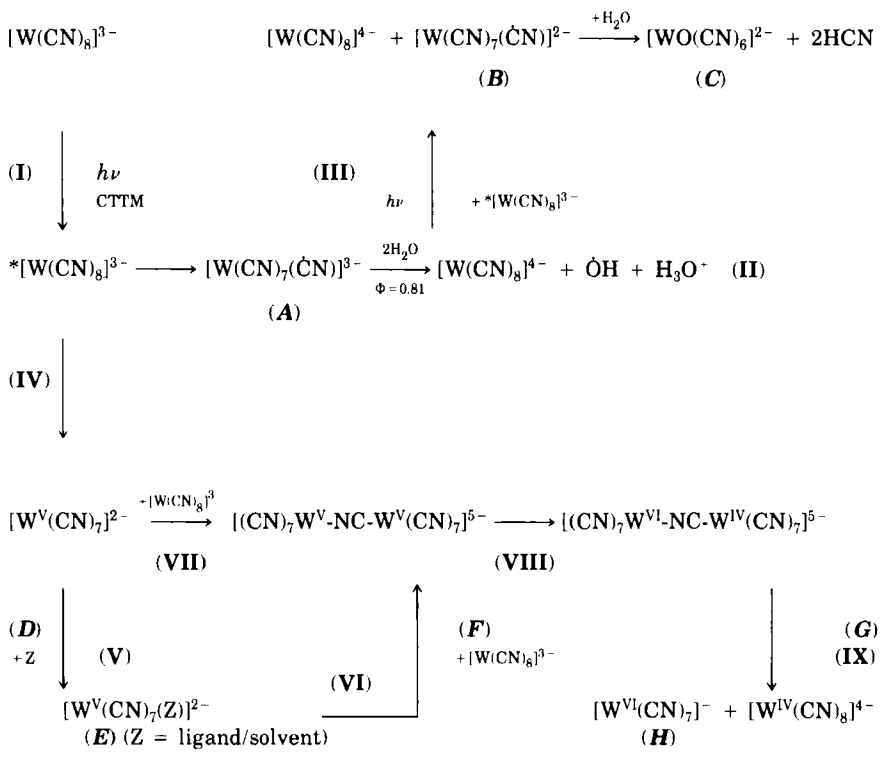

SCHEME 1. Photolytic processes associated with $[M(CN)_8]^{3-}$.

complexes. This has led to the postulation of an intermediate radical complex, $[M(CN)_7(\dot{C}N)]^{3-}$, which is capable of oxidizing the hydroxilic solvent, producing $[M(CN)_8]^{4-}$ in high yield (i.e., for W(V), $\Phi = 0.81$) (*125*). The isolation of the novel dioxygen complexes, $[W(O_2)(CN)_7]^{3-}$ and $[(CN)_7W(O_2)W(CN)_7]^{6-}$, characterized by Raman, ESR, and spin-trapping experiments (*135*), provides further evidence for the operation of a free radical mechanism involving the splitting of water, in direct agreement with step II in Scheme 1.

Monochromatic photolysis of aqueous $[W(CN)_8]^{3-}$ solutions at pH 1–13 results in a two-step sequence involving a primary intermolecular redox process and a consecutive thermal chain reaction, both producing $[W(CN)_8]^{4-}$ as the main product, which has been studied kinetically (*136*). The empirical rate law for the postirradiation reaction under excess of $[W(CN)_8]^{3-}$, at constant pH, was found to be of the form rate $= k_{obs}[R']^2[W(CN)_8]^{3-}$, where R′ is a one-electron reductant such as $OH^{\cdot}$ and $ROH^{\cdot}$ (R=Me) (*136*).

b. Step III. For W(V), under high light intensities, the formation of product C in Scheme 1 in aqueous medium has been positively established and characterized by an X-ray crystal structure determination of the PPh_4^+ salt (*137, 138*) (see Fig. 9). The $[WO(CN)_6]^{2-}$ complex forms upon standing of the photolysed W(IV) solution and is obtained in a low yield (<10%), suggesting that this step is a minor step in the overall process. This is in agreement with the proposed scheme, i.e., the postulation of the photolytically active intermediate $[W(CN)_7(\dot{C}N)]^{3-}$, which reacts less efficient by a second photochemical process, producing the W(VI) species. This two-quantum process accounts for the formation of the novel tungsten d^0 complex.

Similarly, in a water/methanol medium (1/1, v/v), the formation of *trans*-$[WO(CN)_5(OCH_3)]^{2-}$ has been observed, the product isolated as the PPh_4^+ salt and characterized structurally (*137*) (see Fig. 10). The isolation of the methoxide product confirms the labilization of the cyano ligand *trans* to the oxo in the $[WO(CN)_6]^{2-}$ complex, resulting in substitution reactions similar to those observed for the dioxotetracyano species of these and related metal centers (Section IIID).

Both these ions (Figs. 9 and 10) show the pentagonal bipyramidal geometries (*136, 137*) with the ligand *trans* to the apical oxo more weakly coordinated to the metal center than that of the equatorial cyano ligands. The distortion of these anions is similar to that of the systems discussed in Section IIID.

c. Steps IV, VII, VIII, and IX. Evidence for steps IV and VII in Scheme 1 has also been presented for both the Mo(V) and the W(V) systems. Although the production of W(VI) in the photolysis of

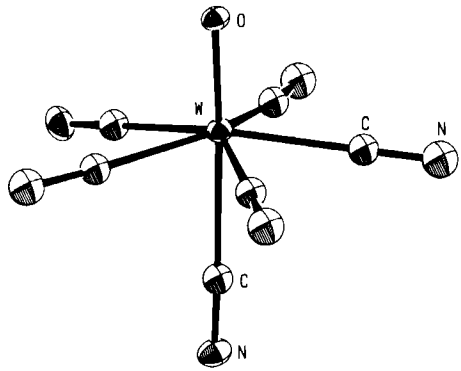

FIG. 9. Perspective view of $[WO(CN)_6]^{2-}$ (*137*). Adapted with permission from Sieklucka *et al.* (*137*). Copyright 1990, Royal Society of Chemistry.

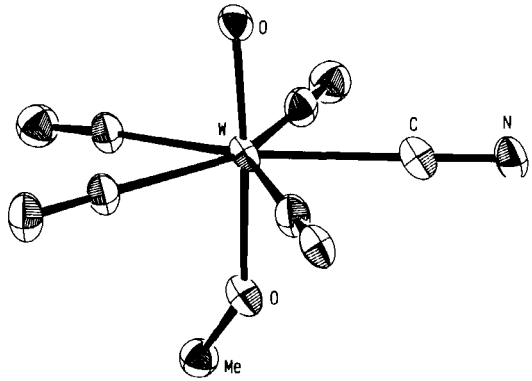

FIG. 10. Perspective view of $[WO(CN)_5(OMe)]^{2-}$ (*137*). Adapted with permission from Sieklucka *et al.* (*137*). Copyright 1990, Royal Society of Chemistry.

$[W(CN)_8]^{3-}$ in hydroxylic solvents is attributed to the two-quantum process, involving the $[W(CN)_7(\dot{C}N)]^{3-}$ species as a light-absorbing intermediate, a different approach had to be taken to explain the observed existence of the W(VI) species in nonaqueous solvents (*122, 123, 125*). The formation of the highly reactive, unsaturated intermediate $[M^{V}(CN)_7]^{2-}$ (D in Scheme 1) was postulated (*125, 139*), which for W produces the dominant $[W^{VI}(CN)_7]^{-}$ (H in Scheme 1) via an inner-sphere redox process with the parent $[W(CN)_8]^{3-}$ complex. The composition of the $[W^{VI}(CN)_7]^{-}$ complex has been verified by X-ray photoelectron spectroscopy (*123*), as well as has that of the di- and trinuclear complexes, formulated as $[(NC)_6W^{VI}–CN–W^{VI}(CN)_6]^{-}$ (resulting from the condensation of two $[W^{VI}(CN)_7]^{-}$ entities) and $[(NC)_7W^{VI}–NC–W^{IV}(CN)_6–CN–W^{VI}(CN)_7]^{6-}$ (formed by two $[W^{VI}(CN)_7]^{-}$ ions and one $[W(CN)_8]^{4-}$ complex) (*137*). In the case of Mo, similar complexes, produced via the reactive intermediate, $[Mo(CN)_7]^{2-}$, have been postulated (*129*).

d. Steps V and VI. The formation of the paramagnetic d^1 species E has been verified, as well as have the different substitution products obtained from ligation of the coordinated Z ligand (*125, 140*), providing further evidence for these proposed steps. ESR techniques were used at 77 and 293 K for these experiments and it was shown that the $[W(CN)_7]^{2-}$ intermediate either becomes rapidly solvated to give $[W^{V}(CN)_7(H_2O)]^{2-}$ or, in high concentrations of X^{-} ions (X = Cl, Br, N_3, NCS) or O_2, reacts to give $[W^{V}(CN)_7X]^{3-}$ or $[W^{V}(CN)_7(O_2)]^{2-}$ (*134, 135*). Ion-pairing interactions in these systems were shown to be very

important, similar to those found in the redox kinetics of these systems (Section IIB). Reaction of E with $[W(CN)_8]^{4-}$, similar to that in step VI in Scheme 1, produces mixed [W(IV/V)] dinuclear complexes, similar to F and G, supplying even further evidence (*125*) for this representation. Furthermore, the formation of products during high-intensity photolysis (200–500 W) of $[W(CN)_8]^{3-}$ in aqueous or aqueous-methanol solutions produced novel dioxygen complexes, formulated as $[W(O_2)(CN)_7]^{3-}$ and $[(CN)_7W(O_2)W(CN)_7]^{6-}$ (*135*), characterized by Raman, ESR, and spin-trapping experiments, and these provide further evidence for the formation of the intermediate $[M(CN)_7]^{2-}$ species. Similarly, the operation of a free radical mechanism as observed in the formation of these two complexes, involving the splitting of water, is again in direct agreement with step I in Scheme 1 (*135*).

2. Octacyano Complexes of Mo(IV) and W(IV)

Although the photolytic activity of the octacyanometalate systems of Mo and W in basic medium, producing the dioxotetracyanometalate(IV) ions as final products, has been known for a long time (*1, 2*), the nature of the mechanism was more recently described. Consequently, the identification of intermediates in this system has contributed substantially to a better understanding of the mechanism. The general photolytic process for the $[M(CN)_8]^{4-}$ complexes of W(IV) (*141*) and Mo(IV) (*142*) are summarized in Scheme 2.

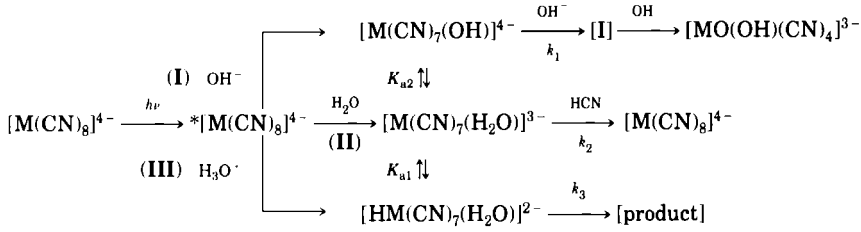

SCHEME 2. Photolytic processes associated with the $[M(CN)_8]^{4-}$ systems ([I] = intermediate species).

The formation of the tetracyano complexes from photolysis of the octacyanometalate(IV) ions in basic medium, step I in Scheme 2, was observed as early as the 1920s and the species formed were later well characterized (*143, 144*) (see also section IIIA). In spite of this fact, later studies (*127, 145*) that gave results similar to those of the initial experiments were conducted, apart from the fact that the existence of the $[M(OH)_2(CN)_4]^{2-}$ complexes (*127*) instead of the crystallographically characterized $[MoO(H_2O)(CN)_4]^{2-}$ (*144*) complex was still claimed

(similar to earlier beliefs (*143, 146*)). Extensive research has been performed on the primary photolysis reaction, i.e., the formation of the activated species $*[W(CN)_8]^{4-}$ in Scheme 2.

The $[Mo(CN)_7(H_2O)]^{3-}$ complex, postulated by Adamson (*147*) and Carassiti (*148*), was isolated as $Ag_3[Mo(CN)_7(H_2O)]$ and characterized by Mitra *et al.* (*146, 149*), who also postulated the formation of the $[Mo(CN)_7(OH)]^{4-}$ species in basic medium. The corresponding W(IV) complex was also isolated and characterized (*150*). The protonation behavior of these heptacyano (*151*) species was first described by Samotus (*152*) and the pK_{a1} and pK_{a2} values as defined in Scheme 2 have been determined as 4.82 and 9.17, respectively, for the W(IV) system. No crystallographic data have been reported for these heptacyano complexes.

The intermediate in step I (Scheme 2) has been proposed to be the $[M(CN)_6]^{2-}$ species (*141, 142*), probably containing coordinated aqua/hydroxo ligands. The first-order rate constant for this base hydrolysis step has been determined as $1.0(2) \times 10^{-4}$ sec^{-1} (0.1 *M*) (*141*) and 1.2×10^{-3} sec^{-1} (0.0028 *M*) (*142*) for W(IV) and 1.1×10^{-3} sec^{-1} for Mo(IV) (*142*). The second-order rate constant for the formation of the octacyanotungstate(IV) has been determined as 2.9 M^{-1} sec^{-1} for the W(IV) system. The product formed (first-order rate constant, $4(1) \times 10^{-4}$ sec^{-1}, [Mo] = 0.1 *M*) (*141*) during acid hydrolysis (step III, Scheme 2) is not well characterized but afforded the study of the decomposition kinetics. The overall quantum yield of the photolysis of $[W(CN)_8]^{4-}$ at pH 1–13 remains constant at ca. 0.98(6) mol/einstein, illustrating also the high-yield conversion of the octacyanotungstate(IV) (*141, 142*).

A few papers have claimed the formation of mixed cyano/bidentate ligand complexes, isolated from the aqueous photolysis of the $[M(CN)_8]^{4-}$ complexes. These include the $[M(OH)_2(CN)_4(BID)]$, with BID=phen, 2,2′-bipy (*153*), and $[M(OH)_3(CN)(phen)]$ (isolated as solids) (M=Mo, W) (*153*), and $[W(CN)_6(en)]^{2-}$ (*154*) complexes. Doubts exist with regard to the correctness of the formulated $[M(OH)_2(CN)_4(BID)]$ complex since this complex in solution displays spectra similar to those of the $[MoO(CN)_3(phen)]^-$ and $[WO(CN)_5]^{2-}$ complexes, suggesting that photolysis of the $[M(CN)_8]^{4-}$ ions produced the $[MO(H_2O)(CN)_4]^{2-}$ ion and, in the case of Mo(IV), resulting in the bidentate substitution of the aqua and a cyano ligand (see Section IIID). In the case of W(IV), the pH is such that the stability constant of the $[WO(CN)_3(phen)]^{2-}$ complex is much less than that of the pentacyano species (Section III), favoring the $[WO(CN)_5]^{3-}$ over the phen complex and accounting for the observed UV/visible spectra. This is in agreement with the results obtained by Samotus (*124*), who isolated the oxopenta-

cyanomolybdate(IV) complex from photolysis of aqueous cyanide solutions of $[Mo(CN)_8]^{4-}$. The corresponding W(IV) complex (*124*) was not observed and its preparation by thermal methods was questioned. It was, however, shown that $[WO(CN)_5]^{3-}$ can be obtained with ease by reducing the total cyanide concentration (*155, 156*).

The postulated above-mentioned monocyano complexes, obtained during the photolysis of the $[W(CN)_8]^{4-}$ complex in the presence of 1,10-phenanthroline and isolated as solids (*153*), most likely stem from decomposition products, of which the postulated composition is unlikely based on the knowledge of these systems. In the case of the claimed $[W(CN)_6(en)]^{2-}$ complex (*154*), questions with regard to characterization exist since the UV/visible data used for the identification are very similar to those for the $[W(CN)_7(H_2O)]^{3-}$ complex (*141, 157*).

The photolysis of $[MCN)_8]^{4-}$ (M=Mo, W) in solvents other than pure water has shown interesting behavior (*126*); for example, in water/MeOH mixtures, the formation of $[Mo(CN)_4(phen)_2]$ was postulated (*158*). In these experiments the octacyanometalate(IV) ions had countercations such as tetramethylammonium to ensure better solubility in organic media. In the case of W(IV) in $CHCl_3$/alcohol (3/1, v/v) mixtures, the formation of paramagnetic alkoxo species, postulated as $[W(OR)_4(phen)]$ (R = CH_3, C_2H_5, n-C_3H_7, n-C_4H_9) (*139*), was observed. These formulations were based on spectroscopic and chemical analyses and on the fact that 8 mol of free cyanide was liberated in the photolytic process. The kinetics of the consecutive thermal reaction following the photolysis of $(PNP)_4[Mo(CN)_8]$ in deoxygenated methanol was studied but the products were not well characterized (*126*).

It is clear that there is much to be investigated with regard to the photolytic reactions associated with both the d^1 and the d^2 molybdenum and tungsten systems, but substantial progress regarding new aspects, which has contributed to the better understanding of these cyano complexes, has been made. More sophisticated apparatus will undoubtedly inspire research in this regard, probably extending the investigations to the periodic neighbors niobium, tantalum, rhenium, and technetium.

III. Tetracyano Complexes Containing Oxo or Nitrido Ligands

A. Synthesis

Although the $[MO_2(CN)_4]^{n-}$ complexes of Mo(IV), W(IV), Re(V), and Os(VI) were prepared in the early half of the 20th century

(*159–162*), the dioxotetracyanotechnetate(V) ion was reported only in 1980 (*163*). Some important syntheses for these complex systems are described below.

The $[MO_2(CN)_4]^{4-}$ complexes for Mo and W can be prepared photochemically (*124, 142, 143, 145, 164*) or thermally (*155, 156*). A very effective form of preparation specifically involves the photolysis of basic solutions of the $[M(CN)_8]^{4-}$ complexes, which produces the corresponding dioxotetracyano-metalate(IV) complexes in >90% yield (*143, 164*). In the absence of a high-intensity photochemical source, sunlight has been found to be more than adequate (*165, 166*). A disadvantage of this method is that it first involves the preparation of the octacyanometalates. Procedures for the effective preparation of these $[M(CN)_8]^{4-}$ ions, involving the reduction of the $[MO_4]^{2-}$ ions by H^+/BH_4^- in the presence of an excess of cyanide ion (*167, 168*), have been developed, thus making the photochemical route more viable.

The thermal preparation of the $[MO_2(CN)_4]^{n-}$ complexes of Mo and W has been described and involves the same procedure for the production of the octacyanometalates but at a much lower cyanide concentration (*155, 156*). Care needs to be taken to limit further substitution toward higher cyanide coordination once the dioxotetracyano complex has been formed in order to reduce the formation of cyano complexes higher than the $[MO(CN)_5]^{3-}$ ion, the reason being that the latter can still be hydrolyzed to the dioxotetracyano complexes by manipulation of solution basicity. Higher cyanide concentrations result in the formation of octacyano complexes (via third-order kinetics, in terms of $[CN^-]$ (*155, 156*), which cannot be converted thermally to the corresponding dioxo complexes. Since higher coordination of the cyanide ion to the W(IV) or Mo(IV) centers proceeds via $[MO(H_2O)(CN)_4]^{2-}$ (Section IIID3), limitation of the concentration of this aqua species therefore also provides an easy way of limiting higher cyanide coordination by pH manipulation. Yields of more than 50% of the dioxotetracyanometalates of Mo(IV) and W(IV) are obtained in a short period of time (less than 2 hr). Preparation of the pentacyano complex $[MO(CN)_5]^{3-}$ has been described (*124, 169, 170*), but it can also be obtained by the above-mentioned BH_4^- reduction (*155, 156*).

A series of procedures for the preparation of $[ReO_2(CN)_4]^{3-}$ that involves cyanide ion substitution of more labile ligands such as py (*171*) and PPh_3 (*172*) from the Re(V) center has been described. A convenient procedure that, as in the case of the Mo(IV) and W(IV) systems described above, produces acceptable yields of dioxotetracyanorhenate(V) directly from the ReO_4^- ion has been described (*173*).

The process is again based on the H^+/BH_4^- reduction of ReO_4^-, followed by careful temperature and pH manipulation.

The radioactivity of technetium and its limited availability have resulted in less research on this metal and probably explains why fewer procedures are available for the preparation of the $[^{99}TcO_2(CN)_4]^{3-}$ complex. A very convenient method (*164, 174*) involves the HCl reduction of $^{99}TcO_4^-$, isolation of $[^{99}TcOCl_4]^-$ as the *n*-tetrabutylammonium salt, *in situ* preparation of the dioxotetrapyridine complex, substitution of the labile pyridine ligands, and isolation of $K_3[^{99}TcO_2(CN)_4]$ in an overall yield of more than 75%. The dioxotetracyanoosmate(IV) complex can be obtained as potassium or cesium salt by refluxing osmium tetroxide in H_2SO_4/HCN medium for a few hours, followed by the addition of the suitable cation, e.g., Cs^+, after evaporation of the reaction solution (*175*).

The preparation of $[MN(CN)_4(H_2O)]^{m-}$, the nitrido complex of Re(V) (*176, 177*), Tc(V) (*178*), and Os(IV) (*179, 180*), is achieved by first introducing the nitrido ligand to the metal center by reflux with acidic sodium azide, with the formation of tetrahalometalate, $[MNX_4]^{n-}$ (*177–179*). Ligation of the halide ions by cyanide ion produces the tetracyanonitridometalate complexes, which can be isolated with a selected cation (*176, 178, 181, 182*), such as tetraphenylphosphonium, in yields greater than 80%.

B. Protonation Reactions

It is well known that the dioxotetracyano complexes of molybdenum(IV), tungsten (IV), technetium(V), and rhenium(V) may be protonated according to Eqs. (164) and (165) (*143, 174, 182–185*):

$$[MO_2(CN)_4]^{n-} + H^+ \rightleftharpoons [MO(OH)(CN)_4]^{(n-1)-} \quad (164)$$

$$[MO(OH)(CN)_4]^{(n-1)-} + H^+ \rightleftharpoons [MO(H_2O)(CN)_4]^{(n-2)-}. \quad (165)$$

The pK_a values for the oxoaqua complexes of the above-mentioned metal ions are listed in Table III. The pK_{a1} values for all these complexes were fairly accurately determined but there is doubt about the pK_{a2} values of the W(IV) and especially the Mo(IV) complex. The pK_{a1} values of $[ReO(H_2O)(CN)_4]^-$ have been determined potentiometrically by Chakravorti (*184*) (see Table III), but these values and the existence of $[ReO(H_2O)(CN)_4]^-$ and $[ReO(OH)(CN)_4]^{2-}$ were questioned (*185*) since it was observed that dimerization occurs upon acidifying $[ReO_2(CN)_4]^{3-}$

TABLE III

pK_a VALUES OF $[MX(H_2O)(CN)_4]^{n-}$ COMPLEXES[a]

M	X	pK_{a1}	pK_{a2}	Reference
Mo(IV)	O	10.0	>14	*174*
W(IV)	O	7.8	>14	*174*
Tc(V)	O	2.9	5.0	*174*
Re(V)	O	1.4	3.7	*174*
Re(V)	N	11.7	—	*192*
Os(VI)	O	—	—	*175*
Os(VI)	N	7.6	—	*193*

[a] See Eqs. (164) and (167).

to give the purple dimer $[Re_2O_3(CN)_8]^{4-}$ (see Fig. 11) (*186*) as a final product (*187, 188*). Leipoldt *et al.*, however, succeeded in obtaining crystalline salts of $[ReO(OH)(CN)_4]^{2-}$ (*189*) and $[ReO(H_2O)(CN)_4]^-$ (*190*), suitable for X-ray analysis, by adding $(PPh_4)Cl$ and $N(C_2H_5)_4Cl$ to solutions of $[ReO_2(CN)_4]^{3-}$ at pH 3.5 and pH 1, respectively. The concentrations of the different salts were such that crystals of $(PPh_4)_2[ReO(OH)(CN)_4]\cdot 5H_2O$ (brown) and $(N(C_2H_5)_4)[ReO(H_2O)(CN)_4]\cdot 2H_2O$ (blue) were obtained within half an hour after adjusting the pH values from about 7 (at this pH the main product is $[ReO_2$

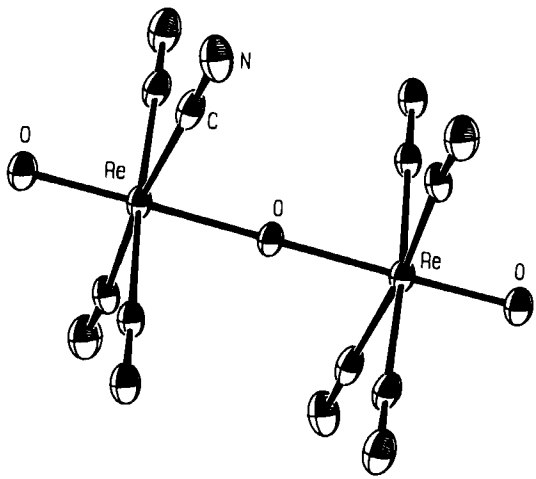

FIG. 11. Perspective view of $[Re_2O_3(CN)_8]^{4-}$ (*186*). Adapted with permission from Basson *et al.* (*186*). Copyright 1987, Chapman & Hall.

$(CN)_4]^{3-}$, which is very stable in solution) to the appropriate pH. Since the dimerization is a slow reaction (*173*), the dimer did not form in significant amounts during the time it took to get the crystals. Since the dimerization of $[TcO(OH)(CN)_4]^{2-}$ is a much faster reaction (*174*), it would be much more difficult to isolate salts of the oxoaqua and oxohydroxo complexes of technetium.

The pK_a values of $[TcO(H_2O)(CN)_4]^-$ and $[ReO(H_2O)(CN)_4]^-$ were also determined kinetically (*174, 191*) during kinetic studies of the substitution reactions of these oxoaqua complexes with thiocyanate ions (see Table III) (*192, 193*). The pK_a values decrease significantly upon going from a second- to a third-row metal complex (from 10 to 7 for the group VI metal ions and from 2.9 to 1.4 for the group VII metal ions) (see Table III), indicating the increase in metal–aqua bond strength. The same tendency was also observed in the relative reactivity of these complexes toward substitution reactions; the substitution reactions of the oxoaqua complexes of the third-row metal ions are orders of magnitude slower than the substitution reactions of the second-row metal ions (see Section IIID).

The effect of charge on the pK_a values of the oxoaqua complexes is very large: The pK_a values decrease by more than five pK_a units upon going from a metal ion with a formal charge of 4+ (Mo(IV) and W(IV)) to a metal ion with a charge of 5+ (Tc(V) and Re(V)) (see Table III). This is an indication of the weakening of the metal–aqua bond by reduction of the charge on the metal ion. This reduction of the charge also has a very large effect on the reactivity of the aqua complexes toward substitution reactions, as will be pointed out in Section IIID.

Increasing the charge on the metal ion to 6 resulted in a complex that cannot be protonated ($[OsO_2(CN)_4]^{2-}$) even at a high hydrogen ion concentration. This is an indication that $[OsO(H_2O)(CN)_4]$ is a very strong acid (as a result of the high charge on the metal ion) and cannot exist in the protonated form (*175*).

Substituting the oxo ligand in these complexes with a nitrido ligand resulted in a very large increase in the pK_a values; the pK_a values of $[ReN(H_2O)(CN)_4]^{2-}$ and $[ReO(H_2O)(CN)_4]^-$ are 12 and 1.4, respectively (*176, 184, 192*). This increase is an indication of the weakening of the metal–aqua bond as a result of the large *trans*-influence of the nitrido ligand in comparison with the *trans*-influence of the oxo ligand. This is in agreement with the fact that the nitrido ligand is one of the strongest π-bonding ligands known. This decrease in the metal–aqua bond strength also has a very large effect on the reactivity of these type of complexes toward substitution reactions (see Section IIID) and on the metal–aqua bond lengths (see Section IIIC).

C. Structure of Protonated Forms

Determination of the crystal structure of salts of the dioxotetracyano complexes of Mo(IV) (*194*), Re(V) (*195*), and Os(VI) (*175*) showed that they are highly symmetrical and that the metal ion is in the center of the plane formed by the carbon atoms of the four cyano ligands (see Fig. 12). There is, however, a significant difference in the metal–oxygen bond distances: 1.834(9) Å in the molybdenum, 1.781(3) Å in the rhenium, and 1.75(1) Å in the osmium complex. This order is what one would expect from the charge of the metal ions: A high positive charge makes the metal ion a good π-acceptor, which increases the metal–oxygen bond strength and thus shortens the bond. The ionic radii of these metal ions also decrease in the order Mo(IV) > Re(V) > Os(VI). This may explain the significant decrease in the metal–carbon bond distance from Mo(IV) to Re(V) and further to Os(VI) (these metal ions are d^2 species (see Table IV).

There is a significant decrease in the metal–oxo bond distance during protonation of the oxygen atom *trans* to the oxo ligand: The Mo=O bond length decreases from 1.834(9) Å in $[MoO_2(CN)_4]^{4-}$ (*194*) to 1.698(7) Å in $[MoO(OH)(CN)_4]^{3-}$ (*143*) and 1.668(5) Å in $[MoO(H_2O)(CN)_4]^{2-}$ (*143, 169, 196*), whereas the Re=O bond distance decreases from 1.781(3) Å in $[ReO_2(CN)_4]^{3-}$ (*195*) to 1.70(1) Å in $[ReO(OH)(CN)_4]^{2-}$ (*189*) and 1.67(1) Å in $[ReO(H_2O)(CN)_4]^{-}$ (*190*). This decrease in the metal–oxo bond distance is accompanied by a large and signifi-

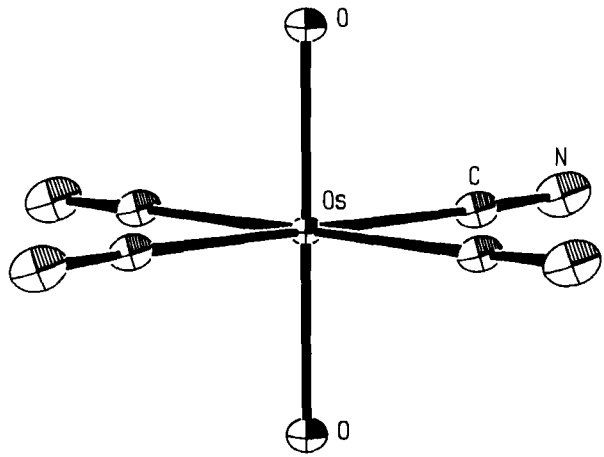

FIG. 12. Perspective view of $[OsO_2(CN)_4]^{2-}$ (*175*). Adapted with permission from Purcell *et al.* (*175*). Copyright 1991, Chapman & Hall.

TABLE IV

BOND DATA FOR ISOELECTRONIC TETRACYANO COMPLEXES OF Mo(IV), W(IV), Tc(V), Re(V), AND Os(VI) CONTAINING OXO OR NITRIDO LIGANDS

Complex	M≡N or M=O (Å)	M—L[a] (Å)	M—C[b] (Å)	D[c] (Å)	Reference
$[MoO_2(CN)_4]^{4-}$	1.834(9)	1.834(9)	2.20(1)	0	*194*
$[MoO(OH)(CN)_4]^{3-}$	1.698(7)	2.077(7)	2.11(1)	0.19	*143*
$[MoO(H_2O)(CN)_4]^{2-}$	1.668(5)	2.271(4)	2.16(1)	0.34	*143, 169*
$[MoO(N_3)(CN)_4]^{3-}$	1.70(1)	2.29(2)	2.17(1)	0.28	*197*
$[MoO(CN)_5]^{3-}$	1.705(4)	2.373(6)	2.18(1)	0.38	*169*
$[MoO(CH_3CN)(CN)_4]^{2-}$	1.658(7)	2.500(7)	2.159	0.46	*196*
$[WO(F)(CN)_4]^{3-}$	1.77(1)	2.017(8)	2.14(2)	0.18	*198*
$[WO(NCS)(CN)_4]^{3-}$	1.61(2)	2.23(2)	2.14(3)	0.35	*199*
$[ReO_2(CN)_4]^{3-}$	1.781(3)	1.781(3)	2.13(1)	0	*195*
$[ReO(OH)(CN)_4]^{2-}$	1.70(1)	1.90(1)	2.11(1)	0.08	*189*
$[ReO(H_2O)(CN)_4]^{-}$	1.67(1)	2.142(7)	2.11(1)	0.30	*190*
$[Re_2O_3(CN)_8]^{4-}$	1.69(1)	1.92(1)	2.12(1)	0.11	*186*
$[ReO(NCS)(CN)_4]^{2-}$	1.67(1)	2.12(1)	2.11(1)	0.30	*200*
$[ReN(H_2O)(CN)_4]^{2-}$	1.64(1)	2.496(7)	2.11(1)	0.35	*176*
$[ReN(N_3)(CN)_4]^{3-}$	1.65(2)	2.36(2)	2.11(1)	0.34	*201*
$[ReN(CN)_5]^{3-}$	1.68(1)	2.39(1)	2.12(1)	0.31	*202*
$[TcO(NCS)(CN)_4]^{2-}$	1.61(1)	2.16(1)	2.11(1)	0.33	*174*
$[OsO_2(CN)_4]^{2-}$	1.75(1)	1.75(1)	2.09(1)	0	*175*
$[OsN(OH)(CN)_4]^{2-}$	1.80(1)	1.98(2)	2.11(1)	0.04	*181*

[a] *trans* to M≡N or M=O bonds.

[b] Equatorial M—CN bonds.

[c] Displacement of the central metal atom from the plane formed by four cyano ligands.

cant increase in the metal–oxygen bond *trans* to the oxo ligand: from 1.834(9) Å in $[MoO_2(CN)_4]^{4-}$ (*194*) to 2.077(7) Å in $[MoO(OH)(CN)_4]^{3-}$ and 2.271(4) Å in $[MoO(H_2O)(CN)_4]^{2-}$ (*143, 169*) and from 1.781(3) Å in $[ReO_2(CN)_4]^{3-}$ (*195*) to 1.90(1) Å in $[ReO(OH)(CN)_4]^{2-}$ (*189*) and 2.142(7) Å in $[ReO(H_2O)(CN)_4]^{-}$ (*190*). This decrease in the metal–oxo bond length (and the simultaneous increase in the metal–oxygen bond distance *trans* to the oxo ligand) is accompanied by a significant distortion of the octahedral geometry of the coordination polyhedron during protonation: The metal ion is pulled out of the plane formed by the carbon atoms of the four cyano ligands toward the oxo ligand by 0.19 and 0.34 Å for $[MoO(OH)(CN)_4]^{3-}$ (*143*) and $[MoO(H_2O)(CN)_4]^{2-}$ (*143, 169, 196*), respectively, and by 0.08 and 0.30 Å for $[ReO(OH)(CN)_4]^{2-}$ (*189*) and $[ReO(H_2O)(CN)_4]^{-}$ (*190*), respectively. The above-mentioned effects of protonation are illustrated in the structures of the different dioxo, oxo-aqua, and oxo-hydroxo complexes (*197–202*) (see Table IV and also Figs. 13 and 14). It is interesting to note that the metal–oxygen

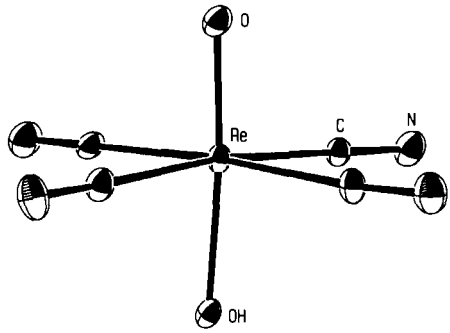

FIG. 13. Perspective view of $[ReO(OH)(CN)_4]^{2-}$ (*189*). Adapted with permission from Purcell *et al.* (*189*). Copyright 1989, Chapman & Hall.

bond distances in $[ReO(OH)(CN)_4]^{2-}$ and the dimer $[Re_2O_3(CN)_8]^{4-}$ (within the O=Re—O—Re=O moiety) are the same within experimental error, whereas the distortion of the octahedral environment of the rhenium ions in these complexes is also about the same.

Noteworthy also is the large difference in the metal–aqua bond distance in the molybdenum(IV) and rhenium(V) complexes: The rhenium–aqua bond is 0.13 Å shorter than the molybdenum–aqua bond, which is more than one would expect from the ionic radii of these metal ions and is probably a result of the higher positive charge on the rhenium atom. The relative strong rhenium–aqua bond resulted in a relative strong acidic water ligand compared with that of the molybde-

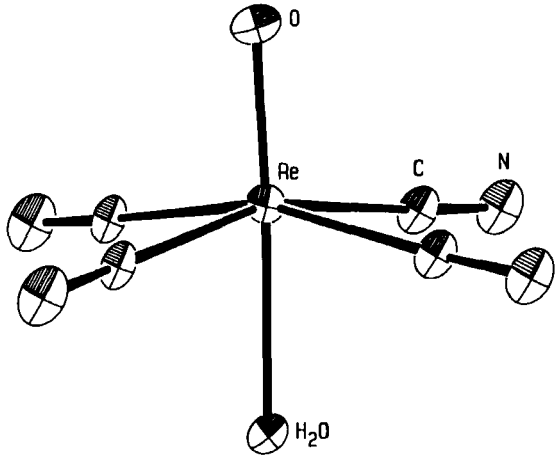

FIG. 14. Perspective view of $[ReO(H_2O)(CN)_4]^-$ (*190*). Adapted with permission from Purcell *et al.* (*190*). Copyright 1990, Chapman & Hall.

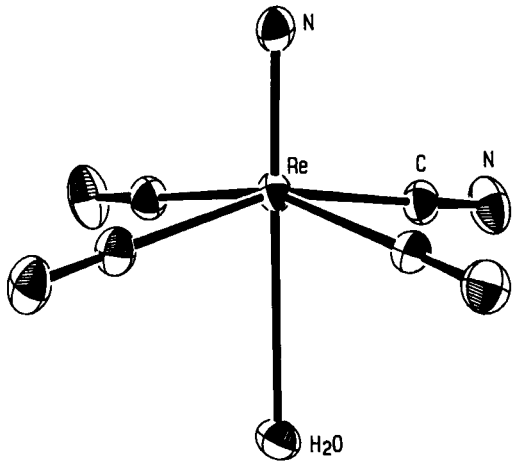

FIG. 15. Perspective view of $[ReN(H_2O)(CN)_4]^{2-}$ (*176*). Adapted with permission from Purcell *et al.* (*176*). Copyright 1992, Chapman & Hall.

num complex. The pK_{a1} value of $[ReO(H_2O)(CN)_4]^-$ is 1.4 compared with a value of about 10 for the molybdenum complex (*143, 182–184*).

The very large *trans*-influence of the nitrido ligand (see Section IIIB) is also evident from the difference in the rhenium–aqua bond lengths for the nitrido and oxo complexes: The rhenium–aqua bond is 0.35 Å longer in $[ReN(H_2O)(CN)_4]^{2-}$ (*176*) than in $[ReO(H_2O)(CN)_4]^-$ (*190*). This weak rhenium–aqua bond explains the weak acidity of the aqua ligand in the nitrido complex. The distortion of the coordination polyhedra is also more pronounced in $[ReN(H_2O)(CN)_4]^{2-}$ than in the corresponding oxo complex: The rhenium atom is displaced by 0.35 Å out of the plane formed by the four carbon atoms in the former complex in comparison with 0.30 Å in the latter complex (see Figs. 14 and 15). The difference in the metal–aqua bond distances (and thus the metal–aqua bond strength) not only affects the acidity of the coordinated water molecule but also has an enormous effect on the lability of the aqua ligand (reactivity toward substitution reactions), as will be pointed out in Section IIID. Some structural results for the dioxo-, oxohydroxo-, and oxoaqua complexes are summarized in Table IV.

D. SUBSTITUTION REACTIONS

1. Reactions with Monodentate Ligands

Investigation of the substitution reactions of the oxo- and nitridotetracyano complexes of Mo(IV), W(IV), Re(V), and Tc(V) was begun

after it was realized that the weakening of the metal–oxygen bond during protonation (see Sections IIIB and IIIC) might lead to the substitution of the hydroxo ligand and more probably the aqua ligand by strong σ-donating ligands. As a result of the large difference between the metal–hydroxo and the metal–aqua bond distances, one would expect that the aqua complex should be much more reactive toward substitution than the hydroxo complex, as was indeed observed. The dioxo complex with two relatively strong metal–oxygen bonds, in comparison with the hydroxo and aqua complexes, is, as may be expected from the short metal–oxygen bonds, totally inert toward substitution reactions.

A number of detailed kinetic studies (*155, 156, 166, 174, 191, 192, 198, 203–205*) (which also included construction of pH profiles) of the substitution reactions of the protonated forms of the dioxo and nitrido complexes of these metal ions showed that the relative reactivity of these complexes toward substitution with a number of σ-donating monodentate nucleophiles is what one would expect from the bond distances (and thus the bond strengths) in these complexes: The dioxo complexes with strong metal–oxygen bonds, observed in crystal structure determinations of $K_3Na[MoO_2(CN)_4]\cdot 6H_2O$ (*194*), $K_3[ReO_2(CN)_4]$ (*195*), and $Cs_2[OsO_2(CN)_4]$ (*175*), are completely inert toward oxo substitution reactions. The oxohydroxo complexes with a relatively short (strong) metal–hydroxo bond, observed in crystal structure determinations of $[Cr(en)_3][MoO(OH)(CN)_4]\cdot H_2O$ (*143*) and $(PPh_4)_2[ReO(OH)(CN)_4]$ (*189*), are also inert, whereas the aqua complexes with a relatively weak (long) metal–aqua bond, observed in $[MoO(H_2O)(CN)_4]^{2-}$ (*143, 169*) and $[ReO(H_2O(CN)_4]^-$ (*190*), are relatively reactive toward substitution.

Preparation of the products of substitution reactions between the aqua complexes of Mo(IV), W(IV), Re(V), and Tc(V) and various incoming ligands such as CN^-, NCS^-, N_3^-, and F^- and the subsequent crystal structure determinations of some of these substitution products (*169, 174, 196–202*) showed that only the aqua (or hydroxo) ligand is substituted by the monodentate ligand even in the presence of a large excess of the incoming ligand. The crystal structures of the following substitution products with monodentate ligands have been determined: $[2,2'\text{-}H_2bipy][TcO(NCS)(CN)_4]$ (*174*), $K_3WOF(CN)_4$ (*198*) $Cs_2Na[MoON_3(CN)_4]$ (*197*), $[4,4'\text{-}H_2bipy][ReO(NCS)(CN)_4]$ (*200*), $[N(CH_3)_4]_3[WO(NCS)(CN)_4]\cdot NaNCS$ (*199*), $(PPh_4)_3[ReN(CN)_5]\cdot 7H_2O$ (*202*), $Cs_2Na[ReN(N_3)(CN)_4]$ (*201*), $[PPh_4]_3[MoO(CN)_5]\cdot 7H_2O$ (*169*), $[PPh_4]_3[MoO(CN)_5]\cdot PPh_4Cl\cdot 2H_2O\cdot 2CH_3CN$ (*196*), and $[(PPh_3)_2N]_2[MoO(MeCN)(CN)_4]$ (*196*).

Some structural results are summarized in Table IV. The structures of some of these substitution products are illustrated in Figs. 16–18. These salts were prepared by adding an excess of the ligand to a relatively concentrated solution of the complex at a pH at which the complex is mainly in the aqua form followed by the excess addition of a salt solution of the appropriate cation, which forms a salt with the complex ion with a convenient solubility in order to get good quality crystals for X-ray analysis. These crystal structure determinations showed that only the aqua ligand is substituted by the excess of the incoming ligand. The cyano ligands are thus not substituted by monodentate ligands. This is not surprising in view of the strong metal–cyano bonds in the equatorial plane of the complex.

The oxo (or nitrido) ligand has about the same effect on the structure (bond lengths and especially the mode of distortion of the coordination polyhedron) of these substitution products as on the structure of the hydroxo and especially the aqua complex: The metal ion is pulled out of the plane formed by the four cyano ligands toward the oxo (or nitrido) ligand. The most important bond lengths and other structural features are summarized in Table IV. The amount of displacement of the heavy atom out of the square plane of the four cyano ligands, as well as the Re=O (or Re≡N) bond length, is sensitive to the nature of the incoming ligand and may be used as an indication of the bond strength and

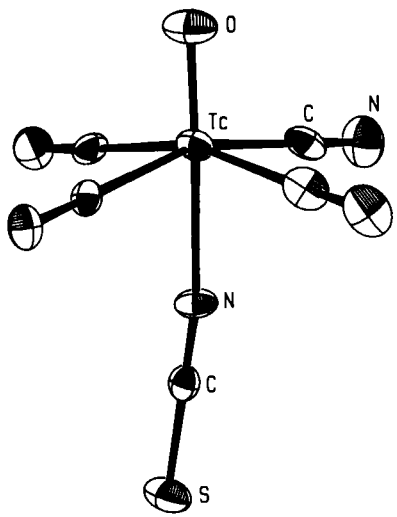

FIG. 16. Perspective view of $[TcO(NCS)(CN)_4]^{2-}$ (*174*). Adapted with permission from Roodt *et al.* (*174*). Copyright 1992, American Chemical Society.

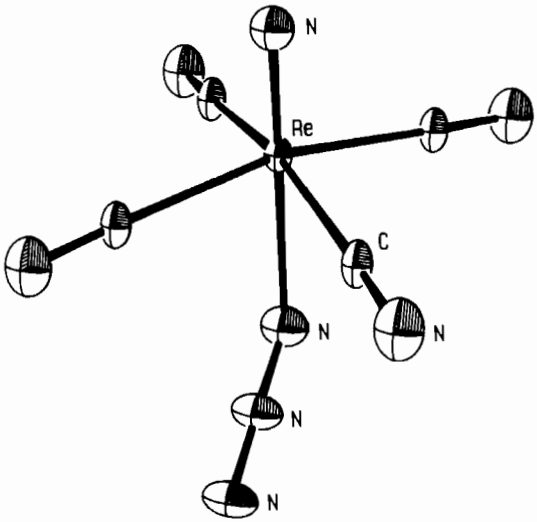

FIG. 17. Perspective view of $[ReN(N_3)(CN)_4]^{3-}$ (*201*). Adapted with permission from Purcell *et al.* (*201*). Copyright 1992, Elsevier–Sequoia.

trans-influence of the incoming ligand. The ν(M=O) value is a more sensitive parameter to compare the relative *trans*-influences of the incoming ligands (*199*). The ν(W=O) values for a number of tungsten complexes are listed in Table V. These values indicate that the *trans*-influences (and thus probably the bond strengths) decrease in the order

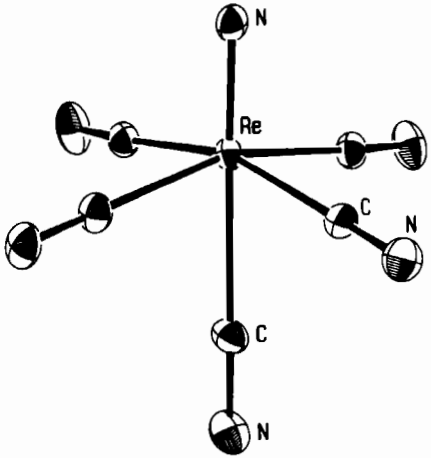

FIG. 18. Perspective view of $[ReN(CN)_5]^{3-}$ (*202*). Adapted with permission from Purcell *et al.* (*202*). Copyright 1991, Champan & Hall.

TABLE V

SELECTED INFRARED DATA FOR SOME OXOCYANO COMPLEXES OF W(IV)[a]

L[b]	ν (W=O)
H_2O	980
Py	964
Phen	962
NCS^-	954
N_3^-	952
F^-	946
Pic^-	944
CN^-	924
OH^-	915
O^{2-}	728

[a] Roodt *et al.* (*199*).
[b] L is *trans* to the W=O bond.

$O^{2-} > OH^- > CN^- > Pic^-$(oxygen atom) $> F^- > N_3^- > NCS^- >$ Phen $>$ Py $> H_2O$. The relative large effect of the fluoride ion (compared with those of N_3^-, NCS^-, and py), which is also evident by the small displacement of the metal ion out of the plane formed by the four cyano ligands as well as the relative long W=O bond distance in $[WOF(CN)_4]^{3-}$ (*198*), may be explained by the strong interaction between F^- (a small anion) and the metal ion, with a formal charge of 4+.

On the basis of the fact that only the aqua (or hydroxo) ligand is substituted by monodentate ligands and the pH profiles (see also Figs. 19–21), the reaction for the substitution reactions of these complexes with monodentate ligands may be represented by Scheme 3.

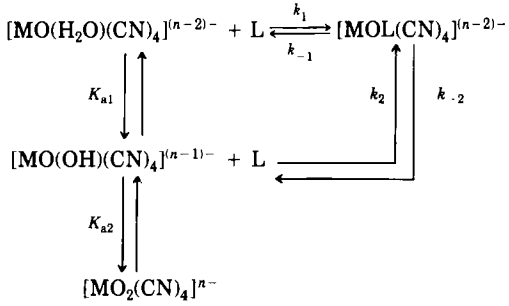

SCHEME 3. Reactions of the protonated forms of $[MO_2(CN)_4]^{n-}$ complexes with monodentate ligands.

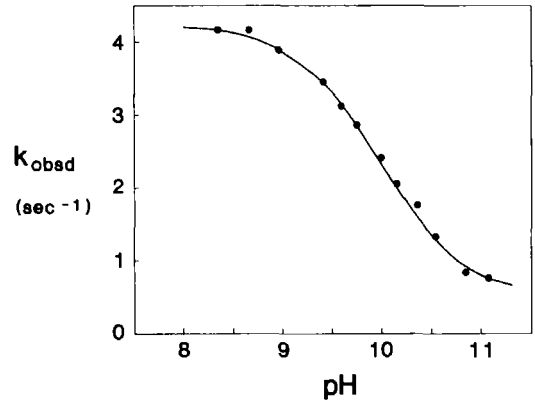

FIG. 19. pH profile for the reaction between $[MoO(H_2O)(CN)_4]^{2-}$ and F^- at 15°C and μ = 1.0 *M* (*166*). Adapted with permission from Potgieter *et al.* (*166*). Copyright 1988, Chapman & Hall.

In accordance with Scheme 3, the rate law, on the condition that $[L] \gg [MO(H_2O)(CN)_4{}^{n-}]$, is given by:

$$k_{obsd} = \left\{\frac{k_1 + k_2K_{a1}/[H^+]}{1 + K_{a1}/[H^+]}\right\}[L] + k_{-1} + k_{-2}[OH^-]. \qquad (166)$$

All the kinetic results for all the reactions studied could be fitted to Eq. (166). Figures 19–21 illustrate the effect of pH on the reaction

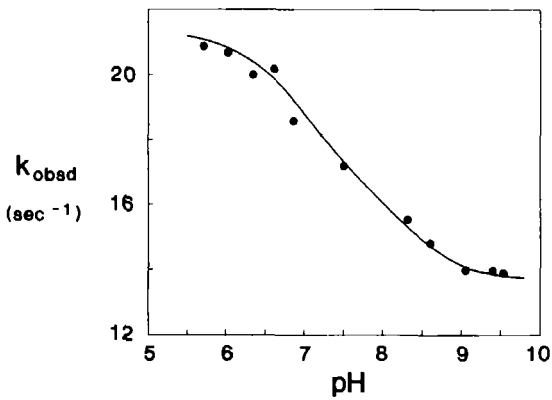

FIG. 20. pH profile for the reaction between $[WO(H_2O)(CN)_4]^{2-}$ and pyridine at 25°C and μ = 1.0 *M* (*203*).

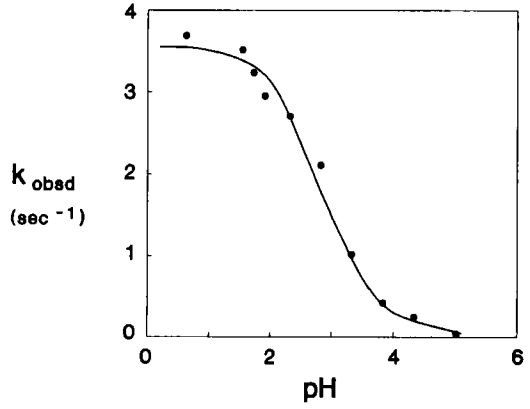

FIG. 21. pH profile for the reaction between $[TcO(H_2O)(CN)_4]^-$ and NCS^- at 25°C and μ = 1.0 *M* (*174*). Adapted with permission from Roodt *et al.* (*174*). Copyright 1992, American Chemical Society.

rates, in agreement with the rate law, Eq. (166). The rate constants k_1, k_2, and k_{-1}, as well as the values of K_{a1} for the reaction of the various complexes with a number of incoming ligands, were determined by means of a least-squares fit of the kinetic results to Eq. (166) (see Table VI). The rate constants for the substitution reactions of the hydroxo complexes (k_2) were zero within experimental error for all the reactions studied. The reactions could not be studied at a pH at which the hydroxo complex is the main species since no reactions were observed due to the low stability constant of the final complex at such a pH. The relative reactivity of the aqua and hydroxo complexes (k_1/k_2) could thus not be determined.

A detailed kinetic study of the ^{17}O water exchange of the dioxo complex of rhenium(V) (*206*), however, gave very valuable information about the relative reactivities of the aqua and hydroxo complexes toward substitution: The ratio of the water exchange rate of the aqua and hydroxo complexes of rhenium(V) was determined to be about 50. The ^{17}O NMR studies of these complexes demonstrate its effectiveness for the characterization of these type of complexes in aqueous solutions (*207*).

The use of multinuclear NMR for the characterization of these types of oxocyano complexes has proved to be valuable. The Re(V) system has been studied this way and an excellent correlation was found to exist among the ^{17}O chemical shift, the Re—O bond distance, and the ν(Re=O) stretching frequency (*207*). The data in Table VI show that

TABLE VI

COMPARISON AMONG STRUCTURAL, INFRARED, AND ^{17}O NMR DATA FOR THE DIOXOTETRACYANORHENATE(V) SYSTEM

Complex ion	Bond	Bond distance (Å)	ν (Re—O)[a] (cm^{-1})	^{17}O-chemical shift (ppm)
$[ReO(H_2O)(CN)_4]^-$	Re=O	1.667(8)[b]	1038	874[c]
$[ReO(NCS)(CN)_4]^{2-}$	Re=O	1.67(1)[d]	1010	869[c]
$[Re_2O_3(CN)_8]^{4-}$	Re=O	1.69(1)[e]	995	765
$[ReO(OH)(CN)_4]^{2-}$	Re=O	1.70(1)[f]	952	752[c]
$[ReO_2(CN)_4]^{3-}$	Re=O	1.783(1)[g]	785	463
$[Re_2O_3(CN)_8]^{4-}$	Re—μO	1.921(1)[e]	700	229
$[ReO(OH)(CN)_4]^{2-}$	Re—OH	1.90(1)[f]	660	119[c]
$[ReO(H_2O)(CN)_4]^-$	Re—OH_2	2.142(7)[b]	600	−19

[a] Leipoldt *et al.* (*173*).
[b] Purcell *et al.* (*190*).
[c] DMSO.
[d] Purcell *et al.* (*200*).
[e] Basson *et al.* (*186*).
[f] Purcell *et al.* (*189*).
[g] Murmann and Schlemper (*195*).

the oxo ligand in the $[ReO(H_2O)(CN)_4]^-$ complex is the most electron deficient as a result of the strongest Re—O bond; this, in turn, is manifested by both the X-ray and the infrared data. Current research includes the study of proton exchange in these systems by means of line broadening affected by pH manipulation (*206*). Both proton and oxygen exchange rate constants have been determined and the results could be used as further evidence of the dissociative activation for the ligation of the coordinated aqua ligand. Some evidence (*206*) suggests that the mechanism shifts to interchange (or associative) for oxygen exchange on the $[MO(OH)(CN)_4]^{m-}$ complexes.

The kinetic results, which gave an indication of the relative reactivities of the aqua and hydroxo complexes, are thus in agreement with the metal–aqua and metal–hydroxo bond distances in these complexes (see Section IIIC) and illustrate the value of accurate structural parameters in predicting relative reactivities of similar complexes (*208*).

The following detailed kinetic studies, including pH profiles, of the substitution reactions of the oxo complexes with various incoming ligands (the reactions with cyanide ligands will be discussed later) were performed (see Table VII).

TABLE VII

KINETIC DATA FOR THE REACTION OF $[MX(H_2O)(CN)_4]^{n-}$ COMPLEXES WITH DIFFERENT INCOMING LIGANDS AT 25°C[a]

M	X	⟨L⟩	k_1 (M^{-1} sec^{-1})	k_{-1} (sec^{-1})	K_1 (M^{-1})	$\Delta H^{\ddagger}$ (k_1) (kJ mol^{-1})	$\Delta S^{\ddagger}$ (k_1) (J mol^{-1} K^{-1})	Reference
Mo	O	F^-[b]	18.7(6)	1.6(4)	12.1(9)	49(3)	−59(13)	*166*
		CN^-[c]	116(2)	1.20(5)	95(5)	51(4)	−53(14)	*156*
		HCN[b]	4.8(2) × 10^2	1.4(3) × 10^2	3(1)	35(1)	−80(4)	*156*
W	O	F^-[c]	1.06(3) × 10^{-1}	1.0(1) × 10^{-3}	1.4(2) × 10^2	70(3)	−28(10)	*198*
		CN^-	1.15(3)	8(2) × 10^{-3}	1.1(1) × 10^3	90(5)	12(20)	*155*
		HCN	9(1)	8(2)	1.0(2)	69(3)	−5(10)	*155*
		N_3^-	4.2(1)	0.20(6)	4.8(11)	67(3)	−10(8)	*204*
		NCS^-	2.88(11)	2.12(5)	2.0(1)	73(3)	8(9)	*203*
		Py	6.9(4)	14.0(2)	0.5(1)	98(2)	101(6)	*203*
Re	O	NCS^-	3.48(4) × 10^{-3}	4.8(4) × 10^{-5}	87(7)	73(8)	−46(20)	*191*
		Tu	3.99(9) × 10^{-2}	7.3(2) × 10^{-3}	7.0(4)	52(1)	−95(3)	*205*
		NMTU	6.7(2) × 10^{-2}	2.6(5) × 10^{-3}	16.0(4)	42(3)	−125(10)	*205*
		NDMTU	5.9(2) × 10^{-2}	2.5(3) × 10^{-3}	31(2)	45(11)	−119(4)	*205*
		H_3N	6.4(2) × 10^{-2}	6.9(6) × 10^{-4}	3.2(3)	60(2)	−87(6)	*205*
Re	N	HCN[b]	66	78	0.9	—	—	*192*
		CN^-[b]	7.2(4) × 10^3	12(2)	600(100)	39(2)	−40(6)	*192*
Tc	O	NCS^-	22.2(3)	0.43(4)	54(2)	62(4)	−9(12)	*174*
Os	N	N_3^-	1.89(7)	9.5(5) × 10^{-3}	189(8)	58(2)	−45(3)	*193*

[a] See also Scheme 3.
[b] 15°C.
[c] 20°C.

(i) The molybdenum(IV) complex with F^- ions (166). The pH profile of this reaction is given in Fig. 19. It is clear from Fig. 19 (and this is the case for all the reactions studied) that the main reactive species is the aqua complex. The reactions of the molybdenum complex with other monodentate ligands were too fast to measure on a stopped-flow instrument, except in the case of cyanide ions (*156*). This reaction could be studied since the stability constant of $[MoO(CN)_5]^{3-}$ is large enough to control the rate of the reaction by means of the aqua-hydroxo equilibrium; the hydroxo complex of molybdenum(IV) is, as already pointed out, very unreactive.

(ii) The tungsten(IV) complex with F^- (198), pyridine, NCS^- (203), N_3^- (204), and cyanide ions (155). The pH profile for the reaction with pyridine is shown in Fig. 20. The rates of these reactions are very insensitive to the nature of the incoming ligand (see Table VII), except in the case of the reaction with F^- and HCN. The observed linear free-

energy relationship (see Fig. 22) points to a dissociative mechanism. The much slower reaction with F^- ions (also found in the case of the reaction with $[MoO(H_2O)(CN)_4]^{2-}$) was a result of the high degree of solvation of the fluoride ions due to the high electronegativity of the fluoride ion. Even more convincing evidence for a dissociative mechanism for these types of reactions was the observed positive volume of activation ($+10.6(5)$ cm^3 mol^{-1}) for the reaction with azide ions (*204*).

(iii) Rhenium(V) complex with NCS$^-$ (191), thiourea, and other incoming ligands (205). The observed linear free-energy relationship also suggests dissociative activation for the substitution reactions of the rhenium complex (*205*).

(iv) Technetium(V) complex with thiocyanate ions (174). The reaction of $[TcO(H_2O)(CN)_4]^-$ was studied with only thiocyanate ions as the incoming ligand. The same rate law (see Scheme 3 and Eq. (166)) as that for the other complexes was observed (see Fig. 21 for the pH profile). The results were also interpreted in terms of a dissociative activation.

The kinetic data for the reaction of the $[MX(H_2O)(CN)_4]^{n-}$ complexes with only NCS^- are summarized for convenience and easier comparison in Table VIII.

For the Group VIB elements, there is a decrease in the reaction rate by a factor of 50–200 (see also Table VII) and for the group VIIB elements, a decrease by a factor of about 6300 upon going from the second- to the third-row element. This suggests that the metal–aqua bond is stronger in the third-row elements than in the second-row

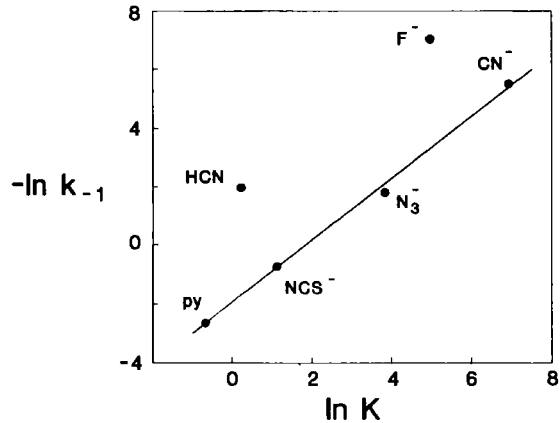

FIG. 22. Linear free-energy relationship for the reaction between $[WO(H_2O)(CN)_4]^{2-}$ and various incoming ligands (*155, 198, 203, 204*).

TABLE VIII

KINETIC DATA FOR THE REACTION OF $[MX(H_2O)(CN)_4]^{n-}$ COMPLEXES WITH NCS^- AT 25°C

Parameter	Mo(IV)	W(IV)	Tc(V)	Re(V)	Re(V)	Os(VI)
X	O	O	O	O	N	N
pK_{a1}	10.0	7.8	2.9	1.4	11.7	7.8
k_1 (M^{-1} sec^{-1})	116[a]	2.9	22.2	0.0035	7200[a]	1.89[b]
$\Delta S^{\neq}$ (J mol^{-1} K^{-1})	Nearly zero in most cases					
$\Delta V^{\neq}$ (cm^3 mol^{-1})	—	10.6	—	—	—	—
Reference	*156*	*203*	*174*	*191*	*192*	*193*

[a] CN^- at 20°C.
[b] N_3^-.

elements, as one would expect. The very large difference in the values of k_1 found for the complexes of the second- and third-row elements (large effect of the metal–aqua bond strength) may also point to a dissociative mechanism for these reactions. A stronger metal–aqua bond for the third-row elements is also evident from the lower pK_a values for the third-row complexes (see Sections IIIB and IIIC): A stronger metal–oxygen bond will weaken the oxygen–hydrogen bond in the aqua ligand with the resulting lower pK_a value.

Another interesting and significant feature about the results in Table VIII is the decrease in the reaction rate upon going from a group VIB metal ion with a formal charge of +4 to a group VIIB metal ion with a formal charge of 5+: $k_1^{Mo}/k_1^{Tc} = 10$ and $k_1^{W}/k_1^{Re} = 820$. This indicates that the aqua ligands are more strongly bonded to the metal ion with the higher formal charge, probably as a result of stronger dipole–ion interaction between the aqua ligand and the metal ion with the higher charge. This stronger metal–aqua bond for the group VIIB metal ions compared with that for the group VIB metal ions is also evidenced by the very large decrease in the pK_a values of the aqua complexes upon going from a metal ion with a formal charge of 4+ to one with a formal charge of 5+ (see also Section IIIB). The above-mentioned decrease in the rate constants with an increase in the formal charge of the metal ion (increase in the bond strength of the metal–aqua bond) also suggests a dissociative activation since ease of bond breaking is apparently very significant in the determination of the relative reactivity of these complexes.

An even more spectacular effect of bond strength on the relative reactivity of these complexes is found upon comparing the values of

k_1 in Table VIII for the reactions of the oxo and nitrido complexes of rhenium(V); the nitrido complex with the weak metal–aqua bond (Re—OH_2 = 2.496(7) Å) reacts about 10^6 times faster than the oxo complex with the much stronger metal—aqua bond (Re—OH_2 = 2.142(7) Å) (see Table IV). The comparison of the rate constants given in Table VIII was not made with the same incoming ligands as those used for these two complexes since it was not possible to study the reaction of the oxo complex with cyanide ions (the $[ReO(H_2O)(CN)_4]^-$ complex exists only at a low pH value (Section IIIB)) and of $[ReN(H_2O)(CN)_4]^{2-}$ with thiocyanate ions since this reaction is too fast at the high NCS^- concentration that is necessary as a result of the relative low stability constant of the tiocyanato complex. It is, however, reasonable to assume that the rate constants of these complexes with CN^- should be about the same as those with NCS^- since it was shown that the substitution reactions of these types of complexes proceed via a dissociative mechanism. The effect of the incoming ligand will thus be relatively small. The effect of the rhenium–aqua bond strengths in the oxo and nitrido complexes (see Table IV for bond distances and also Sections IIIB and IIIC) is also evidenced by the very large increase in the pK_{a1} value of 1.4 for the oxo complex to about 12 for the nitrido complex. This very high value for the nitrido complex points to a very weakly bonded aqua ligand, in agreement with the observed rhenium–aqua bond distance. The large dependency of the rate of substitution on the rhenium–aqua bond distances, as observed in comparing the oxo and nitrido complexes, also suggests a dissociative mechanism, and this also explains the high reactivity of the nitrido complex.

The large effect of the metal–aqua bond strengths (and thus the pK_a values of the $[MX(H_2O)(CN)_4]^{n-}$ complexes) (see Tables III and IV) on the reaction rate is nicely illustrated by the plot of log k_1 versus the pK_{a1} value of $[MX(H_2O)(CN)4]^{n-}$ (see Fig. 23). The observed LFER also points to a dissociative mechanism. The large deviation for the technetium complex (with interesting consequences for nuclear medicinal applications of Tc complexes) is difficult to explain (*174*).

Although one may expect that there is a large probability that these substitution reactions may proceed via an associative activation since it is well known that these metal ions have a great tendency to form stable coordination compounds with coordination numbers of 7 and also 8, all the kinetic results discussed earlier clearly point to a dissociative activation. Considering the results of the structure determinations of both reactants (especially of the aqua complexes) and the substitution products of these reactants, a dissociative mechanism is not so surprising for the following reasons (*208*).

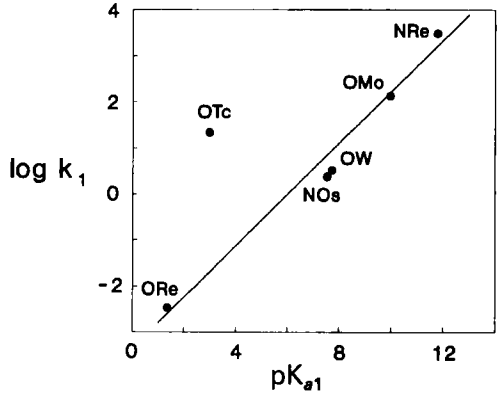

FIG. 23. Linear free-energy relationship for the reactions between various $[MX(H_2O)(CN)_4]^{n-}$ complexes and NCS^- (see Table VIII); ORe = $[ReO(H_2O)(CN)_4]^-$, OTc = $[TcO(H_2O)(CN)_4]^-$, OW = $[WO(H_2O)(CN)_4]^{2-}$, OMo = $[MoO(H_2O)(CN)_4]^{2-}$, NOs = $[OsN(H_2O)(CN)_4]^-$, and NRe = $[ReN(H_2O)(CN)_4]^{2-}$.

(i) The structural results indicate a very large *trans*-influence of the oxo and especially the nitrido ligand as illustrated by the following examples. The crystal structure determination of salts of $[MoO(Phen)(CN)_3]^-$ (*209, 210*) (see also Section IIID2) showed that the Mo—N bond distance *trans* to the oxo ligand is much longer than the Mo—N bond distance *trans* to the cyano ligand; the difference is about 0.91 Å, which is an indication of the very large *trans*-influence of the oxo ligand. The large *trans*-influence of the oxo ligand is also demonstrated by the long metal–aqua bond distances in $[MoO(H_2O)(CN)_4]^{2-}$ (*143, 169*) and in $[ReO(H_2O)(CN)_4]^-$ (*190*). The large *trans*-influence of the oxo and nitrido ligand is also very nicely illustrated by the Re—CN and Mo—CN bond distances in $[ReN(CN)_5]^{3-}$ (*202*) and $[MoO(CN)_5]^{3-}$ (*169*), respectively: The distance of the axial Re—C bond (*trans* to the nitrido ligand) is 0.27 Å longer than the average of the four equatorial Re—C bond distances, whereas the corresponding difference in the molybdenum complex is 0.19 Å (see also Section IIID3). The crystal structure determinations for $[ReO(H_2O)(CN)_4]^-$ (*190*) and $[ReN(H_2O)(CN)_4]^{2-}$ (*176*) showed also that the *trans*-influence of the nitrido ligand is much larger than that of the oxo ligand. From the above-mentioned examples it is clear that the large *trans*-influence of the oxo and nitrido ligands results in a weakening of the metal–aqua bonds. This ground-state destabilization will promote a dissociative mechanism and not an associative mechanism.

(ii) The structural results of both the reactants and the reaction products showed that the coordination polyhedra are significantly distorted from an ideal octahedral geometry (see Table IV). The central metal ion is displaced toward the oxo (or nitrido) ligand, out of the plane formed by the four carbon atoms of the four cyano ligands, by 0.35 Å, for example, in the case of $[ReN(H_2O)(CN)_4]^{2-}$ (*176*). This type of distortion is a frequently occurring phenomenon for octahedral complexes containing a strongly π-bonded ligand such as an oxo or nitrido ligand. This type of distortion results in a carbon–metal–aqua bond angle that is significantly smaller than the 90° for an ideal octahedron, only 80.6° in the case of $[ReN(H_2O)(CN)_4]^{2-}$ (*176*). This mode of distortion causes the aqua complex to be crowded in the most probable region of attack of the incoming ligand (i.e., the position of the aqua ligand) in an associative mechanism. An associative mechanism will therefore be less likely, whereas a dissociative mechanism will actually be promoted as a result of the repulsion between the four cyano ligands and the aqua ligand.

2. *Reactions with Bidentate Ligands*

The reaction between 1,10-phenanthroline and the protonated forms of $[MoO_2(CN)_4]^{4-}$ was the first substitution reaction of these complexes that was studied (*209–211*). The sodium salt of the substitution product, which gave a chemical analysis of Na:Mo:Phen:CN = 1:1:3:3, was structurally characterized by means of the crystal structure determinations of $Na[MoO(Phen)(CN)_3]\cdot 2Phen$ and $Na[MoO(Phen)(CN)_3]\cdot 2Phen\cdot CH_3OH\cdot H_2O$. These structure determinations showed that the incoming bidentate ligand substituted the aqua (or hydroxo) ligand as well as one cyano ligand (see Fig. 24). The very large *trans*-influence (mentioned in previous sections) of the oxo ligand was also observed in the structure of $[MoO(Phen)(CN)_3]^-$; the Mo—N bond *trans* to the oxo ligand is 0.19 Å longer than the Mo—N bond *trans* to the cyano ligand (*209*). Similar results were obtained for the complex $[WO(bpy)(CN)_3]^-$ (*212, 213*). Since a metal–aqua bond is usually much weaker than a metal–cyano bond (and this is especially the case in these complexes, as a result of the large *trans*-influence of the oxo ligand), one would expect that the aqua ligand will first be substituted during this two-step process. The crystal structure determination of $(AsPh_4)_2[WO(Pic)(CN)_3]\cdot 2H_2O$ showed that the oxygen atom of the carboxylic acid group of 2-picolinic acid is *trans* to the oxo ligand (*165*) (see Fig. 25). This was interpreted to mean that the aqua ligand was indeed first substituted since it is known that the oxygen atom in these types of ligands (such as 2-picolinic acid) will bond before the nitrogen atom.

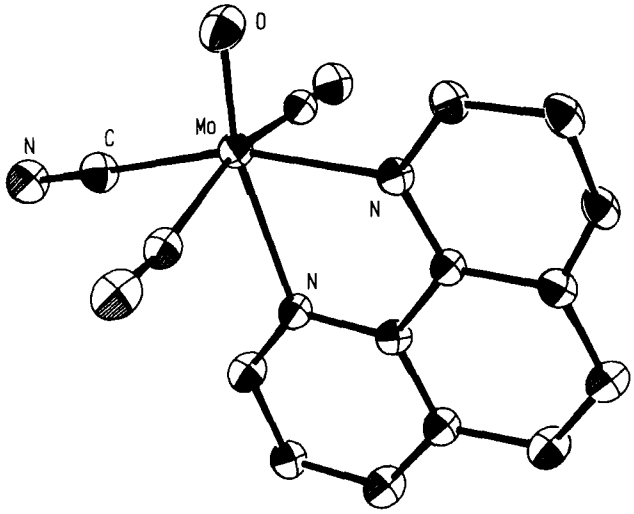

FIG. 24. Perspective view of $[MoO(Phen)(CN)_3]^-$ (*209, 210*).

The fact that the substitution reactions of the tungsten complex with monodentate ligands (see Table VII) are about 1000 times faster than those with bidentate ligands (2-picolinic acid) (*214*), whereas the kinetic results point to a dissociative mechanism (see Section IIID1), is

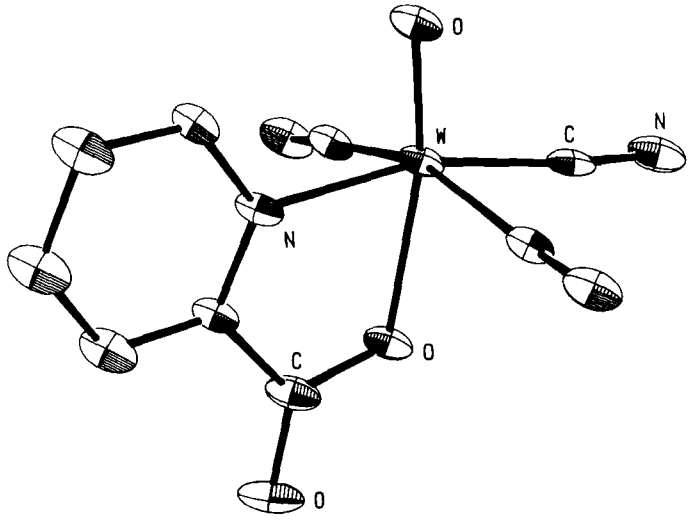

FIG. 25. Perspective view of $[WO(Pic)(CN)_3]^{2-}$ (*165*). Adapted with permission from Leipoldt *et al.* (*165*). Copyright 1986, Chapman & Hall.

a strong indication that the substitution of the aqua ligand is a relative fast reaction, whereas the substitution of the cyano ligand (ring closure) is a relative slow reaction (*198, 203, 204, 214*). The large difference in the reaction rates for the reaction of $[MoO(H_2O)(CN)_4]^{2-}$ with monodentate ligands (*156, 166*) and bidentate ligands (*211, 215*) also suggests that the ring-closure step (substitution of the cyano ligand) is the rate-determining step. This is not so surprising since the metal–cyano bond is expected to be much stronger than the metal–aqua bond. Scheme 4 (based on the structural as well as kinetic results) represents the reaction with a bidentate ligand.

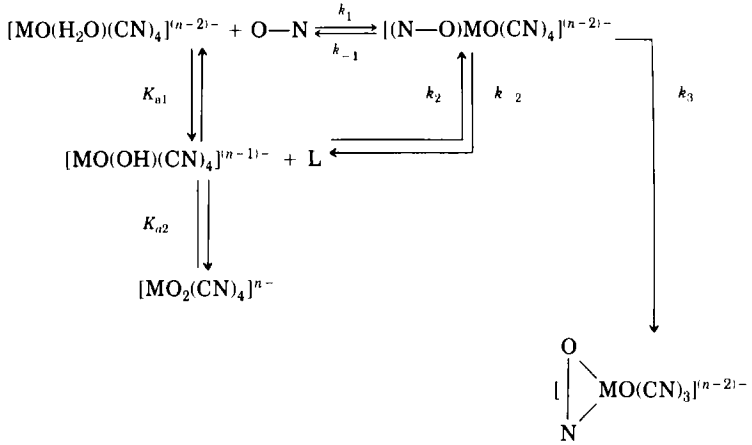

SCHEME 4. Reaction of the protonated forms of $[MO_2(CN)_4]^{n-}$ complexes with a bidentate ligand O—N; $k_3 \ll k_1$.

The reaction of $[MoO(H_2O)(CN)_4]^{2-}$ with 1,10-phenanthroline (*211*) and 2,2′-dipyridyl (*215*) has also been studied by means of reaction kinetics. It is clear that there are still uncertainties and questions regarding the mechanism of the reaction of these bidentate ligands: For example, why is the reaction of the molybdenum complex faster at high pH values at which there is less of the aqua and more of the hydroxo) complex in solution (*211*)? Scheme 5 was proposed for reaction with 2,2′-bipyridyl (*215*).

This study showed that $[MoO)(H_2O)(CN)_4]^{2-}$ is the only reactive species. It was proposed that the rate-determining step is the substitution of the aqua ligand and that the substitution of the cyanide ligand is fast. It is, however, more probable that the substitution of the aqua ligand is too fast to be observed under the experimental conditions used by the authors (*215*) (see also Section IIID1). The authors also

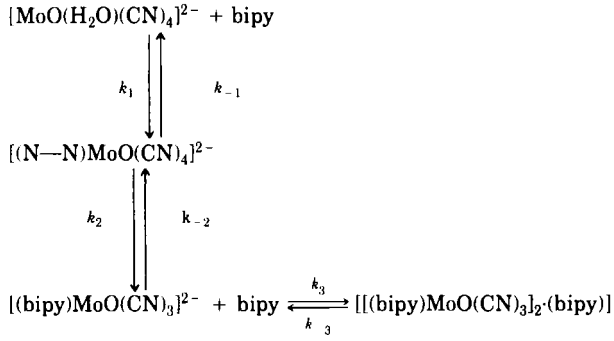

SCHEME 5. Scheme for reaction between $[MoO(H_2O)(CN)_4]^{2-}$ and 2,2'-bipyridyl (*215*); N—N = monocoordinated bipy.

observed the formation of a second product in the presence of an excess of bipy, which they formulate as $[[(bipy)MoO(CN)_3]_2 \cdot bipy]$ (*215*).

3. *Reactions with Cyanide Ions*

The reactions of the molybdenum(IV) and tungsten(IV) complexes with cyanide ions proceed via the same scheme as those of other monodentate ligands (see Scheme 3) with the formation of the pentacyano complex (*155, 156*). This very fast reaction is followed by a much slower reaction with the production of the octacyano complex in the presence of an excess of cyanide ions.

Although the octacyano complexes of Mo(IV) and W(IV) have been known for many years (see Section IIIA) and more convenient methods for synthesizing these complexes have been described, little is actually known about the mechanism of the formation of these complexes. A recent kinetic study of the formation of these complexes, however, suggested the overall reaction presented in Scheme 6 (*155, 156*).

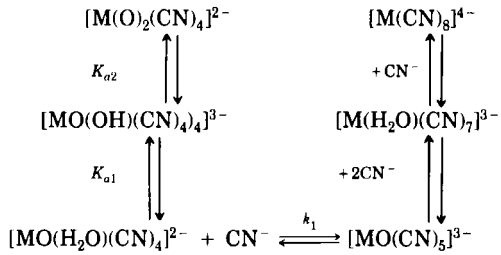

SCHEME 6. Reaction scheme for the formation of the octacyano complexes of Mo(IV) and W(IV).

In this reaction scheme, the formation of the pentacyano complex is a relatively fast reaction, with rate constants of about 116 and 2.9 M^{-1} sec^{-1} for the molybdenum (20°C) and tungsten (25°C) complexes, respectively, whereas the formation of the octacyano complex from the pentacyano complex is a relative slow reaction, with a half-life of several minutes at a cyanide ion concentration of 1 M for both the molybdenum and the tungsten complexes. The formation of the octacyano complex from the pentacyano complex is third order in the cyanide ion concentration (*155, 156*). This suggests that the rate-determining step is the reaction of the heptacyano complex with cyanide ions. It seems, however, that the pentacyano complex is a necessary intermediate in the synthesis of the octacyano complex. This proposed reaction scheme makes it possible for the first time to explain why the octacyano complex of rhenium(V), which is also a d^2 species, is still unknown in spite of several attempts (and claims of success) by different groups in the past (see Section IIA) to synthesize this complex: The reactive complexes $[ReO(H_2O)(CN)_4]^-$ and $[ReO(OH)(CN)_4]^{2-}$ do not exist at a pH > 8, at which there are enough free cyanide ions since the pK_a values of $[ReO(H_2O)(CN)_4]^-$ are only 1.4 and 4.2. The formation of the intermediate $[ReO(CN)_5]^{2-}$ (see Scheme 6) is thus not possible. Thus one cannot proceed beyond the tetracyano complex in this way.

The dimer $[Re_2O_3(CN)_8]^{4-}$, instead of $[ReO_2(CN)_4]^{3-}$, was used as a starting material in an attempt to synthesize $[Re(CN)_8]^{3-}$ since it is stable over a large pH range (*173*) (from pH 2 to pH 12), and it is expected to have the same reactivity as $[ReO(OH)(CN)_4]^{2-}$ based on the equal bond distances in these two complexes (see Section IIIC and Table IV). A recent kinetic study of the reaction of $[Re_2O_3(CN)_8]^{4-}$ with CN^- showed that this reaction indeed took place (breaking of the Re—O bond), with a half-life of about 2 hr at $[CN^-]$ = 1.0 M (*216*). This observed rate is in good agreement with the expected rate (based on the rate of the reaction of the aqua complex with thiocyanate ions and the value of the ratio of the reactivities of the aqua and hydroxo complexes as determined from the kinetic study of the water-exchange reaction (*206*) mentioned earlier) if one assumes the same reactivity of $[ReO(OH)(CN)_4]^{2-}$ and $[Re_2O_3(CN)_8]^{4-}$ toward substitution reactions. These results thus showed that accurate bond distances may indeed give important indications about the relative reactivities of coordination compounds (*208*). The rhenium(V) was, however, reduced in this process to rhenium(III), a d^4 species, which resulted in the formation of $[Re(CN)_7]^{4-}$ as a final product.

It was mentioned (see Section IIID1) that $[ReN(H_2O)(CN)_4]^{2-}$ reacts very rapidly with cyanide ions; about 10^6 times faster than the substitu-

tion reactions of $[ReO(H_2O)(CN)_4]^-$. The reaction product ($[ReN(CN)_5]^{3-}$) was characterized by means of the crystal structure determination of $(PPh_4)_3[ReN(CN)_5]\cdot 7H_2O$ (*202*). The large *trans*-influence of the nitrido ligand is also observed in this structure determination as well as those of $Cs_2Na[ReN(N_3)(CN)_4]$ (*201*) and $(AsPh_4)_2[ReN(H_2O)(CN)_4]\cdot 5H_2O$ (*176*), a very long bond *trans* to the nitrido ligand.

A kinetic study of the reaction of $[ReN(H_2O)(CN)_4]^{2-}$ with cyanide ions (*192*) showed that this reaction may also be represented by Scheme 3. It was observed that this complex (as well as $[MoO(H_2O)(CN)_4]^{2-}$ and $[WO(H_2O)(CN)_4]^{2-}$) reacts with the free cyanide ions as well as HCN, with the formation of the pentacyano complex (*155, 156, 192*). The possibility that the CN group may coordinate by means of the nitrogen atom was illustrated by the crystal structure determination of the $(PPh_3)_2N^+$ salt of $[MoO(CN)_4(CH_3CN)]^{2-}$ (*196*). The CH_3CN group is weakly coordinated to the molybdenum atom by means of the nitrogen atom in this compound.

4. *Reactions with Dioxygen and Related Compounds*

It was recently found that $[MoO(CN)_5]^{3-}$ can take up one molecule of dioxygen with the formation of the peroxo complex $[MoO(O_2)(CN)_4]^{2-}$, which was structurally characterized by means of the crystal structure determination of $(PPh_4)_2[MoO(O_2)(CN)_4]$ (*170*) (see Fig. 26). The peroxo complex $[MoO(O_2)(CN)_3(HMPA)]^-$ was synthesized from the above-mentioned peroxo complex and also characterized by means of the crystal structure determination of $(Ph_3PCH_2Ph)[MoO(O_2)(CN)_3(HMPA)]$, where HMPA is hexamethylphosphoramide. The O—O bond

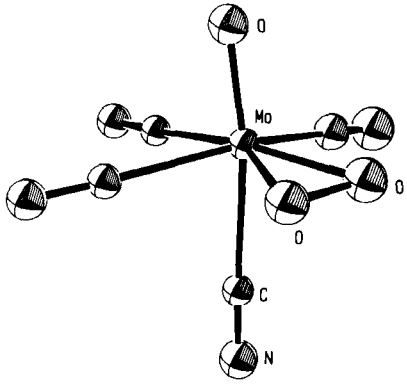

FIG. 26. Perspective view of $[MoO(O_2)(CN)_4]^{2-}$ (*170*). Adapted with permission from Arzoumanian *et al.* (*170*). Copyright 1988, American Chemical Society.

distances in these complexes are 1.416(5) and 1.397(10) Å (*170*), respectively. These values are in agreement with literature values for peroxo complexes (*217*) and point to a substantial weakening of the oxygen—oxygen bond in dioxygen. This oxygen uptake thus apparently leads to the activation of the dioxygen molecule as is indicated by the fact that this complex readily reacts with PPh_3 and cyclooctene, with the formation of $O{=}PPh_3$ and cyclooctene oxide (*170*). Similar reactions are observed with different Mo(IV) complexes, and it has also been shown recently that the corresponding W(IV) system behaves similarly. Different complexes are currently being actively investigated for the elucidation of their mechanisms and future application in catalytic oxidations (*155, 156*). There are, however, several problems associated with these studies with regard to the stability of the systems as well as questions with regard to the mechanisms that exist at this point in time.

It was also found that the oxopentacyano complex of Mo(IV) can facilitate oxygen atom transfer from dimethylsulfoxide and N_2O. The two reactions studied may be represented by the following equations (*218*).

$$(CH_3)_2SO + PPh_3 \xrightarrow{[MoO(CN)_5]^{3-}} (CH_3)_2S + OPPh_3 \qquad (167)$$

$$N_2O + PPh_3 \xrightarrow{[MoO(CN)_5]^{3-}} N_2 + OPPh_3 \qquad (168)$$

The crystal structure determination of tetraphenylphosphonium tetracyano[*N*-*o*-tolylhydroxylaminato(2-)-*O*,*N*]molybdate(VI) indicates the same mode of bonding of the -*N*-*O* substituent as that for dioxygen in the case of the above-mentioned dioxygen complexes (*219*).

References

1. Griffith, W. P., *Coord. Chem. Rev.* **17,** 177 (1975).
2. Sharpe, A. G., "The Chemistry of Cyano Complexes of the Transition Metals." Academic Press, London, 1976.
3. Colton, R., Peacock, R. D., and Wilkinson, G., *J. Chem. Soc.*, p. 1374 (1960).
4. Lock, C. J., and Wilkinson, G., *J. Chem. Soc.*, p. 2281 (1964).
5. Skolozdra, O. E., Mikhalevich, K. N., and Sergeeva, A. M., *Visn. L'viv. Politekh. Inst.* **60,** 23 (1971).
6. Griffith, W. P., Kiernan, P. M., and Bregeault, J.-M., *J. Chem. Soc., Dalton Trans.*, p. 1411 (1978).
7. Basson, S. S., and Leipoldt, J. G., *Transition Met. Chem.* **7,** 207 (1982).
8. Kepert, D. L., "Inorganic Stereochemistry." Springer-Verlag, Berlin, 1982.

9. Hoard, J. L., Hamor, T. A., and Glick, M. D., *J. Am. Chem. Soc.* **90,** 3177 (1968).
10. Bombieri, G., Moseley, P. T., and Brown, D., *J. Chem. Soc., Dalton, Trans.* p. 1520 (1975).
11. Countryman, R., and McDonald, W. S., *J. Inorg. Nucl. Chem.* **33,** 2213 (1971).
12. Hoard, J. L., and Silverton, J. V., *Inorg. Chem.* **2,** 235 (1963).
13. Lippard, S. J., *Prog. Inorg. Chem.* **8,** 109–193 (1967).
14. Bok, L. D. C., Leipoldt, J. G., and Basson, S. S., *Acta Crystallogr. Sect. B: Struct. Crystallogr. Cryst. Chem.* **B26,** 684 (1970).
15. Basson, S. S., Bok, L. D. C., and Leipoldt, J. G., *Acta Crystallogr., Sect. B: Struct. Crystallogr. Cryst. Chem.* **B26,** 1209 (1970).
16. Bok, L. D. C., Leipoldt, J. G., and Basson, S. S., *Z. Anorg. Allg. Chem.* **392,** 303 (1972).
17. Chojnaki, J., Grochowski, J., Lebioda, L., Oleksyn, B., and Stadnicka, K., *Rocz. Chem.* **43,** 273 (1969).
18. Meske, W., and Babel, D., *J. Alloys Compd.* **183,** 158 (1992).
19. Corden, B. J., Cunningham, J. A., and Eisenberg, R., *Inorg. Chem.* **9,** 356 (1970).
20. Basson, S. S., Leipoldt, J. G., and van Wyk, A. J., *Acta Crystallogr., Sect. B: Struct. Crystallogr. Cryst. Chem.* **B36,** 2025 (1980).
21. Leipoldt, J. G., Basson, S. S., and Bok, L. D. C., *Inorg. Chim. Acta* **44,** L99 (1980).
22. Basson, S. S., Leipoldt, J. G., Bok, L. D. C., van Vollenhoven, J. S., and Cilliers, P.J., *Acta Crystallogr., Sect. B: Struct. Crystallogr. Cryst. Chem.* **B36,** 1765 (1980).
23. Muetterties, E. L., and Guggenberger, L. J., *J. Am. Chem. Soc.* **96,** 1748 (1974).
24. Burdett, J. K., Hoffman, R., and Fay, R. C., *Inorg. Chem.* **17,** 2553 (1978).
25. Hursthouse, M. B., and Galas, A. M., *J. Chem. Soc., Chem. Commun.* p. 1167 (1980).
26. Laing, M., Gafner, G., Griffith, W. P., and Kiernan, P. M., *Inorg. Chim. Acta* **33,** L119 (1979).
27. Orgel, L. E., *J. Inorg. Nucl. Chem.* **14,** 136 (1960).
28. Meske, W., and Babel, D., *Z. Naturforsch., B: Chem. Sci.* **43,** 1167 (1988).
29. Meske, W., and Babel, D., *Acta Crystallogr., Sect. A: Found. Crystallogr.* **A40,** Suppl., C230 (1984).
30. Semenishin, D. I., Glowiak, T., and Mys'kiv, M. G., *Koord. Khim.* **11,** 122 (1985).
31. Ali, S. I., and Murtaza, Z., *Polyhedron* **4,** 463 (1985).
32. Malik, W. U., Srivastava, S. P., Thallam, K.K., and Gupta, V.K., *Acta Chim. Acad. Sci. Hung.* **109,** 345 (1982).
33. Mentasti, E., Secco, F., and Venturini, M., *Inorg.Chem.* **21,** 2314 (1982).
34. Gupta, V. K., Kumar, A., and Singh, P., *Proc. Indian Natl. Sci. Acad.* **57(A),** 485 (1991).
35. Malik, W. U., Srivastava, S. P., Thallam, K. K., and Gupta, V. K., *Acta Chim. Hung.* **112,** 5 (1983).
36. Ali, S. I., Murtaza, Z., and Khan, A. A., *Z. Phys. Chem. (Leipzig)* **266,** 1250 (1985).
37. Sykes, A. G., *Adv. Inorg. Chem. Radiochem.* **10,** 153 (1967).
38. Wilkins, R. G., "Kinetics and Mechanism of Reactions of Transition Metal Complexes," 2nd ed. VCH Verlagsges., Weinheim, 1991.
39. Thomas, L., and Hicks, K. W., *Inorg. Chem.* **13,** 749 (1974).
40. Leipoldt, J. G., Bok, L. D. C., van Vollenhoven, J. S., and Maree, J. P., *Z. Anorg. Allg. Chem.* **434,** 293 (1977).
41. Hicks, K. W., *J. Inorg. Nucl. Chem.* **38,** 1381 (1976).
42. Bailey, N., Carrington, A., Lott, K. A. K., and Symons, M. C. R., *J. Chem. Soc.*, p. 290 (1960).
43. Rawoof, M. A., and Sutter, J. R., *J. Phys. Chem.* **71,** 2767 (1967).
44. Hicks, K. W., and Sutter, J. R., *J. Phys. Chem.* **75,** 1107 (1971).

45. Leipoldt, J. G., Dennis, C. R., and Grobler, E. C., *Inorg. Chim. Acta* **77,** L45 (1983).
46. Borish, E. T., Kirschenbaum, L. J., and Mentasti, E., *J. Chem. Soc., Dalton Trans.*, p. 1789 (1985).
47. Potgieter, I. M., M. Sc. Dissertation, University of the Orange Free State (1979).
48. Stedman, G., *Adv. Inorg. Chem. Radiochem.* **22,** 113 (1979).
49. Hayon, E., and Simic, M., *J. Am. Chem. Soc.* **94,** 42 (1972).
50. Jindal, V. K., Agrawal, M. C., and Mushran, M. C., *Z. Naturforsch. B: Anorg. Chem., Org. Chem., Biochem., Biophys., Biol.* **25B,** 188 (1970).
51. Leipoldt, J. G., Bok, L. D. C., van Wyk, A. J., and Dennis, C. R., *React. Kinet. Catal. Lett.* **6,** 467 (1977).
52. Dennis, C. R., van Wyk, A. J., Basson, S. S., and Leipoldt, J. G., *Inorg. Chem.* **26,** 270 (1987).
53. Stanbury, D. M., *Inorg. Chem.* **23,** 2879 (1984).
54. Pelizzetti, E., Mentasti, E., and Pramauro, E., *Inorg. Chem.* **17,** 1688 (1978).
55. Pelizzetti, E., Mentasti, E., and Barni, E., *J. Chem. Soc., Perkin Trans. 2*, p. 623 (1978).
56. Brown, G. M., and Sutin, N., *J. Am. Chem. Soc.* **101,** 883 (1979).
57. Pelizzetti, E., Mentasti, E., and Pramauro, E., *Inorg. Chem.* **17,** 1181 (1978).
58. Holzwarath, J., and Jürgensen, H., *Ber. Bunsenges. Phys. Chem.***78,** 526 (1974).
59. Hodali, H. A., and El-Zaru, R. A., *Dirasat* [*Ser.*]: *Nat. Sci. (Univ. Jordan)* **16,** 7 (1989).
60. El-Zaru, R. A., and Hodali, H. A., *Polyhedron* **9,** 113 (1990).
61. Nichols, P. J., and Grant, M. W., *Aust. J. Chem.* **42,** 1085 (1989).
62. Bruhn, H., and Holzwarth, J., *Ber. Bunsenges. Phys. Chem.* **82,** 1006 (1978).
63. Pelizzetti, E., and Pramauro, E., *Inorg. Chem.* **18,** 882 (1979).
64. Pelizzetti, E., and Pramauro, E., *Inorg. Chim. Acta* **46,** L29 (1980).
65. Scherer, G., and Willig, F., *J. Electroanal. Chem.* **85,** 77 (1977).
66. Holzwarth, J., and Strohmaier, L., *Ber. Bunsenges. Phys. Chem.* **77,** 1145 (1973).
67. Bruhn, H., Nigam, S., and Holzwarth, J., *Faraday Discuss., Chem. Soc.* **74,** 129 (1982).
68. Lemire, R. J., and Lister, M. W., *J. Solution Chem.* **6,** 429 (1977).
69. Sanchez, F.; Nasarre, M. J., Graciani, M. M., Jimenez, R., Moya, M. L., Burgess, J., and Blandamer, M. J., *Transition Met. Chem.* **13,** 150 (1988).
70. Ford-Smith, M. H., and Rawsthorne, J. H., *J. Chem. Soc. A*, p. 160 (1969).
71. Bok, L. D. C., Leipoldt, J. G., and Basson, S. S., *J. Inorg. Nucl. Chem.* **37,** 2151 (1975).
72. Majid, Y. A., and Howlett, K. E., *J. Chem. Soc. A*, p.679 (1968).
73. Ferranti, F., and Indelli, A., *Gazz. Chim. Ital.* **107,** 543 (1977).
74. Dennis, C. R., Leipoldt, J. G., Basson, S. S., and van Wyk, A. J., *Inorg. Chem.* **25,** 1268 (1986).
75. Leipoldt, J. G., Bok, L. D. C., Basson, S. S., van Vollenhoven, J. S., and Maree, J. P., *React. Kinet. Catal. Lett.* **5,** 203 (1976).
76. Almeida, M. B., Ferranti, F., Alvarez, A. M., and Indelli, A., *Gazz. Chim. Ital.* **110,** 129 (1980).
77. Chlebek, R. W., and Lister, M. W., *Can. J. Chem.* **44,** 437 (1966).
78. Dennis, C. R., Basson, S. S., and Leipoldt, J. G., *Polyhedron* **2,** 1357 (1983).
79. Connick, R. E., Tam, T. M., and von Denster, E., *Inorg. Chem.* **21,** 103 (1982).
80. Swinehart, J. H., *J. Inorg. Nucl. Chem.* **29,** 2313 (1967).
81. Jindal, V. K., Agrawal, M. C., and Mushran, S. P., *J. Chem. Soc. A*, p. 2060 (1970).
82. Bridgart, G. J., Waters, W. A., and Wilson, I. R., *J. Chem. Soc., Dalton Trans.*, p. 1582 (1973).
83. Ayoko, G. A., Iyun, J. F., and Okechukwu, R. C., *Bull. Chem. Soc. Ethiop.* **4,** 33 (1990).

84. van Wyk, A. J., Dennis, C. R., Leipoldt, J. G., and Basson, S. S., *Polyhedron* **6,** 641 (1987).
85. Bok, L. D. C., Leipoldt, J. G., and Basson, S. S., *Z. Anorg. Allg. Chem.* **415,** 81 (1975).
86. Dennis, C. R., van Wyk, A. J., Basson, S. S., and Leipoldt, J. G., *Transition Met. Chem.* **17,** 471 (1992).
87. Dennis, C. R., van Wyk, A. J., Basson, S. S., and Leipoldt, J. G., *Polyhedron* **7,** 2193 (1988).
88. Leipoldt, J. G., Bok, L. D. C., and Dennis, C. R., *J. Inorg. Nucl. Chem.* **38,** 1655 (1976).
89. Leipoldt, J. G., Bok, L. D. C., van Wyk, A. J., and Dennis, C. R., *J. Inorg. Nucl. Chem.* **39,** 2019 (1977).
90. Lamprecht, G. J., Leipoldt, J. G., Dennis, C. R., and Basson, S. S., *React. Kinet. Catal. Lett.* **13,** 269 (1980).
91. Dennis, C. R., Leipoldt, J. G., Basson, S. S., and Lamprecht, G. J., *Polyhedron* **4,** 1621 (1985).
92. Howlett, K. E., and Wedzicha, B. L., *Inorg. Chim. Acta* **18,** 133 (1976).
93. Dinegar, R. H., Smellie, R. H., and la Mer, V. K., *J. Am. Chem. Soc.* **73,** 2050 (1951).
94. Leipoldt, J. G., Dennis, C. R., van Wyk, A. J., and Bok, L. D. C., *Inorg. Chim. Acta* **31,** 187 (1978).
95. Leipoldt, J. G., Dennis, C. R., van Wyk, A. J., and Bok, L. D. C., *Inorg. Chim. Acta* **34,** 237 (1979).
96. Solymosi, F., and Csik, J., *Chemist-Analyst* **49,** 12 (1960).
97. Guardado, P., Maestre, A., and Balon, M., *J. Inorg. Nucl. Chem.* **43,** 1391 (1981).
98. Hussein, M. A., and Sulfab, Y., *Transition Met. Chem.* **7,** 181 (1982).
99. Sulfab, Y., *J. Inorg. Nucl. Chem.* **38,** 2270 (1976).
100. Abdel-Khalek, A. A., and Elsemongy, M. M., *Monatsh. Chem.* **115,** 1385 (1984).
101. de Toro, P., Maestre, A., and Balon, M., *React. Kinet. Catal. Lett.* **27,** 221 (1985).
102. Birk, J. P., and Kozub, S. G., *Inorg. Chem.* **12,** 2460 (1973).
103. Faraggi, M., *J. Phys. Chem.* **80,** 2316 (1976).
104. Zehavi, D., and Rabani, J., *J. Phys. Chem.* **76,** 3703 (1972).
105. Shoute, L. C. T., Alfassi, Z. B., Neta, P., and Huie, R. P., *J. Phys. Chem.* **95,** 3238.
106. Huie, R. E., Shoute, L. C. T., and Neta, P., *Int. J. Chem. Kinet.* **23,** 541 (1991).
107. Basson, S. S., Bok, L. D. C., Leipoldt, J. G., and Grobler, S. R., *J. Inorg. Nucl. Chem.* **39,** 377 (1977).
108. Olatunji, M. A., and Okechukwa, R. C., *Transition Met. Chem.* **12,** 205 (1987).
109. Leipoldt, J. G., Bok, L. D. C., Basson, S. S., van Wyk, A. J., Dennis, C. R., and Cilliers, P. J., *React. Kinet. Catal. Lett.* **8,** 93 (1978).
110. Janssen, M. J., *Recl. Trav. Chim. Pays-Bas.* **81,** 650 (1962).
111. Olatunji, M. A., and Okechukwu, R. C., *Inorg. Chim. Acta* **131,** 89 (1987).
112. Hodali, H. A., and El-Zaru, R. A., *Polyhedron* **9,** 2299 (1990).
113. El-Zaru, R. A., and Hodali, H. A., *Dirasat [Ser.]: Nat. Sci. (Univ. Jordan)* **15,** 108 (1988).
114. Taniguchi, I., Miyamoto, S., Tomimura, S., and Hawkridge, F. M., *J. Electroanal. Chem.* **240,** 333 (1988).
115. McKnight, G. F., and Haight, G. P., *Inorg. Chem.* **12,** 1619 (1973).
116. Hicks, K. W., and Hurless, M. A., *Inorg. Chim. Acta* **74,** 229 (1983).
117. Birk, J. P., *J. Am. Chem. Soc.* **91,** 3189 (1969).
118. Leipoldt, J. G., Basson, S. S., Lamprecht, G. J., and Rabie, D. R., *Inorg. Chim. Acta* **51,** 67 (1981).
119. Rosenheim, A., Garfunkel, A., and Kohn, F., *Z. Anorg. Chem.* **65,** 166 (1910).
120. Goodenow, E. L., and Garner, C. S., *J. Am. Chem. Soc.* **77,** 5268 (1955).

121. Balzani, V., and Carassiti, V., "Photochemistry of Coordination Compounds." Academic Press, London, 1970.
122. Sieklucka, B., *Inorg. Chim. Acta* **186,** 179 (1991).
123. Sieklucka, B., Dziembaj, R., and Witkowski, S., *Inorg. Chim. Acta* **187,** 5 (1991).
124. Dudek, M., and Samotus, A.,. *Transition Met. Chem.* **10,** 271 (1985).
125. Kemp, T. J., *J. Inf. Rec. Mater.* **17,** 421 (1989).
126. Hennig, H., Billing, R., Salvetter, J., and Rehorek, D., *Z. Chem.* **26,** 304 (1986).
127. Nya, A. E., and Mohan, H., *Polyhedron* **3,** 743 (1984).
128. Gray, G. W., and Spence, J. T., *Inorg. Chem.* **12,** 2751 (1971).
129. Rehorek, D., Salvetter, J., Hantschmann, A., Hennig, H., Stasicka, Z., and Chodkowska, A., *Inorg. Chim. Acta* **37,** L471 (1979).
130. Rehorek, D., Rehorek, A., Thomas, P., and Hennig, H., *Inorg. Chim. Acta* **64,** L225 (1982).
131. Rehorek, D., and Janzen, E. G., *Z. Chem.* **25,** 451 (1985).
132. Rehorek, D., and Janzen, E. G., *Z. Chem.* **22,** 64 (1982).
133. Rehorek, D., and Hennig, H., *Can. J. Chem.* **60,** 1565 (1982).
134. Butter, K. R., Kemp, T. J., Sieklucka, B., and Samotus, A., *J. Chem. Soc., Trans., Dalton* p. 1217 (1986).
135. Sieklucka, B., Samotus, A., Sostero, S., and Traverso, O., *Inorg. Chim. Acta* **86,** L51 (1984).
136. Sieklucka, B., Kanas, A., and Samotus, A., *Transition Met. Chem.* **7,** 131 (1982).
137. Sieklucka, B., Alcock, N. W., Kemp, T. J., and Stufkens, D. J., *J. Chem. Soc., Trans., Dalton* p. 2331 (1990).
138. Sieklucka, B., Alcock, N. W., Kemp, T. J., Vincze, L., and Stufkens, D. J., *Inorg. Chim. Acta* **163,** 127 (1989).
139. Thomas, P., Saidi, C., and Hennig, H., *Inorg. Chim. Acta* **82,** L11 (1984).
140. Kemp, T. J., Shand, M. A., and Rehorek, D., *J. Chem. Soc., Dalton Trans.,* p. 285 (1988).
141. Sieklucka, B., and Samotus, A., *J. Inorg. Nucl. Chem.* **42,** 1003 (1980).
142. Kiessling, D., Nagorsnik, E., Thomas, P., and Hennig, H., *J. Prakt. Chem.* **322,** 843 (1980).
143. Lippard, S. J., and Russ, B. J., *Inorg. Chem.* **6,** 1943 (1967).
144. Robinson, P. R., Schlemper, E. O., and Murmann, R. K., *Inorg. Chem.* **14,** 2035 (1975).
145. Nagorsik, E., Thomas, P., and Hoyer, E., *Inorg. Nucl. Chem. Lett.* **10,** 353 (1974).
146. Mitra, R. P., and Mohan, H., *J. Inorg. Nucl. Chem.* **36,** 3739 (1974).
147. Adamson, A. W., and Perumareddi, J. R., *Inorg. Chem.* **4,** 247 (1965).
148. Carasitti, V., and Balzani, V., *Ann. Chim. (Rome)* **50,** 630 (1960).
149. Mitra, R. P., Sharma, B. K., and Mohan, H., *Can. J. Chem.* **47,** 2317 (1969).
150. Mohan, M., *J. Inorg. Nucl. Chem.* **38,** 1303 (1976).
151. Samotus, A., *Adv. Mol. Relax. Process.* **5,** 121–128 (1973).
152. Samotus, A., and Sieklucka, B., *J. Inorg. Nucl. Chem.* **40,** 315 (1978).
153. Ali, S. I., and Murtaza, Z., *Polyhedron* **4,** 821 (1985).
154. Ali, S. I., and Kaur, H., *Transition Met. Chem.* **16,** 450 (1991).
155. Smit, J. P., Purcell, W., Roodt, A., and Leipoldt, J. G., *Polyhedron* (accepted for publication).
156. Smit, J. P., Roodt, A., Purcell, W., and Leipoldt, J. G., to be published.
157. Samotus, A., and Sieklucka, B., *J. Inorg. Nucl. Chem.***40,** 315 (1980).
158. Thomas, P., Geissler, D., and Hennig, H., *Z. Chem.* **18,** 148 (1978).
159. Bucknall, W. R., and Wardlow, W., *J. Chem. Soc.* p. 2981 (1927).
160. Collenberg, O., *Z. Anorg. Allg. Chem.* **136,** 246 (1924).

161. Morgan, G., and Davies, G. R., *J. Chem. Soc.*, p. 1858 (1938).
162. Kraus, F., and Schrader, G., *J. Prakt. Chem.* **30,** 36 (1928).
163. Trop, H. S., Jones, A. G., and Davison, A. N., *Inorg. Chem.* **19,** 1993 (1980).
164. Samotus, A., Kanas, A., and Dudek, M., *J. Inorg. Nucl. Chem.***41,** 1129 (1979).
165. Leipoldt, J. G., Basson, S. S., Roodt, A., and Potgieter, I.M., *Transition Met. Chem.***11,** 323 (1986).
166. Potgieter, I. M., Basson, S. S., Roodt, A., and Leipoldt, J. G., *Transition Met. Chem.* **13,** 209 (1988).
167. Leipoldt, J. G., Bok, L. D. C., and Cilliers, P. J., *Z. Anoarg. Allg. Chem.* **407,** 350 (1974).
168. Leipoldt, J. G., Bok, L. D. C., and Cilliers, P. J., *Z. Anorg. Allg. Chem.* **409,** 343 (1974).
169. Wieghardt, K., Backes-Dahmann, G., Holzbach, W. J., Swiridoff, W. J., and Weiss, J., *Z. Anorg. Allg. Chem.* **499,** 44 (1983).
170. Arzoumanian, H., Petrignani, J. F., Pierrot, M., Ridouane, F., and Sanchez, J., *Inorg. Chem.* **27,** 3377 (1988).
171. Chakravorti, M. C., *J. Inorg. Nucl. Chem.* **34,** 893 (1972).
172. Lock, C. J. L., and Wilkinson, G., *J. Chem. Soc.* p. 2281 (1964).
173. Leipoldt, J. G., Basson, S. S., Roodt, A., and Purcell, W., *Transition Met. Chem.* **12,** 209 (1987).
174. Roodt, A., Leipoldt, J. G., Deutsch, E. A., and Sullivan, J. C., *Inorg. Chem.* **31,** 1080 (1992).
175. Purcell, W., Roodt, A., Basson, S. S., and Leipoldt, J. G., *Transition Met. Chem.* **16,** 60 (1991).
176. Purcell, S., Potgieter, I. M., Damoense, L. J., and Leipoldt, J. G., *Transition Met Chem.* **17,** 387 (1992).
177. Johnson, N. P., *J. Chem. Soc. A.* p. 1843 (1969).
178. Baldas, J., Boas, J. F., Colmanet, S. F., and Mackay, M. F., *Inorg. Chim. Acta* **170,** 233 (1990).
179. Griffith, W. P., and Pawson, D., *J. Chem. Soc., Dalton Trans.*, p. 1315 (1973).
180. Che. C.-M., Lam, M.H., and Mak, T. C. W., *J. Chem. Soc., Chem. Commun.*, p. 1529 (1989).
181. Purcell, W., Van der Westhuizen, H. J., Leipoldt, J. G., and Basson, S. S., (submitted).
182. Hejmo, E., Kanas, A., and Samotus, A., *Bull. Acad. Pol. Sci., Ser. Sci. Chim.* **21,** 311 (1973).
183. van de Poel, J., and Neumann, H. M., *Inorg. Chem.* **7,** 2086 (1968).
184. Chakravorti, M. C., *Inorg. Nucl. Chem.* **34,** 893 (1972).
185. Toppen, D. L., and Murmann, R. K., *Inorg. Nucl. Chem. Lett.* **6,** 139 (1970).
186. Basson, S. S., Leipoldt, J. G., Roodt, A., and Purcell, W., *Transition Met. Chem.* **12,** 82 (1987).
187. Shandles, R., Schlemper, E. O., and Murmann, R. K., *Inorg. Chem.* **10,** 2785 (1971).
188. Lumme, P. O., Turpeinen, U., and Stasicka, Z., *Acta Crystallogr., Sect. C: Cryst. Struct. Commun.* **C47,** 501 (1991).
189. Purcell, W., Roodt, A., Basson, S. S., and Leipoldt, J. G., *Transition Met. Chem.* **14,** 5 (1989).
190. Purcell, W., Roodt, A., Basson, S. S., and Leipoldt, J. G., *Transition Met. Chem.* **15,** 239 (1990).
191. Purcell, W., Roodt, A., Basson, S. S., and Leipoldt, J. G., *Transition Met. Chem.* **14,** 224 (1989).

192. Leipoldt, J. G., Purcell, W., and Damoense, L. J., to be published.
193. Purcell, W., Basson, S. S., van der Westhuizen, H. J., and Leipoldt, J. G., to be published.
194. Day, V. W., and Hoard, J. L., *J. Am. Chem. Soc.* **90,** 3374 (1968).
195. Murmann, R. K., and Schlemper, E. O., *Inorg. Chem.* **10,** 2352 (1971).
196. Arzoumanian, H., Pierrot, M., Ridouane, F., and Sanchez, J.,*Transition Met. Chem.* **16,** 422 (1991).
197. Basson, S. S., Leipoldt, J. G., Potgieter, I. M., and Roodt, A., *Inorg. Chim. Acta* **103,** 121 (1985).
198. Leipoldt, J. G., Basson, S. S., Roodt, A., and Potgieter, I. M., *S. Afr. J. Chem.* **39,** 179 (1986).
199. Roodt, A., Leipoldt, J. G., Basson, S. S., and Potgieter, I. M., *Transition Met. Chem.* **15,** 439 (1990).
200. Purcell, W., Roodt, A., Basson, S. S., and Leipoldt, J. G., *Transition Met. Chem.***14,** 369 (1989).
201. Purcell, W., Damoense, L. J., and Leipoldt, J. G.,*Inorg. Chim. Acta* **195,** 217 (1992).
202. Purcell, W., Potgieter, I. M., Damoense, L. J., and Leipoldt, J. G., *Transition Met. Chem.* **16,** 473 (1991).
203. Roodt, A., Leipoldt, J. G., Basson, S. S., and Potgieter, I. M., *Transition Met. Chem.* **13,** 336 (1988).
204. Leipoldt, J. G., van Eldik, R., Basson, S. S., and Roodt, A., *Inorg. Chem.* **25,** 4639 (1986).
205. Purcell, W., Roodt, A., and Leipoldt, J. G., *Transition Met. Chem.* **16,** 339 (1991).
206. Roodt, A., Leipoldt, J. G., Helm, L., and Merbach, A. E., to be published.
207. Roodt, A., Leipoldt, J. G., Helm, L., and Merbach, A. E.,*Inorg. Chem.* **31,** 2864 (1992).
208. Leipoldt, J. G., Basson, S. S., Roodt, A., and Purcell, W.,*Polyhedron* **11,** 2277 (1992).
209. Basson, S. S., Leipoldt, J. G., and Potgieter, I. M., *Inorg. Chim. Acta* **87,** 71 (1984).
210. Basson, S. S., Leipoldt, J. G., and Potgieter, I. M., *Inorg. Chim. Acta* **90,** 57 (1984).
211. Leipoldt, J. G., Basson, S. S., Potgieter, I. M., and Roodt, A., *Inorg. Chem.* **26,** 57 (1987).
212. Samotus, A., Szklarzewicz, J., and Alcock, N. W.,*Inorg. Chim. Acta* **172,** 129 (1990).
213. Szklarzewicz, J., Samotus, A., Alcock, N. W., and Moll, M., *J. Chem. Soc., Dalton Trans.*, p. 2959 (1990).
214. Roodt, A., Basson, S. S., and Leipoldt, J. G., *Polyhedron* (accepted for publication).
215. Samotus, A., Kanas, A., Glug, W., and Szklarzewicz, J., *Transition Met. Chem.* **16,** 614 (1991).
216. Purcell, W., Leipoldt, J. G., and Roodt, A., to be published.
217. Mimoun, H., *J. Mol. Catal.* **7,** 1 (1980).
218. Arzoumanian, H., Nuel, D., and Sanchez, J., *J. Mol. Catal.* **65,** L9 (1991).
219. Ridouane, F., Sanchez, J., Arzoumanian, H., and Pierrot, M., *Acta Crystallogr., Sect. C: Cryst. Struct. Commun.* **C46,**1407 (1990).